INFLUENCE OF LIGHTWEIGHT AGGREGATE AND CALCIUM SULFOALUMINATE CEMENT ON DEFORMATION OF ORDINARY PORTLAND CEMENT MORTAR AND CONCRETE

BY

DI WU

THESIS

Submitted in partial fulfillment of the requirements
for the degree of Master of Science in Civil Engineering
in the Graduate College of the
University of Illinois at Urbana-Champaign, 2015

Urbana, Illinois

Adviser:

Assistant Professor Paramita Mondal

ABSTRACT

Cracking due to shrinkage is a predominant cause of concrete constructions degradation. Several strategies were developed to mitigate shrinkage in concrete. The addition of pre-soaked lightweight aggregate (LWA) and usage of calcium sulfoaluminate (CSA) cement are two common methods applied in shrinkage mitigation. Pre-soaked LWA supplies additional moisture to cement paste during hydration, thereby compensating for the water consumption that occurs during hydration and drying. CSA cement induces expansion of the matrix, which counteracts shrinkage.

This thesis presents the results from a wide range of tests that examined the effectiveness of LWA and CSA cement on shrinkage mitigation of mortar and concrete. The results indicate that the addition of pre-soaked LWA could reduce the shrinkage under sealed conditions, and the effectiveness is influenced by the dosage of pre-soaked LWA, w/c ratio and soaking time of LWA. Under unsealed conditions, the addition of pre-soaked LWA is not an effective way on shrinkage mitigation. However, LWA does affect the shrinkage of the matrix by influencing the stiffness of the entire matrix. The combined use of pre-soaked LWA and CSA cement could more effectively mitigate shrinkage, and the effect was more significant with increasing dosage of LWA.

To My Father and Mother

ACKNOWLEDGMENTS

I would like to express gratitude to my advisor Prof. Paramita Mondal for giving me the opportunity to work on this project under her guidance. I would not have been able to accomplish the needed tasks without her valuable suggestions and patience. She is an excellent researcher and teacher, and I benefited tremendously from working with her.

I would like to acknowledge my fellow colleagues in CEE, Piyush Chaunsali, Ardavan Ardeshirilajimi, Ang Li, Agustin Spalvier, Sravanthi Puligilla and Jaymie Kaiser. Among them, I would like to especially thank Piyush Chaunsali, who spent a lot of time introducing me to this topic. I appreciate the efforts he spent on teaching and helping me with the experiments and also the valuable suggestions he gave me. I also like to thank Ardavan Ardeshirilajimi for his help on my experiments.

I greatly appreciate the support from the CEE staff, especially Timothy Prunkard and Jamar Brown. The help they provided on the experimental materials and devices is what made the experiments possible.

I would like to give special thanks to my parents for their unconditional support and love.

Table of Contents

CHAPTER 1

INTRODUCTION

1.1. Introduction

In this chapter, the scope of this thesis is presented. Additionally, the main objectives of this research are discussed.

1.2. Scope of this thesis

Concrete structures are generally regarded as durable. However, the long-term performance of concrete structures can be significantly compromised by cracking. Cracking speeds up the ingress of aggressive chemicals, such as chloride and sulfate ions, resulting in degradation of cement-based materials. One informal estimate from the industry places this as a $500 million problem in America, with some ready-mix companies experiencing cracking issues on as many as 70% of their jobs. (Bentz and Weiss, 2008). The cracking arises from the restrain of volume changes associated with shrinkage due to hydration reactions, drying and thermal deformation. Therefore, the mitigation of shrinkage is a very urgent issue that needs to be resolved.

Several strategies for reducing shrinkage in concrete were developed. These include the use of higher aggregate volumes, modified cement binders, and shrinkage reducing admixtures (ACI Committee 231, 2010). Two of the strategies that are related to this research are the use of expansive additives and water saturated porous inclusions. They are described briefly as follows (Hansen, 2011):

Internal curing: Internal curing can mitigate shrinkage by introducing a water reservoir into the concrete that will release water to compensate for the water consumed by hydration and

drying. The medium commonly used as reservoirs are lightweight aggregates and superabsorbent polymers.

Expansive additives: Expansive additives can reduce cracking by offering expansion to counteract the shrinkage rather than reducing the shrinkage directly. These expansions may be obtained through ettringite formation or calcium hydroxide formation.

1.3. Objectives of this thesis

This thesis deals with autogenous and drying shrinkage of cementitious materials. Internal curing (lightweight aggregates) and expansive cement (calcium sulfoaluminate cement) are studied as methods to reduce shrinkage. This thesis is divided in two main parts, corresponding to studies on mortar and concrete.

1.3.1. Mortar

Several factors that affect the deformation of ordinary Portland cement (OPC) mortar are investigated, including dosages of pre-soaked lightweight aggregate (LWA), w/c ratios and soaking times of LWA. Additionally, the effectiveness of different LWA are compared. Additional objective is investigating the combined effects of pre-soaked LWA and calcium sulfoaluminate (CSA) cement on shrinkage mitigation of mortar.

1.3.2. Concrete

The effects of pre-soaked LWA on the deformation of ordinary Portland cement concrete is investigated. Additionally, the combined effects of pre-soaked LWA and CSA cement on deformation of concrete are studied.

CHAPTER 2

LITERATURE REVIEW

2.1. Introduction

In this chapter, the hydration and microstructure formation process of ordinary Portland cement (OPC) and calcium sulfoaluminate (CSA) cement paste, shrinkage mechanism and internal curing theory are discussed in order to provide a theoretical background for shrinkage behavior, expansion and internal curing.

2.2. Hydration process of ordinary Portland cement (OPC)

2.2.1. Hydration Reaction

The major components in the ordinary Portland cement are tricalcium silicate (C_3S), dicalcium silicate (C_2S), tricalcium aluminate (C_3A), and tetracalcium aluminoferrite (C_4AF) and the added gypsum ($C\bar{S}H_2$). Upon addition of water, these components start a series of hydration reactions. The most important hydration products are calcium silicate hydrate gel (C-S-H gel), calcium hydroxide (CH) and calcium sulphoaluminate hydrates (AFt and AFm). Other hydration products includes aluminum, iron and sulfur constituents. The main hydration reactions are listed as follows (Gartner et al., 2002; Chaunsali et al., 2013).

$$C_3S + (3 - x + n)H \rightarrow C_xS_2H_n + (3 - x)CH$$

$$C_2S + 4.3H \rightarrow C_{1.7}SH_4 + 0.3CH$$

$$C_3A + 3C\bar{S}H_2 + 26H \rightarrow C_6A\bar{S}_3H_{32}$$

$$2C_3A + C_6A\bar{S}_3H_{32} + 4H \rightarrow 3C_4A\bar{S}H_{12}$$

$$2C_3A + 27H \rightarrow C_4AH_{19} + C_2AH_8 \rightarrow 2C_3AH_6 + 15H$$

$$2C_4AF + 3C\bar{S}H_2 + 28H \rightarrow 3C_4(A,F)\bar{S}H_{12} + (F,A)H_3$$

According to Gartner et al. (2002), hydration process can be divided into four stages: first minutes, induction period, acceleration period and post-acceleration period. The corresponding chemical processes, physical processes and relevance to physical properties of concrete to each of the stage are showed in Table 2.1. The Figure 2.1 indicates the corresponding heat evolution curves.

Table 2.1 Four principal hydration stages of Portland cement concretes (Gartner et al., 2002)

Processing Stage (in concrete)	Chemical processes	Physical processes	Relevance to physical properties of concrete
First minutes (wetting and mixing)	Rapid dissolution of free lime, sulphate and aluminate phases; immediate formation of "Aft"; Superficial hydration of C3S. Hemihydrate dissolves but gypsum or syngenite can form.	Large initial burst of heat, mainly from dissolution of aluminate phases, plus some from alite and CaO. (Dissolution of alkali sulphates is endothermic.)	Rapid formation of aluminate hydrates, plus gypsum and syngenite influences rheology and may also affect the subsequent microstruture.
Induction period (agitation, transport, placing and finishing)	Nucleation of "C-S-H (m)"; Rapid decrease in [SiO2] and [Al2O3] to very low levels; [CH] becomes supersaturated and portlandite nucleates; [R+], [SO4+] stay fairly stable.	Low heat evolution rate; slow formation of early C-S-H and more Aft leads to continuous increase of viscosity (in absence of admixtures)	Continued formation of Aft and Afm phases. Can influence workability, bit it is formation of C-S-H that usually leads to the onset of normal set.

Table 2.1 (cont.)

Processing Stage (in concrete	Chemical processes	Physical processes	Relevance to physical properties of concrete
Acceleration period (setting and early hardening.)	Hydration of C3S (to C-S-H and portlandite) accelerates and reaches maximum; CH supersaturation decreases. [R+], [SO42-] stay fairly stable.	Rapid formation of hydrates leads to solidification and decreases in porosity; high rate of heat evolution.	Change from plastic to rigid consistency (initial and final set); early strength development.
Post-acceleration period (demolding continued hardening)	Decelerating rate of formation of C-S-H and portlandite from both C3S and C2S; [R+] and [OH-] increase but [SO42-] falls to very low levels; renewed hydration of aluminates to give (mainly) Afm phases. Aft may redissolve and/or recrystallize.	Decrease in rate of heat evolution. Continuous decreasing in porosity Particle-to-aggregate bond formation.	Continuous strength increase due to decreasing porosity, but at an ever-diminishing rate. Decrease in creep capacity. Hydration continuous for years of water is available. Paste will shrink due to drying.

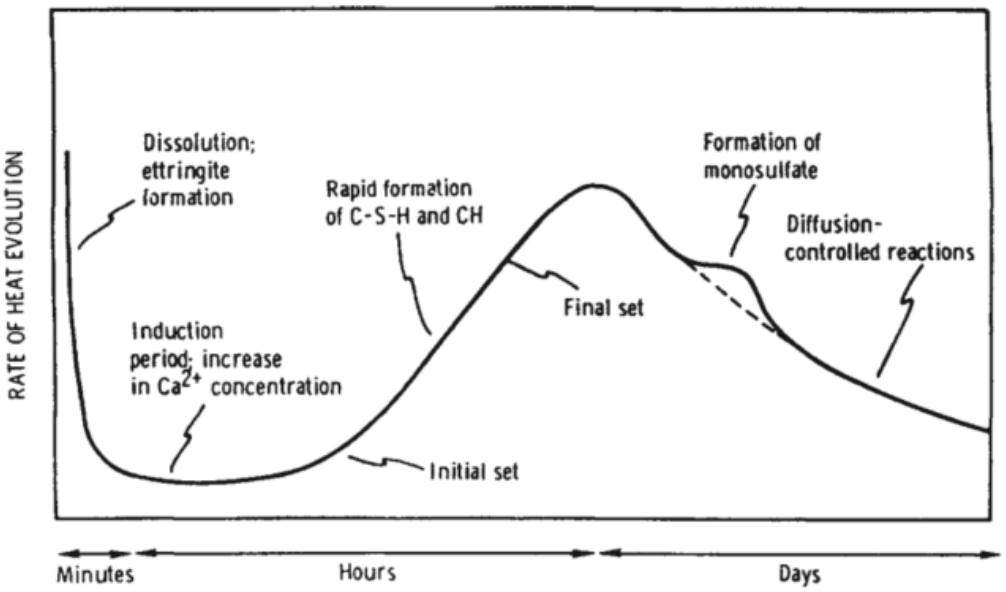

Figure 2.1 Schematic representation of heat evolution during hydration of cement (Gartner et al., 2002)

2.2.2. Microstructure formation

Cementing matrix is composite materials whose properties depend on both the properties of individual component and their spatial relationship and connections to each other (the microstructure). Figure 2.2 shows schematically the sequence of structure formation with hydration processing. Figure 2.2a shows the fluid paste in which the individual cement grains are separated by water. As hydration processes, solid hydration products form a continuous matrix and fit the unhydrated cement grains together, which is illustrated in Figure 2.2b-d (Mindess and Young, 2003).

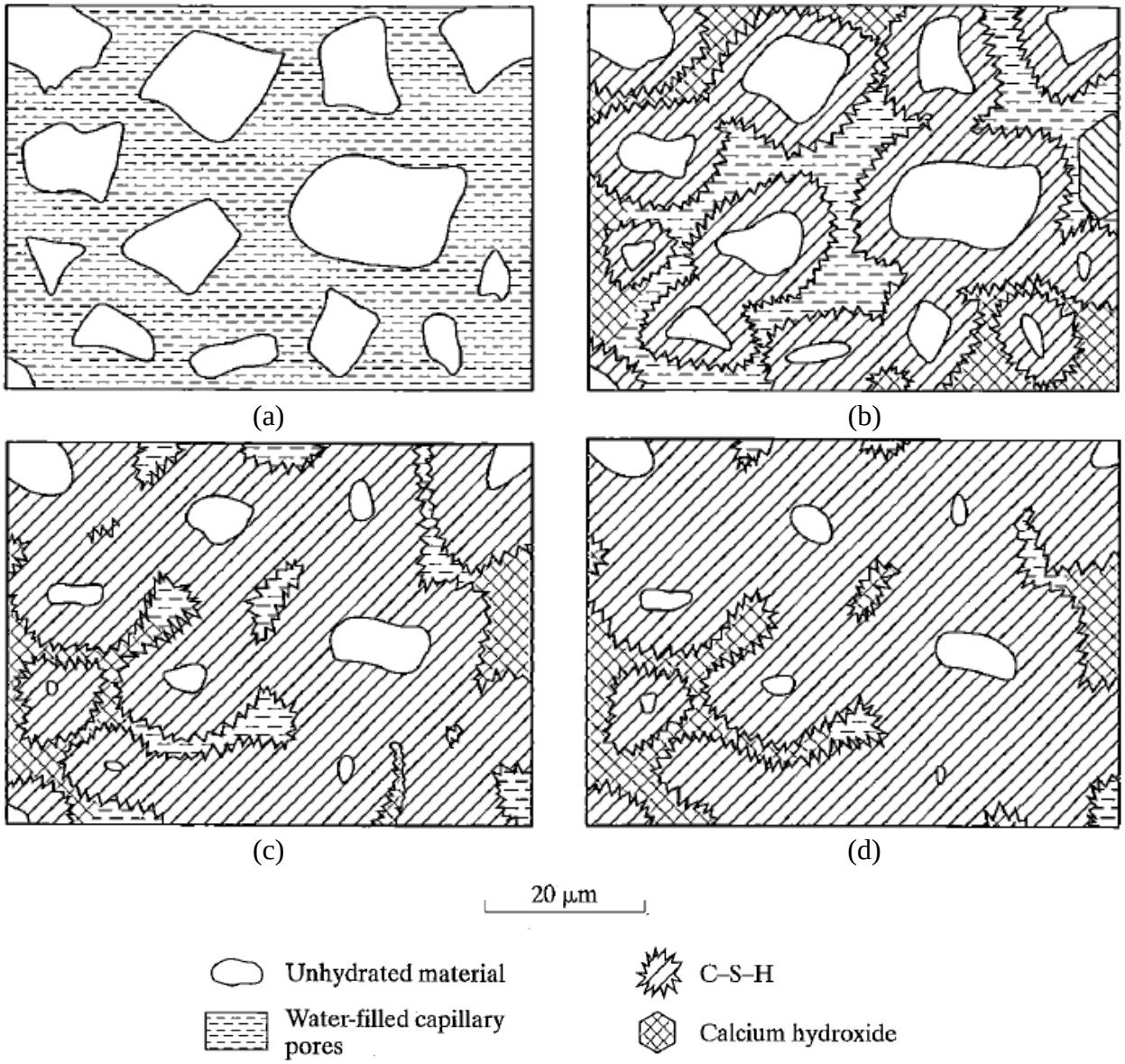

Figure 2.2 Schematic outline of microstructural development in Portland cement paste: (a) initial mix; (b) 7 days; (c) 28 days; and (d) 90 days (Mindess and Young, 2003) (Calcium sulfoaluminates are included as part of C-S-H for simplification, although they crystallize as separate phases)

2.2.3. Pore Structure

Hardened cement paste contains a wide range of pore sizes. The total porosity, size distribution and connectivity are very important parameters to the properties of concrete. A general agreement of pore classification is summarized in Table 2.2. Larger pores are extrinsically introduced into the hardened cement paste and they adversely influence the strength as the weak

links. The interconnected network formed from macropores provides pathway for easy mass transport, but frequently they are isolated by mesopores. Mesopores are of the size at which capillarity is dominant leading to the development of internal stress as mecopores emptied or high suction pressure as water added. Micropores are considered as the intrinsic part of C-S-H gel. (Powers et al., 1959; Mindess and Young, 2003; Gartner et al., 2002).

Capillary pores are formed when the water between cement particles is consumed as hydration proceeds. Hence, their volume and sizes depend on the w/c ratio and degree of hydration. Because the volume of solid phase increases, as hydration proceeds, the solid hydration products start filling the capillary pores. Contrarily, as more hydration gel is formed the volume of gel pores increases. However, the volume of capillary pores decreases much faster than the volume of gel pores increases. Thus, the total porosity decreases as hydration processes. This trend was clearly verified by the mercury intrusion porosimetry results showed in Figure 2.3 (Mindess and Young, 2003).

Table 2.2 Pores in hardened Portland cement paste

Designation	Diameter	Description	Origins	Properties Affected
Large Pore	> 10,000 nm (> 10 μm)	air voids	extrinsically entrapped	Strength; permeability; diffusivity
Macropores	10,000-50 nm (10-0.05 μm)	large capillaries	Remnants of water-filled space	Permeability; diffusivity
Mesopores	50-10 nm	medium capillaries	Remnants of water-filled space	Permeability in the absence of macropores; shrinkage above 80% RH
	10-2.5 nm	small, isolated capillaries	Part of outer product C-S-H	Shrinkage between 80% RH and 50% RH

Table 2.2 (cont.)

Designation	Diameter	Description	Origins	Properties Affected
Micropores	2.5-0.5 nm	gel pores	Intrinsic part of C-S-H	Shrinkage at all RH; creep
	< 0.5 nm	interlayer spaces	Intrinsic part of C-S-H	

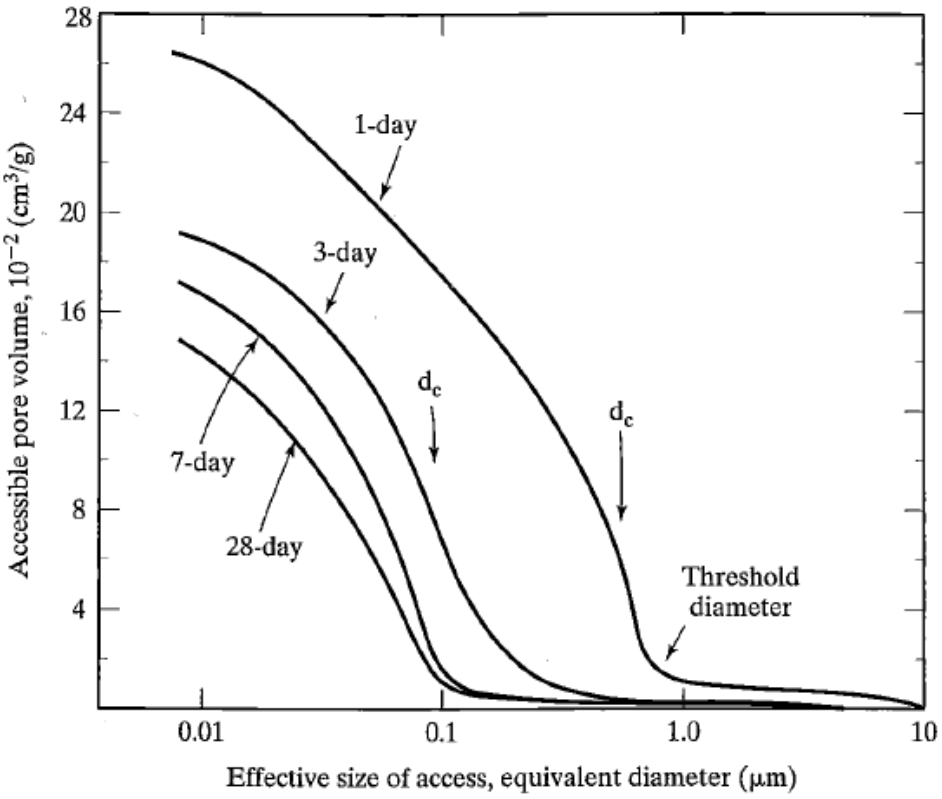

Figure 2.3 Mercury intrusion porosimetry curves for Portland cement paste (Mindess and Young, 2003)

2.3. Mechanisms of shrinkage

2.3.1. Chemical shrinkage

According to Jensen and Hansen (2001), chemical shrinkage is the internal volume reduction associated with the hydration reactions in a cementitious material. The mechanisms of chemical shrinkage are summarized by Wittmann (1982) as hydration shrinkage, thermal

shrinkage, dehydration shrinkage, crystallization swelling, conversion shrinkage and carbonation shrinkage.

Hydration shrinkage: Generally, nearly all the chemical reactions are accompanied by volume change. It is observed that the hydration of all four main clinker constituents causes reduction in volume. Powers (1935) reported the directly measured volume reduction of pure phases. The results he obtained is shown in Table 2.3.

Table 2.3 Volume reduction of pure clinker phases

Phase	1 day (ml/g)	3 days (ml/g)	7 days (ml/g)	14 days (ml/g)	28 days (ml/g)
C_3S	0.0188	0.0300	0.0336	0.0409	0.0481
C_2S	0.0110	0.0126	0.0106	0.0140	0.0202
C_3A	0.0632	0.0759	0.1133	0.1201	0.1091
C_4AF	0.0190	0.0202	0.0415	0.0352	0.0247

The Portland cement is observed a reduction of volume about 6-7 ml/100g of cement reacted (Powers and Brownyard, 1948). An even greater shrinkage is observed in the reaction of silica fume with calcium hydroxide: about 20 ml/100g of the silica fume reacted (Jensen and Hansen, 2001). Compared to the volume of reactants, while the absolute volume of hydration products decreases, the solid volume increases markedly. This increases causes the building up of the microstructure. The volume reduction mainly comes from consumption of water.

Thermal shrinkage: Since cement hydration is exothermal reaction, a certain degree of heat is liberated. Considering a typical mineralogical composition of Portland cement, the value of about 110 cal/g of cement hydrated can be liberated. A big portion of heat is liberated when concrete is still fresh and plastic. Thus, thermal expansion can occur in this stage, especially in massive element. As the rate of hydration decreases, the temperature decreases and, therefore, the matrix undergoes thermal shrinkage (Wittmann, 1982).

Dehydration shrinkage: Some of the hydration products are not stable with respect to a decrease of the relative humidity. Well-crystallized phases can loss their hydrate water at precise values of relative humidity. This loss of hydrate water is accompanied by a volume change, i.e. dehydration shrinkage (Wittmann, 1982).

Crystallization swelling: In a solid skeleton the expansion caused by crystal growth of hydration products is hindered and as a consequence internal stress is built up. This internal stress can induce swelling of matrix (Wittmann, 1982).

Conversion shrinkage: Some hydration products, especially aluminate hydrates, convert slowly to more stable form. This conversion is associated with volume change (Wittmann, 1982).

Carbonation shrinkage: In the presence of water the calcium hydroxide reacts with carbon dioxide in the surroundings. This reaction is called carbonation and it is accompanied by a decreased of the cement paste volume, i.e. carbonation shrinkage (Wittmann, 1982).

2.3.2. Self-desiccation

Before set, when cement paste is still fluid, the chemical shrinkage is totally converted to the external volume change, i.e. autogenous shrinkage. This occurs since the fluid paste is still not able to sustain the internal voids created by chemical shrinkage and collapses on itself. However, at the time of set, chemical shrinkage diverge from autogenous shrinkage as shown in Figure 2.4. The solidification of the paste prevents the matrix from further self-collapse. Hereafter, chemical shrinkage creates inner, empty cavities if the cement paste is under sealed condition. As hydration proceeds, these voids grow and penetrate into finer and finer pores. This results in the formation of vapor-water menisci and relative humidity drops according to Kelvin-Laplace equation. The drop of RH induces capillary pressure (Kelvin's law) and also accompanied by changes in both

surface tension and disjoining pressure. Thus, self-desiccation is the main reason for shrinkage under sealed condition (Henkensiefken et al., 2009; Lura et al., 2003; Jensen and Hansen, 2001).

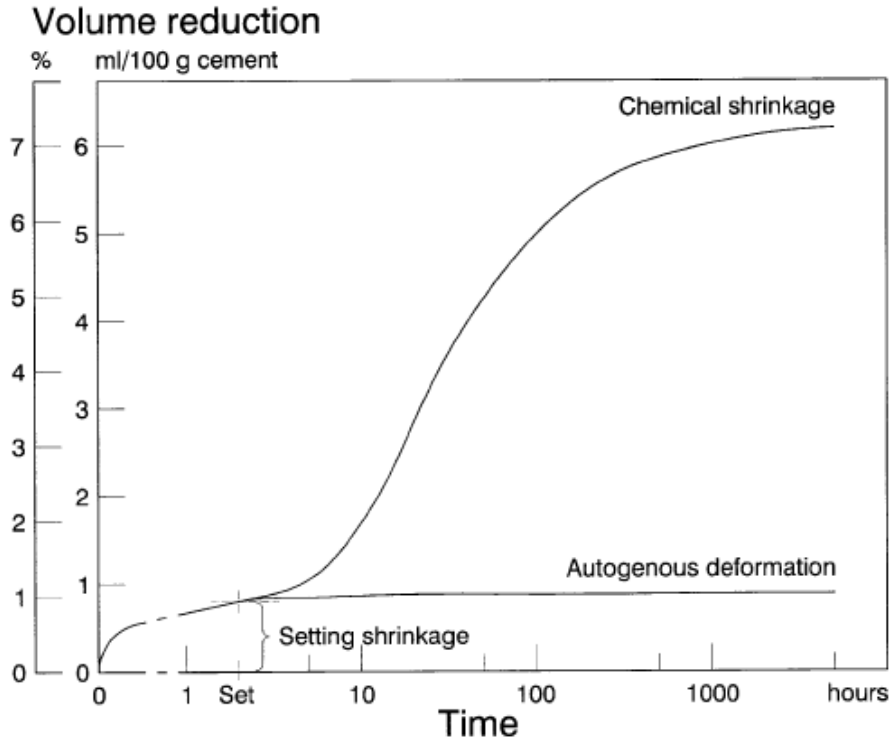

Figure 2.4 Chemical shrinkage and autogenous shrinkage volumes during hydration (Jensen and Hansen, 2001)

2.3.3. Shrinkage due to moisture change

The mechanisms of shrinkage due to moisture loss are poorly understood and the real mechanisms are still under discussion. However, there is a general agreement that the shrinkage is related to RH change of the hardening cement paste. Capillary tension, surface tension and disjoining pressure are the most popular mechanisms to explain the shrinkage due to moisture change.

2.3.3.1. Capillary tension

When vapor pressure over plane surface liquid (P) is equal to the saturation vapor pressure (P_0), liquid and vapor reach the equilibrium, i.e. number of molecules leaving the liquid equals to the number of molecules returning back to the liquid. This state is designated as relative humidity of 100%. If relative humidity drops below 100%, evaporation happens.

In capillary pores, the vapor pressure over meniscus is different from that over a plane surface liquid. Thus, at presence of meniscus, equilibrium is achieved at a lower vapor pressure than the saturated vapor pressure, in other words, at a lower relative humidity. Additionally, because of surface tension difference between the liquid and vapor, the difference in pressure between liquid and vapor can be calculated by Young-Laplace equation. The water-air meniscus, the equation is:

$$P_c \equiv P_a - P_w = -\frac{2\gamma}{r}$$

where γ (N/m) is surface tension at air-water interface, r (m) is the radius of menisci curvature, P_a (Pa) is the pressure in the air and P_w (Pa) is the pressure in the water. The difference between pressure in the air and in the water is capillary pressure, P_c (Pa). The capillary pressure given by the air pressure minus water pressure is always negative. This means the water is in the state of tension (Kovler and Zhutovsky, 2006).

The capillary pressure can also be related to the internal relative humidity as shown by Kelvin's equation:

$$P_c = \frac{RT \ln RH}{V_m}$$

where R is the universal gas constant (8.314 J/mol K), T (K) is the thermodynamic temperature, V_m is the molar volume of pore solution ($\approx 18\times10^{-6}$ m^3/mol).

The Kelvin's equation and Young-Laplace equation can be combined as Kelvin-Laplace equation, giving the relation between radius of menisci curvature and internal relative humidity:

$$\ln RH = -\frac{2\gamma V_m}{RTr}$$

According to Kelvin-Laplace equation, with a decrease in relative humidity, water starts to evaporate until the radius of menisci curvature reduces to the one corresponding to Kelvin-Laplace

equation. The minimum radius of menisci curvature is the radius of the capillary pores. If relative humidity drops lower than the relative humidity corresponding to the minimum radius of menisci curvature, evaporation takes place until the all water in that pore evaporates.

As shown by Young-Laplace equation, water in capillary pores is in the tension state. This tensile stress is balanced by compressive stress from the surrounding solid. Thus, emptying of capillary pores in cement paste by external drying or by self-desiccation subjects cement paste to compressive stress and results in volume decrease, i.e. shrinkage.

The linear strain of shrinkage, ε, of a partially saturated porous medium due to capillary pressure, σ_{cap}, could be estimated by the equation by Bentz et al. (1998), which is modified originally by Mackenzie (1950):

$$\varepsilon = \frac{SP_c}{3}\left(\frac{1}{K_p} - \frac{1}{K_s}\right)$$

where S (m^3 water/m^3 pore) is the saturation fraction, K_p (Pa) is the bulk modulus of the whole porous body and K_s (Pa) is the bulk modulus of the solid material within the porous body. As hydration proceeds, smaller and smaller pores are emptied and, as a consequence, the capillary pressure increases. However, as water lost, the saturation fraction decreases. This mechanism is effective only when capillary water becomes continuous. Powers (1965) reported that the capillary pressure becomes important at relative humidity in the range of 50-100%, while others consider this range as 35-100% (Feldman and Sereda, 1970).

2.3.3.2. Surface tension

In solid, the interaction forces between a molecule in the bulk and its neighbors are balanced form all the sides and the pressure in the bulk of the solid is uniform. However, at the surface of the bulk, the interaction forces on the surface molecules for the interior of the solid are not balanced by similar forces from the outside of the solid. Equilibrium condition require that at

the surface equal but opposite forces are applied to the surface molecules. This force is the surface tension of the solid (Visser, 1998).

The surface tension induces compressive stress to the solid. In particles of colloidal size, such as the cement gel particles which have large specific surface area, surface tension induce a huge compressive stress. Changes in surface tension would lead to volume change of the solid. After absorbing water, the adsorbed water molecules partly balance the attraction forces on the solid surface molecules from the interior molecules. Thus, the absorbing water results in reduction of surface tension. The solid strain then reduces and the solid expands in order to get a new equilibrium. The reduction of surface tension, $\Delta\gamma$, and the film thickness, Γ, of the adsorbed water is:

$$\Delta\gamma = \gamma_0 - \gamma = RT \int \Gamma d\,(\ln(P))$$

where R is the gas constant (8.314 J/mol K), T (K) is the thermodynamic temperature and P (Pa) is the vapor pressure.

The length changes caused by changes in surface tension is expressed by Bangham equation:

$$\Delta l/l = \lambda \cdot \Delta\gamma$$

where $\Delta l/l$ is the length change and λ is a proportionality factor that could be expressed by the equation proposed by Hiller (1964):

$$\lambda = \frac{\Sigma \cdot \rho}{3E}$$

where Σ is the specific surface area, ρ is specific gravity and E is elasticity modulus. It should be noted that the mechanism of change in surface tension is only important at lower humidity. This is because the changes in the surface tension of the solids due to the adsorption of

water molecules are of significance only for the first three layers of physically adsorbed water (Lura et al., 2003). For this reason, the surface tension mechanism is valid only up to the relative humidity of 40% (Kovler and Zhutovsky, 2006).

2.3.3.3. Disjoining pressure

C-S-H particles of the cement consist of laminar sheets. When they are placed in water, charged or polar layers attract water molecules at interfaces up to a few layers. These attracted water layers induce repulsive forces at solid surfaces to repel the C-S-H layers apart. By the adsorption of interlayer water, not only repulsive forces arise, but also the attractive forces decrease. The net surface force of the repulsion forces and loss of attraction forces is called disjoining pressure. The repulsion forces of disjoining pressure are composed of double layer repulsion and structural repulsion and the attraction forces are van der Waal's forces.

In the range of 50%<RH<100%, the attractive capillary pressure in the narrow gaps between particles and the repulsive disjoining pressure coexist. This is schematically shown in Figure 2.5.

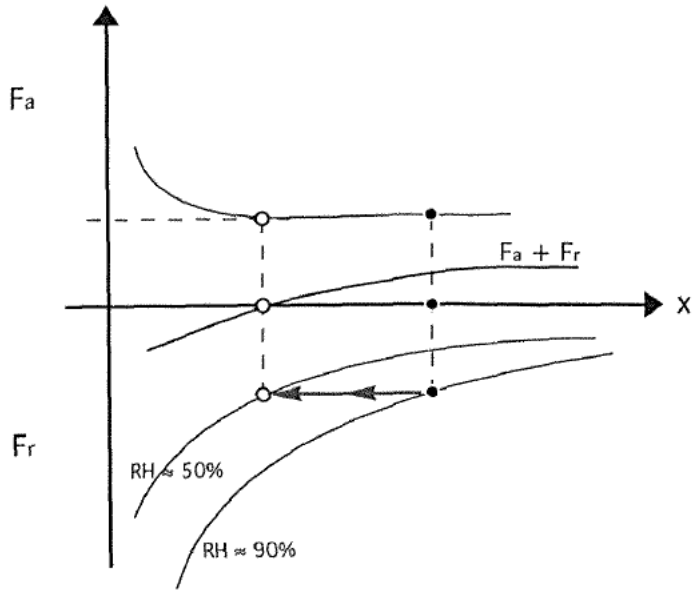

Figure 2.5 Interacting attractive and repulsive forces as a function of separation distance (Beltzung, 2001)

At very low distances attractive forces is composed of both capillary and van der Waals forces. Capillary forces are approximately independent of relative humidity while disjoining forces decrease with drying. Capillary forces are assumed independent of relative humidity because of the balancing effect between change of capillary pressure and change of surface (Schubert, 1982). Thus, as illustrated in Figure 2.5, in the case of drying the surfaces come closer as disjoining forces and equilibrium distance are lowered. This reducing in distance between surfaces appears as shrinkage in macro scale (Beltzung, 2001).

2.4. Internal curing by using lightweight aggregate (LWA)

2.4.1. Motivation of internal curing

Internal curing refers to provide the water as needed for hydration or to replace moisture lost through evaporation or self-desiccation by using reservoirs such as pre-wetted lightweight aggregate.

Traditionally, people use external curing techniques such as ponding, fogging, misting, and wet burlap to provide additional water for hydrating and reducing self-desiccation. However, in the higher-performance concretes the capillary porosity becomes isolated during the first few days of hydration (Powers et al., 1959). Thus, the external water can only penetrate a few millimeters into the concrete, whereas the interior of the concrete undergoes significant self-desiccation (Bentz, 2002). On the contrary, internal curing is able to distribute the water more equally across the cross section from inner side. The comparison between external and internal curing is illustrated in Figure 2.6.

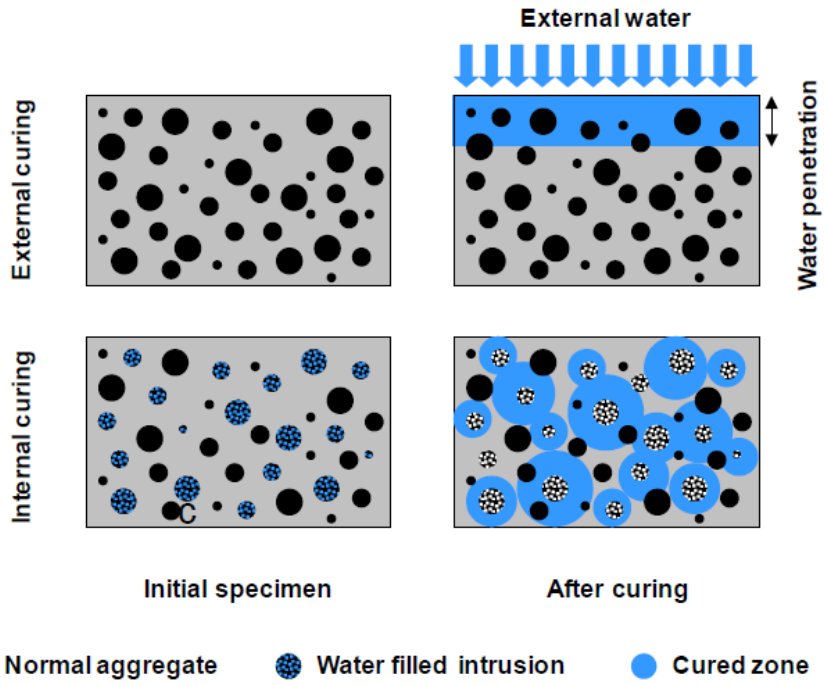

Figure 2.6 Illustration of the difference between external and internal curing (Castro et al., 2010)

The goal of internal curing is to provide a proper amount of additional water with a proper spatial distribution in order to maximize the hydration of cementitious component and to minimize the autogenous stresses and strains. Therefore, internal curing could potentially increase strength, reduce transport coefficients and mitigate cracking (Bentz and Weiss, 2011).

2.4.2. Mixture proportioning with internal curing

Mixture proportioning with internal curing is to achieve the goal of internal curing. Thus, based on this concern, three key questions should consider in this design process: 1) How much internal curing water (or what amount of internal reservoirs) is necessary for a given set of mixture proportions, 2) How far from the surfaces of the internal reservoirs into the surrounding cement paste can the internal curing water travel and 3) How are the reservoirs spatially distributed in the hydrating matrix?

Assuming that no water evaporation to surrounding environment happens, the amount of required internal reservoirs can be determined by simply equating the water demand of the

hydrating mixture to the supply that is readily available from the internal reservoirs. In other words, the volume of the internal curing water should be equal to the volume of the voids created by chemical shrinkage. Castro et al. (2011) provided an equation shows this relationship and the solution obtained for the required mass of dry LWA:

$$M_{LWA} = \frac{C_f \times CS \times \alpha_{max}}{S \times \phi_{LWA24h} \times \psi}$$

where C_f (kg/m^3) is the cement content of the mixture, CS (g of water/ g of cement) is the chemical shrinkage of the binder at 100% reaction, α_{max} (0 to 1) is the maximum degree of hydration, S the saturation degree based on the 24-hour absorption, ϕ_{LWA24h} (g of water/ g of dry LWA) is the 24-hour absorption and ψ (0 to 1) is the fraction of water released from the LWA at high relative humidity.

In a pure Portland cement system, for a water-to-cement ratio of 0.36 or higher, the maximum degree of hydration is expected as 1. For a lower water-to-cement ratio, it can be estimated by $(w/c)/0.36$ (Bentz et al., 2005). Chemical shrinkage could be obtained by conducting experiment according to ASTM C1608-12 or theoretically calculating according to the method proposed by Bentz et al. (2005). Saturation degree, absorption and desorption of LWA will be discussed in details in the next section.

2.4.3. Characterization of LWA for internal curing

The X-ray absorption studies of cement based materials have indicated that during drying, water will preferentially move from coarser pores to finer pores (Bentz et al., 2001). In the case of internal curing, the coarser pores are expected as those in LWA. Thus, for LWA to function successfully as an internal curing reservoir, the pores containing the water must be large than those in the surrounding cement paste, so that water will preferentially more form the LWA to the hydrating cement.

The ability of LWA to release water can be quantified by measuring absorption/desorption properties of LWA. Thus, absorption/desorption properties of LWA are critical to its successful performance as an internal reservoir. ASTM C1761/C1761M-13b provides standard methods to measure absorption and desorption properties of LWA for internal curing. This standard suggests using paper towel method to determine the absorption. It should be noted that absorption of LWA is a time-dependent property, so that absorption must be clarified with a time descriptor. The most commonly used absorption is of 24 hours. Table 2.4 presents the time-dependent absorption values for numerous types of LWA which are commonly used throughout the US (Castro et al., 2011). The results indicate a wide range of 24-hour absorption form 6% to 31%. It should be noticed that the amount of LWA required for internal curing is inversely proportional to its absorption capacity. Thus, a higher absorption is preferred for internal curing.

Table 2.4 Lightweight aggregate absorption at different times

LWA #	Water absorption at 6 h (%)	Water absorption at 24 h (%)	Water absorption at 48 h (%)
1	13.2	16.0	17.6
2	13.1	15.0	16.7
3	25.4	30.5	32.6
4	15.3	17.7	18.4
5	15.6	17.5	18.3
6	12.4	14.1	14.6
7	7.4	10.0	11.1
8	12.9	15.6	16.5
9	12.5	15.0	16.1
10	16.4	19.1	20.5
11	14.9	17.9	19.1
12	15.9	18.9	20.1
13	15.6	18.5	19.4
14	9.9	12.2	13.1
15	5.2	6.0	6.5

For LWA is suitable for internal curing, its absorbed water should be released readily at high relative humidity. The saturated salt solutions method is recommended by ASTM

C1761/C1761M-13b to determine the desorption capacity of LWA for internal curing at 94% relative humidity. Several studies shows that approximately 90% of the 24-hour absorbed water is readily released at high relative humidities (> 93%) for the LWA commonly used in US (Bentz et al., 2005; Radlinska et al., 2008 and Castro et al., 2011). However, it should be mentioned that some undesirable LWA may only release 60% to 70% of adsorbed water (Lura, 2003). Figure 2.7 shows an illustration of desirable and undesirable desorption behavior (Castro et al. 2011). Same as absorption capacity, desorption capacity is also inversely proportional to the amount of LWA required for internal curing. Thus, a higher desorption is preferred.

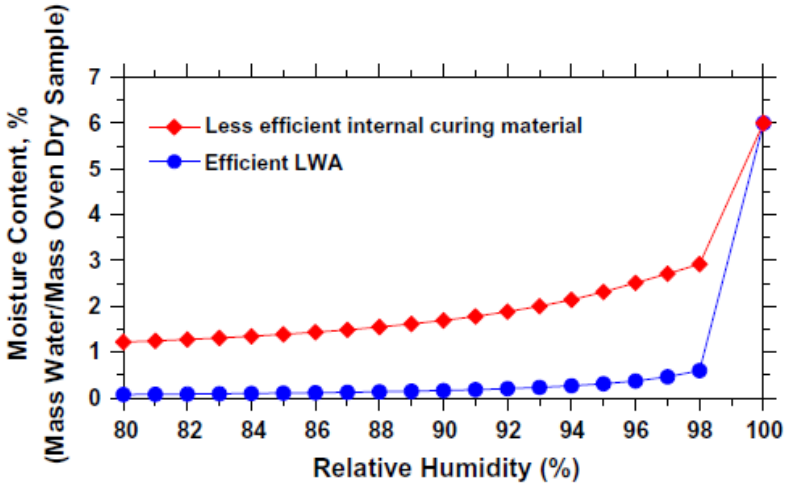

Figure 2.7 Illustration of desirable and undesirable desorption behavior

2.4.4. Spatial distribution of LWA for internal curing

Two remaining questions are how far the adsorbed water can travel from the reservoirs into the cement paste and what fraction of the cement paste can be protected by internal curing? An estimate for the travel distance can be obtained by equating the projected water flow rate to the value needed to maintain saturation in the surrounding cement paste at its current rate of hydration (Weber and Reinhardt, 1999). Supplying reasonable inputs to this equation at early, middle and late age, Bentz et al. (2006) estimated the adsorbed water travel distances shown in Table 2.5.

Several later studies by using neutron and x-ray tomography observed slightly different travel distance (4 mm, 1.8 mm, 3 mm) at early age, however, generally at least few millimeters (Lura et al., 2006; Henkensiefken et al., 2011; Trtick et al., 2011). At later age (28 days and beyond), as the permeability of the cement paste decreases by several orders of magnitude, water movement limits to distances of 100 to 200 μm (Bentz and Snyder, 1999).

Table 2.5 Travel distance of adsorbed water in internal reservoirs

Age	Travel distance (mm)
Early (< 1 day)	20
Middle (1 day to 3 days)	5
Late (3 days to 7 days)	1
Worst Case (> 28 days)	0.25

It is observed that much of the water within the pre-wetted LWA was released during the first 24 hours of hydration (Bentz et al., 2006). Under sealed condition, in the first 3 to 4 hours, both dry lightweight aggregate and pre-soaked aggregate absorb some water from the fresh cement paste, and then, up to 7 hours, very little water movement is observed. The majority of water movement from the lightweight aggregate to the paste occurs between 7 and 11 hours, which corresponds to the rapid rate of hydration and the development of pore pressure (Trtik et al., 2011).

Once an estimate of travel distance has been established, the remaining question concerns the fractions of the cement paste that is protected. This question can be solved by the "Hard Core/Soft Shell Microstructural Model" developed by Bentz et al. (1999). In this model, the user provides the sieve size distribution for the original NWA, the fractional replacement of LWA for NWA for each sieve on a volume basis, and the volume fraction of each aggregate in the mixture to obtain a table of the protected paste volume (0 to 1) as a function of distance from the LWA surfaces. By using this model, Henkensiefken et al. (2009) modeled 16 different mixtures with aggregates of different sizes and sands of different fineness modulus. The results shows that,

assuming same water travel distance, finer aggregates could protect larger fraction of paste than coarse aggregates. When 30% of fine aggregate is replaced on volume basis, if the LWA had a lower fineness modulus, nearly all the paste would be within 2 mm of the LWA surfaces.

2.4.5. Effect of internal curing

2.4.5.1. Effect of internal curing on plastic shrinkage

Since the supply of additional water in lightweight aggregate reduces the magnitude of the capillary stresses that are developed during drying, replacement of normal weight sand with pre-wetted lightweight aggregate can provide a significant reduction of plastic shrinkage cracking. If a sufficient volume of pre-wetted lightweight aggregate is used, plastic shrinkage cracking could even be eliminated (Henkensiefken et al., 2010).

2.4.5.2. Effect of internal curing on autogenous shrinkage

As shown in Figure 2.8, at lower replacement amount of pre-soaked LWA, the autogenous shrinkage of LWA mortar is similar to plain mortar mixture, however, when higher volume replacements are used, after the initial expansion, the mixture remain nearly volumetrically stable (Henkensiefken et al., 2009). Another important feature is that there is no significant improvement of using replacement volumes larger than that is needed to eliminate self-desiccation in sealed system (Henkensiefken et al., 2009).

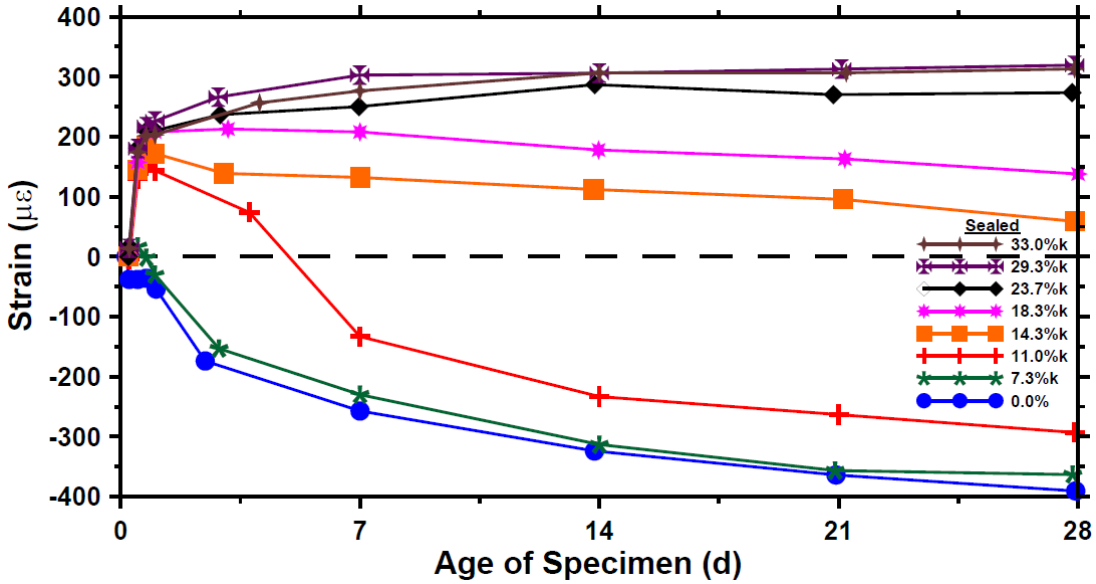

Figure 2.8 Free shrinkage results of mortar mixtures with different LWA replacement volumes in sealed curing condition (Henkensiefken et al., 2009)

Bentz (2007) observed that the application of pre-soaked LWA could provide a significant reduction of autogenous shrinkage in blended cement mortars (SF, FA and slag), while for the SF mortar more pre-soaked LWA are needed to effectively mitigate the autogenous shrinkage.

Golias et al. (2012) reported that when same amount of internal curing water is added, by using a higher amount of oven-dry LWA it is possible to achieve the nearly identical autogenous shrinkage improvement as using pre-soaked LWA.

Using the ASTM C1581 standard (ring test), Henkensiefken (2009) demonstrated that the reduction in autogenous shrinkage resulted in a reduction in cracking as shown in Figure 2.9. At low pre-soaked LWA replacement volume crack happens at early age which is similar to plain mortar, however, as the replacement volumes are increased to a sufficient percentage, the time to cracking is greatly extended. Also, the LWA mortars show a decreasing residual strain at the time of cracking (Henkensiefken et al., 2009).

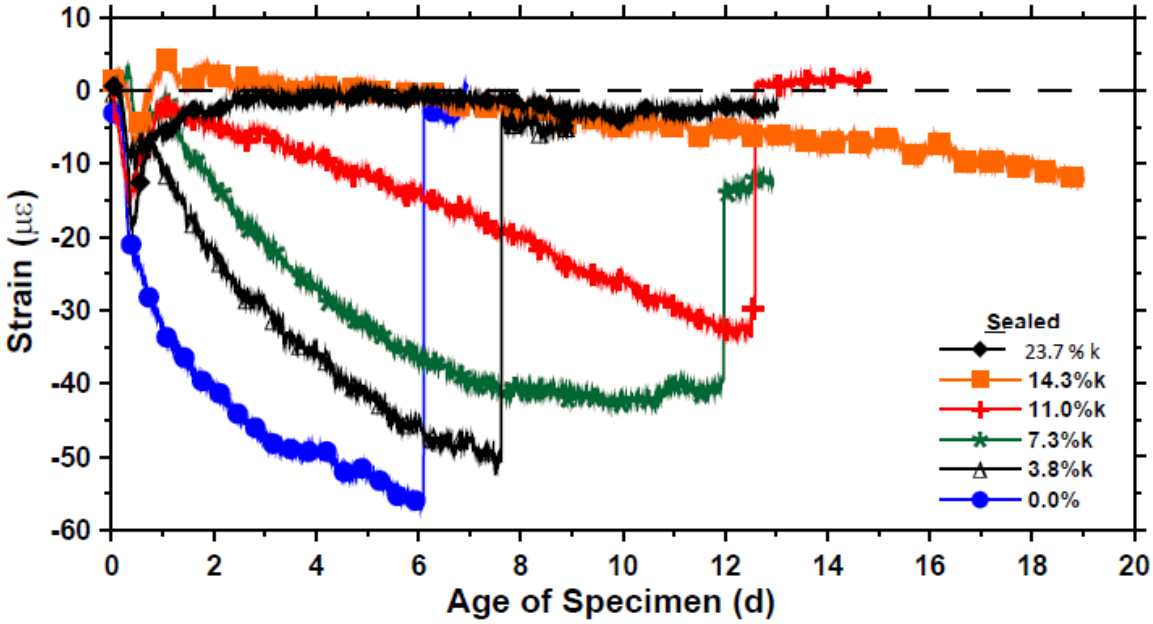

Figure 2.9 Restrained shrinkage results of mortar mixtures with different LWA replacement volumes in sealed curing condition (Henkensiefken et al., 2009)

2.4.5.3. Effect of internal curing on drying shrinkage

As shown in Figure 2.10, Henkensiefken et al. (2009) reported that low replacement volumes of pre-soaked LWA prove to be ineffective in mitigating drying shrinkage caused by the combined effects of external and internal drying, however, when the replacement volume is increased beyond a critical level, the shrinkage is decreased and when even higher replacement volumes are used, the improvements are similar.

Radlinska et al. (2008) also observed that replacing of natural sand with pre-soaked LWA could reduce the early-age shrinkage in unsealed system, however, he indicated that when internal relative humidity reached equilibrium with ambient, the ultimate drying shrinkage of LWA concrete should be comparable with that of the plain concrete, excluding the effect of LWA on the concrete stiffness.

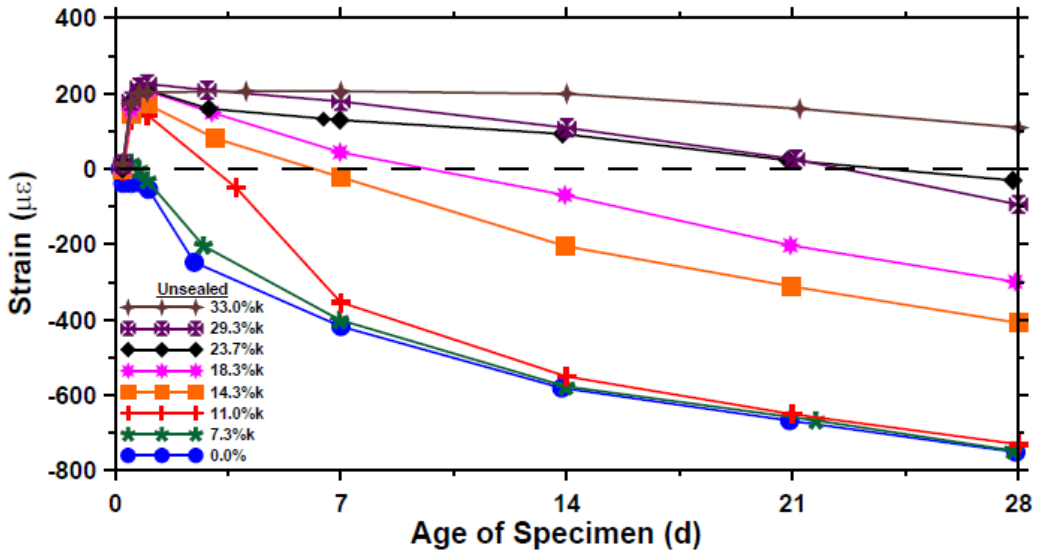

Figure 2.10 Free shrinkage results of mortar mixtures with different LWA replacement volumes in unsealed curing condition (Henkensiefken et al., 2009)

Using the ASTM C1581 standard (ring test), Henkensiefken et al. (2009) reported mortars with low pre-soaked LWA replacement volumes crack at an early age in unsealed system; however as the replacement volume is increased to a sufficient percentage, the time to cracking is greatly extended or cracking is eliminated as shown in Figure 2.11.

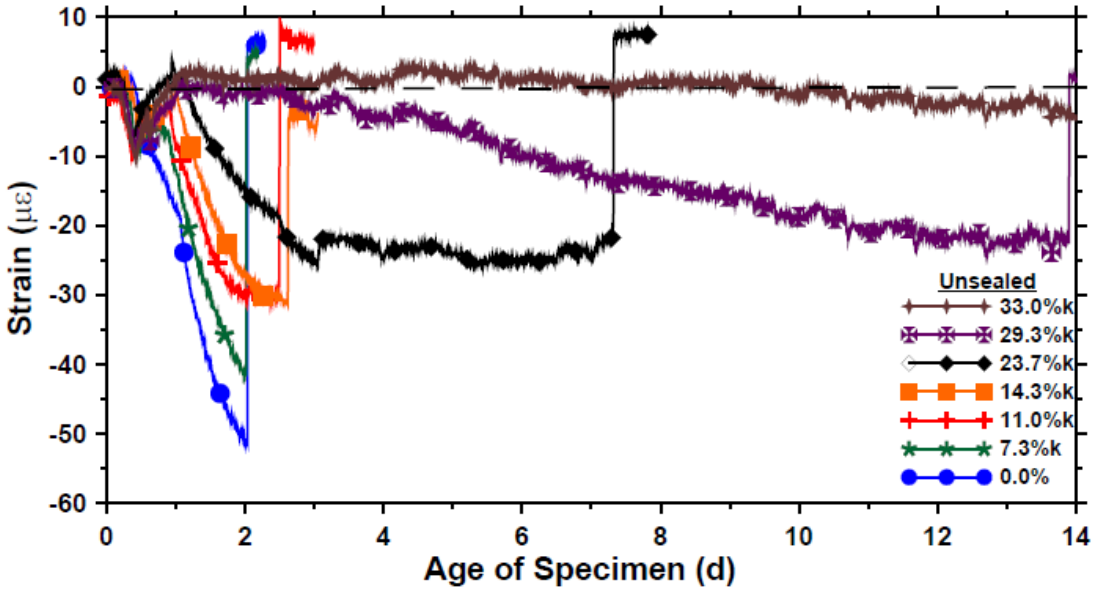

Figure 2.11 Restrained shrinkage results of mortar mixtures with different LWA replacement volumes in unsealed curing condition (Henkensiefken et al., 2009)

2.4.5.4. Effect of internal curing on mechanical properties

The effects of internal curing on elastic modulus, compressive and tensile strength depend on the specific mixture proportions, curing conditions and testing age. A decrease in strength could be observed because LWAs are commonly mechanically weaker than NWAs, however, mixtures with internal curing could also increase strengths and moduli due to an increase in the degree of hydration of the cement. In practice, both increases and decreases in strengths have been observed because these converse effects. Generally, decreases are observed at earlier age while increases are observed at later age (Bentz and Weiss, 2011).

2.4.5.4.1. Compressive strength

Golias et al. (2012b) reported that under water and moist cured conditions, there is no increase in strength associated with the using of pre-soaked LWA, while under sealed and drying conditions, the using of pre-wetted LWA results in higher compressive strength and this improvement is more significant at later age. Bentz (2007) observed around a 10% increase in the compressive strength of blended cement mortars (SF, FA and slag) at later ages. Wasserman and Bentur (1996) indicated that for lightweight aggregates of similar strength, the aggregate of higher absorption will provide higher strength concrete due to its denser interfacial transition zone and lightweight aggregates with pozzolanic reactivity can increase the compressive strength.

However, Zhutovsky et al. (2004) observed that concrete made with pre-soaked LWA have slightly lower strength with and without silica fume. Zhutovsky and Kovler (2012) observed that by internal curing with pre-soaked LWA compressive strength was almost the same at the w/c ratio of 0.33, but reduced by 10% and 4% in mixes with w/c ratio of 0.25 and 0.21, respectively.

2.4.5.4.2. Tensile strength

Shin et al. (2010) reported that the splitting tensile strength of LWA mortars decreases with the increase in the replacement volume of pre-soaked LWA. Golias et al. (2012b) observed that at lower w/c ratio, i.e., 0.3, the splitting tensile strengths of the internally cured samples were lower than the strengths of the plain samples and the reduction of split tensile strength became smaller as the increasing of age, however, at higher w/c ratio, 0.5, the splitting tensile strengths of the internally cured samples were higher than the strengths of the plain samples for samples at all curing conditions (water, moist, sealed and drying).

2.4.5.4.3. Elastic modulus

Golias et al. (2012b) observed that under all curing conditions (water, moist, sealed and drying), the plain samples have a higher elastic modulus than the internally-cured samples. Shin et al. (2010) reported that the elastic modulus decreases with the increase in the replacement volumes of pre-soaked LWA.

2.5. Expansive cement

According to ACI 223R-10, expansive cement is a cement that when mixed with water, produces a paste that, after setting, increases in volume to a significantly greater degree than does Portland cement paste and used to compensate for volume decrease due to shrinkage or to induce tensile stress in reinforcement.

ACI 223R-10 classifies four types of expansive cements: Type K, Type M, Type S and Type G, in which Type K, Type M and Type S expand because of the formation of ettringite while Type G expands due to the formation of calcium hydroxide platelet crystals. The component of each expansive cement is listed following:

Type K: a mixture of Portland cement, anhydrous tetracalcium trialuminate sulfate (ye'elimite), calcium sulfate, and lime.

Type M: a mixture of Portland cement, calcium-aluminate cement, and calcium sulfate.

Type S: a mixture of Portland cement, tricalcium aluminate, and calcium sulfate.

Type G: a mixture of Portland cement, calcium oxide and alumina.

2.5.1. Hydration of calcium sulfoaluminate cement

Calcium sulfoaluminate (CSA) cement is produced by grinding CSA clinker, which has $C_4A_3\bar{S}$, C_2S and Al rich ferrite as its major minerals, together with added gypsum ($C\bar{S}H_2$) (Zhang and Glasser, 2002). The following reactions are suggested taking place during hydration of CSA cement (Mehta and Klein, 1966; Collepardi et al., 1972):

$$C_4A_3\bar{S} + 18H \rightarrow C_3A \cdot C\bar{S} \cdot 12H + 2AH_3$$

$$C_4A_3\bar{S} + 2CSH_2 + 34H \rightarrow C_3A \cdot 3C\bar{S} \cdot 32H + 2AH_3$$

$$C_4A_3\bar{S} + 6CH + 8CSH_2 + 74H \rightarrow 3C_3A \cdot 3C\bar{S} \cdot 32H$$

$$C_2S + H \rightarrow \text{C-S-H}$$

where $C = CaO, A = Al_2O_3, \bar{S} = SO_3, S = SiO_2, H = H_2O$.

According to the aforementioned equations, the possible hydration products are $C_3A \cdot C\bar{S} \cdot 12H$ (monosulfoaluminate), $C_3A \cdot 3C\bar{S} \cdot 32H$ (ettringite), C-S-H and amorphousAH_3. It is shown that Equation 5.1 does not lead to expansion while Equation 5.2 and 5.3 result in expansion due to the formation of ettringite (Mehta, 1967). Thus, the presence of calcium sulfate is critical for expansion since it leads to the formation of ettringite. Moreover, compared to Equation 5.2, Equation 5.3, as calcium hydroxide presents, produces more ettringite. Therefore, the presence of calcium hydroxide is also of great importance to the expansion of CSA cement.

2.5.2. Theories of expansion

The expansion behavior related to the ettringite formation in expansive cement has been widely studied but the mechanisms of expansion are still not fully understood. A variety of mechanisms of expansion are proposed. Most of their arguments is that the expansion is associated with ettringite formation. Several theories are summarized below.

Increase of solid volume: The simplest way used to explain expansion is that the formation of ettringite leads to an increase of solid volume (Polivka, 1973). However, in portland cement there is a similar increase in volume solid while there is no expansion in practice. Furthermore, Mehta (1972) indicated that when the reactants are converted into ettringite, instead of the volume increase of solid, there should be 7-8% reduction in the total volume.

Swelling of colloidal ettringite: Mehta (1973) reported that in the presence of lime the ettringite is colloidal, and not long lath-like crystals. The colloidal ettringite is able to adsorb water molecules which could cause interparticle repulsion, thus causing an expansion of the system. Mehta and Hu (1978) observed a direct relation between the mass gain of adsorption and the expansion of samples. However, found that this swelling force is weak and does not contribute much to expansion. Furthermore, Bizzozero (2014) indicated that when lime is absent the expansion also could occur.

Crystallization pressure: In 150 years ago, Lavalle (1853) observed that crystals growing from their solutions were pushed upward during growth by precipitation of matter on their bottom (Steiger, 2005). Later, Becker and Day (1905) found that a growing alum crystal submerged in a saturated solution could not only lift itself but even a substantial additional load (Steiger, 2005).

Based on this theory, in order to generate crystallization pressure, the crystal must grow from a supersaturated solution (Steiger, 2005). The saturation index (SI) is defined by the following equation (Bizzozero, 2014):

$$SI = \log_{10}\left(\frac{K}{K_{sp}}\right)$$

where, K is the ion activity product and K_{sp} is the solubility product of a given phase.

The formation of ettringite are:

$$6Ca^{2+} + 2Al(OH)_4^- + 4OH^- + 3SO_4^{2-} + 26H_2O \rightarrow Ca_6[Al(OH)_6]_2 \cdot 3SO_4 \cdot 26H_2O$$

Thus, K for ettringite formation is:

$$K = (\alpha_{Ca^{2+}})^6 \cdot \left(\alpha_{Al(OH)_4}\right)^2 \cdot (\alpha_{OH^-})^4 \cdot \left(\alpha_{SO_4^{2-}}\right)^3 \cdot \left(\alpha_{H_2O}\right)^{26}$$

where, α is the activity.

Supersaturation provides the driving force for the development of crystallization pressure (P_c) and the corresponding expansion. For crystals growing in large pores above 0.1-1μm where the size effects are negligible, the crystallization pressure could be calculated using following equation (Steiger, 2005; Bizzozero, 2014):

$$P_c = \frac{RT}{v_m}\ln\left(\frac{K}{K_{sp}}\right)$$

where, R is the universal gas constant (8.314 J/mol K), T (K) is the thermodynamic temperature and v_m is the molar volume of the crystal.

For crystals growing in small pores, which is below 0.1-1μm, where the size effects are relevant, it is important to consider the interfacial free energy of the crystal-liquid interface. The equation for small pores is shown following (Steiger, 2005; Bizzozero, 2014):

$$\Delta P = P_c - P_w = \frac{RT}{v_m}\ln\left(\frac{K}{K_{sp}}\right) - \gamma_{CL}\frac{2}{r_p - \delta}$$

where, ΔP is the net crystallization pressure, P_w is the pressure which is relevant to the size effects for pores below 0.1-1μm, γ_{CL} is the interfacial free energy between the crystal and the liquid, r_p is the radius of the pores and δ (estimated to be 1-2 nm) is the thickness of a film of solution between the crystal and the pore wall.

The aforementioned equation takes both the effects of a supersaturated crystal growing in a small pore and generating a positive pressure on it and of the curvature of crystal-liquid interface generating a negative pressure opposing its growth into account resulting in a net crystallization pressure ΔP (Bizzozero, 2014).

CHAPTER 3

TESTING METHODS

3.1. Introduction

In this chapter, the testing methods that used in this research are described which include unrestrained autogenous and drying deformation of mortar specimens, unrestrained deformation of concrete specimens, restrained deformation of concrete specimens with CSA cement, method to stop cement hydration, thermogravimetric analysis (TGA), X-ray diffraction (XRD), dynamic modulus, absorption test and desorption test.

3.2. Unrestrained autogenous deformation of mortar specimens

3.2.1. Corrugated tubes

The autogenous deformations of mortar specimens by using corrugated tubes were measured according to ASTM C1698. Two specimens were prepared for each mix. The molds consist of corrugated plastic tubes, having a length of 420 ± 5 mm and an outer diameter of 29 ± 0.5 mm. The mold is tightly closed with two tapered end plugs having a length of 19 ± 0.5 mm and a diameter from 21 ± 0.1 mm to 22.4 ± 0.1 mm. The length change of the corrugated tubes were monitored with a dilatometer. The testing setup is shown in Figure 3.1. The length change started being recorded at the time of final setting which was determined according to ASTM C403. The corrugated mold transforms volumetric deformations into linear deformations when the paste is in a fluid state because the mold has a greater stiffness in the radial direction than it does in the longitudinal direction (Sant et al., 2006). The restraint force is very small. According to Jensen (1996), a maximum restraint force of 0.5 N (corresponding to a stress of 0.001 MPa) on the paste was measured for a deformation of 10,000 μstrain (Lura, 2003). The molds were watertight: water

loss from a tube filled with water kept at 20ºC and RH close to 0% for one week was about 0.04 g, corresponding to 0.03% of the water content (Jensen, 1996; Lura, 2003).

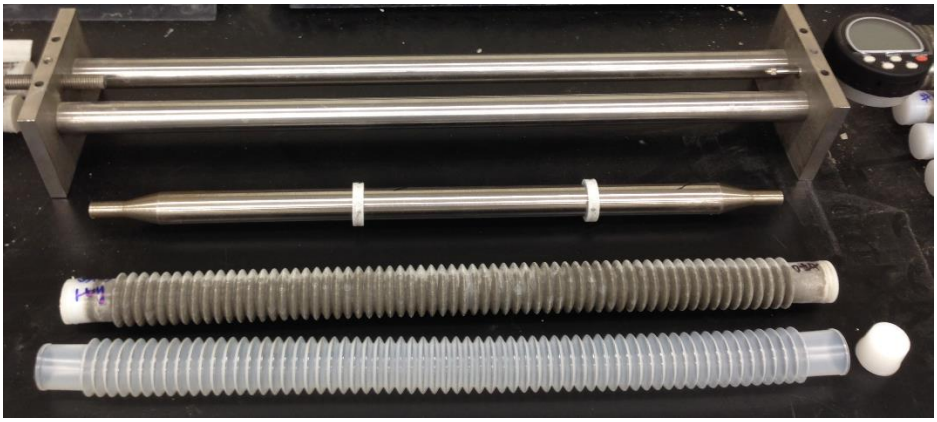

Figure 3.1 Dilatometer and corrugated tubes

3.2.2. Sealed prisms

The autogenous deformations of mortar specimens by using sealed prisms were measured according to ASTM C157. Two prisms of the size of 1 in (25 mm) × 1 in (25 mm) × 11.25 in (285 mm) were prepared for each mix. The samples were demolded at the age of 24±0.5 h after the addition of water to the cement during the mixing. These two prisms were wrapped properly with aluminum tape on all sides as shown in Figure 3.2. The first reading was took right after demolding. After the initial comparator reading, the sealed specimens were stored in environment-controlled room at 25 ± 2ºC and 50 ± 3 % RH. The length change was determined at various ages according to ASTM C490. The length change before 24 hours from corrugated tubes was added to the measurements of sealed prisms. The length comparator is shown in Figure 3.3. The weight of specimens was also measured at each age to the nearest of 0.1 g in order to monitor the moisture loss.

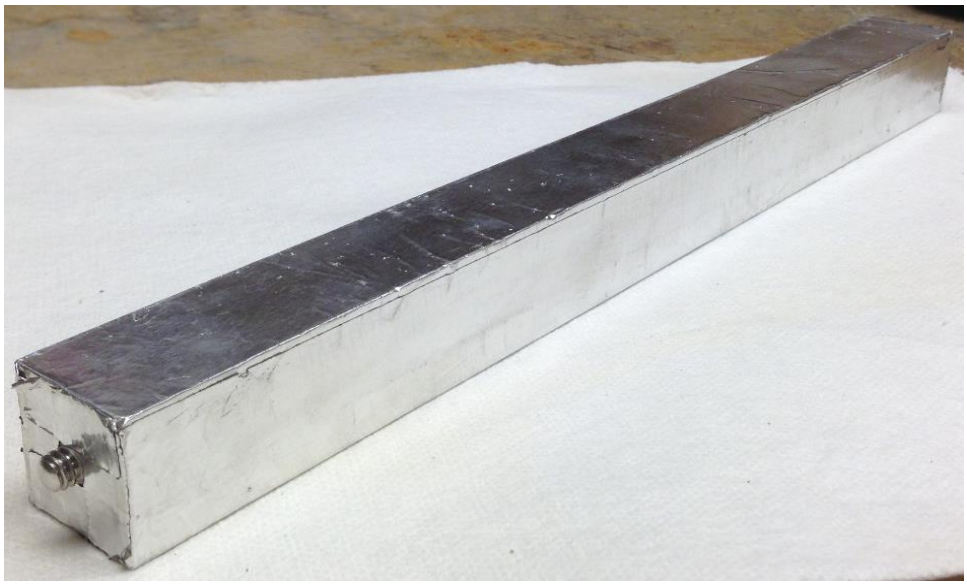

Figure 3.2 Sealed mortar prism

Figure 3.3 Length comparator

3.3. Unrestrained drying deformation of mortar specimens

3.3.1. Unsealed prisms

The drying deformations of mortar specimens by using unsealed prisms were measured according to ASTM C157. Two prisms of the size of 1 in (25 mm) × 1 in (25 mm) × 11.25 in (285 mm) were prepared for each mix. The samples were demolded at the age of 24±0.5 h after the addition of water to the cement during the mixing. The first reading was took right after demolding. After the initial comparator reading, the specimens were stored in lime-saturated water until the age of 7 days. After that, the unsealed prisms were exposed to air at 25 ± 2ºC and 50 ± 3 % RH. These two prisms were not wrapped on any sides as shown in Figure 3.4. The length change was determined at various ages according to ASTM C490. The length change before 24 hours from corrugated tubes was added to the measurements of unsealed prisms. The weight of specimens was also measured at each age to the nearest of 0.1 g in order to monitor the moisture loss.

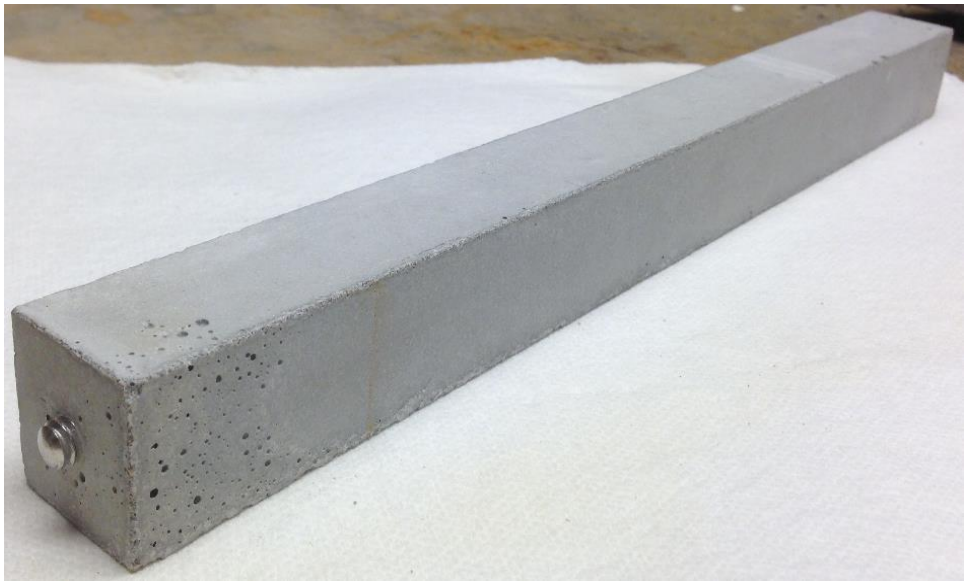

Figure 3.4 Unsealed mortar prism

3.4. Unrestrained deformation of concrete specimens

3.4.1. Sealed prisms for autogenous deformation

The autogenous deformations of concrete specimens by using sealed prisms were measured according to ASTM C157. Two prisms of the size of 3 in (75 mm) × 3 in (75 mm) × 11.25 in (285 mm) were prepared for each mix. These two prisms were wrapped properly with aluminum tape on all sides as shown in Figure 3.5. The curing method and the length measurement method are the same as discussed in the section of 3.2.2. The weight of specimens was also measured at each age to the nearest of 0.1 g in order to monitor the moisture loss.

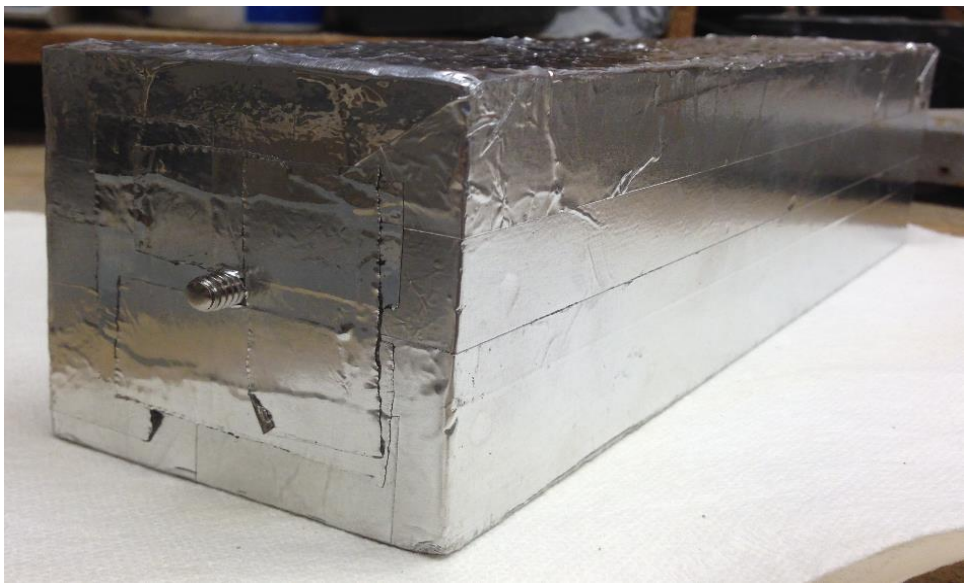

Figure 3.5 Unrestrained sealed concrete prism

3.4.2. Unsealed prisms for drying deformation

The drying deformations of concrete specimens by using unsealed prisms were measured according to ASTM C157. Two prisms of the size of 3 in (75 mm) × 3 in (75 mm) × 11.25 in (285 mm) were prepared for each mix. These two prisms were not wrapped on any sides as shown in Figure 3.6. The curing method and the length measurement method are the same as discussed in

the section of 3.3.1. The weight of specimens was also measured at each age to the nearest of 0.1 g in order to monitor the moisture loss.

Figure 3.6 Unrestrained unsealed concrete prism

3.5. Restrained deformation of concrete specimens with CSA cement

3.5.1. Unsealed prisms for drying deformation

The drying deformations of concrete specimens by using restrained unsealed prisms were measured according to ASTM C878. The molds were the same as those used for unrestrained prisms of the size of 3 in (75 mm) × 3 in (75 mm) × 11.25 in (285 mm). The restrained cage consists of a threaded low-carbon steel rod of the length of 10 in (250 mm) with steel end plates of the size of 3 in (75 mm) × 3 in (75 mm) and held in place by hex nuts. The molds and restrained cage are shown in Figure 3.7. Four restrained prisms were prepared for each mix. Two of the four prisms were demolded at the age of 6±0.5 h and the other two were demolded at the age of 24±0.5 h after the addition of water to the cement during the mixing. The first reading was took right after demolding. After the initial comparator reading, the specimens were stored in lime-saturated water until the age of 7 days. After that, the unsealed prisms were exposed to air at 25 ± 2ºC and 50 ± 3

% RH. These prisms were not wrapped on any sides as shown in Figure 3.8. The length change was determined at various ages according to ASTM C490. The weight of specimens was also measured at each age to the nearest of 0.1 g in order to monitor the moisture loss.

Figure 3.7 Mold and restrained cage for restrained concrete prisms

Figure 3.8 Restrained unsealed concrete prism

3.5.2. Sealed prisms for autogenous deformation

The autogenous deformations of concrete specimens by using restrained sealed prims were measured according to ASTM C878. Two restrained prisms were prepared for each mix. The prisms were the same as discussed in section of 3.5.1. The samples were demolded at the age of 24±0.5 h after the addition of water to the cement during the mixing. These two prisms were wrapped properly with aluminum tape on all sides as shown in Figure 3.9. The first reading was took right after demolding. After the initial comparator reading, the sealed specimens were stored in environment-controlled room at 25 ± 2ºC and 50 ± 3 % RH. The length change was determined at various ages according to ASTM C490. The length change between 6 to 24 hours from restrained unsealed prisms was added to the measurements of restrained sealed prisms. The weight of specimens was also measured at each age to the nearest of 0.1 g in order to monitor the moisture loss.

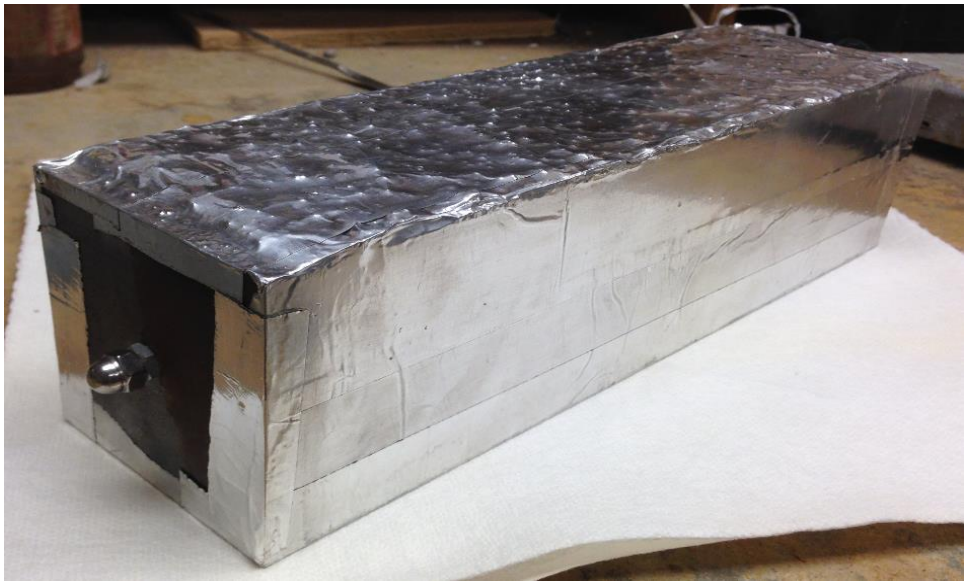

Figure 3.9 Restrained sealed concrete prism

3.6.Method to stop cement hydration

In this study, in order to explain the expansion behavior, the consumption of ye'elimite and formation of ettringite were tracked at various ages. Therefore, hydration of cement was arrested at the certain age. The method used in this study is solvent exchange method. A detailed review could be found in Zhang and Scherer (2011). The solvent exchange method was chosen because its minimum effect on the properties of sample. However, it should be noticed that a possibility that this method may cause some dehydration of ettringite and C-S-H (Zhang and Scherer, 2011). It is believed that the results should be comparable if the same method is used for all samples. First, the rounded slices of 2-3mm thick and 25 mm diameter were cut and immersed into the isopropyl alcohol for at least 24 hours. After that, the rounded slices were kept in a vacuum desiccator with drierite for at least 24 hours. Finally, the dried slices were grounded into very fine powder passing through 45 μm (325 No.) sieve.

3.7.Thermogravimetric analysis (TGA)

Thermogravimetric analysis was performed on powdered samples prepared with the method discussed in the section of 3.6. The type of thermogravimetric analyzer used in this study is Q50-TA Instrument. The samples were heated up to 900 ºC at the rate of 15 ºC per minute in a nitrogen environment.

3.8.X-ray diffraction (XRD)

X-ray diffraction analysis was performed on a powered samples prepared with the method discussed in the section of 3.6. The type of x-ray diffraction system used in this study is Siemens-

Bruker D5000. A quartz sample holder was used to minimize the background noise. The samples were scanned in the range of 5º to 25º with 0.02 increment and 0.4 deg/min scan speed.

3.9. Dynamic modulus

The dynamic modulus was measured according to ASTM C215. Three prisms were prepared of the size of 40 mm × 40 mm × 150 mm for each mix which is shown in Figure 3.10. The specimens were demolded at the age of 24±0.5 hours after the addition of water to cement during mixing. The first reading was took right after demolding. After that, specimens were cured in lime-saturated water until 7 days. Longitudinal resonant frequency was measured to calculate the dynamic modulus.

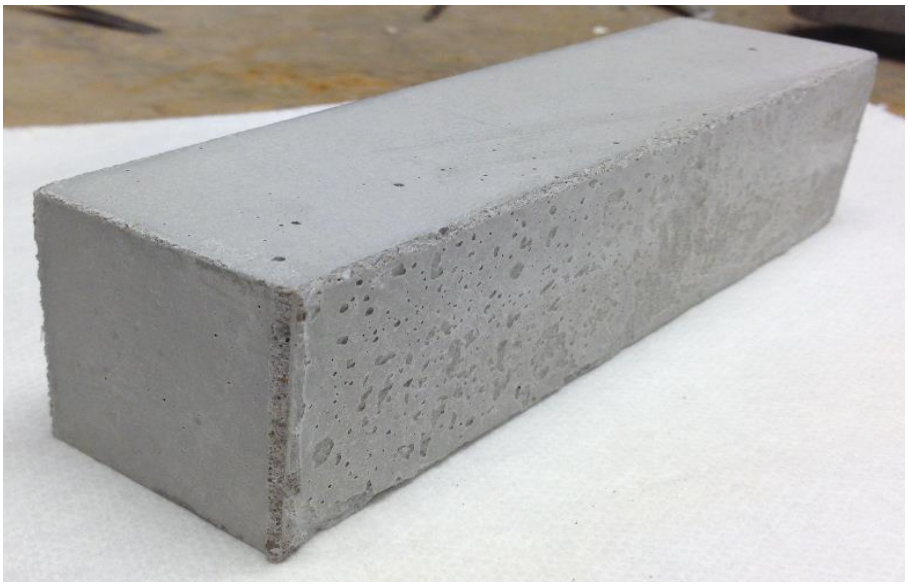

Figure 3.10 Prism for dynamic modulus test

3.10. Absorption test

The absorption test was conducted according to ASTM C128. Test samples were dried in the oven for 24 hours and cooled down to room temperature. The cooled samples were covered with water and stand for a required amount of time which depends on the absorption for how long

was tested. After that, the wetted particles were spread on a flat glass plate and exposed to a gently moving current of warm air. The particles were stirred frequently to guarantee homogeneous drying. The surface moisture was tested at frequent intervals by using cone method until the samples reached a surface-dry condition. A certain amount of surface-dry sample was dried in the oven for 24 hours. The weight of surface-dry sample and oven-dried sample were recorded. The absorption was calculated as follows:

$$\text{Absorption}, \% = \frac{\text{S} - \text{A}}{\text{A}} \times 100$$

where A is the mass of oven dry sample (g), S is the mass of saturated surface-dry sample (g).

3.11. Desorption test

The desorption test was conducted according to ASTM C1761. A specimen of lightweight aggregate in the surface-dry condition was obtained using the method mentioned in section 3.10. Approximately 25 g of specimens were weighed out. The mass of the empty weighing pan and the mass of weighing pan and surface-dry aggregate were recorded to the nearest 0.01 g. The pan with test specimen was placed in the controlled relative humidity environment. The controlled relative humidity environment was provided by supersaturated solution. The relative humidity of 94%, 85% and 75% were obtained by preparing the supersaturated solution of potassium nitrate, potassium chloride and sodium chloride. The supersaturated solutions were placed into desiccators with tight-fitting lids as shown in Figure 3.11. The mass of the specimens were measured on a daily basis until equilibrium was reached. The equilibrium was defined as when there was not more than 0.01 g change in mass in a 24-hour period. The equilibrium mass was measured to the nearest 0.01 g. After equilibrium was achieved, the specimens were placed into the drying oven for at least 24 hours. The oven-dried mass was measured to the nearest 0.01 g. The desorption was calculated as follows:

$$\text{Desorption}, \% = \frac{M_{SSD} - M_E}{M_{SSD} - M_{OD}} \times 100$$

where, M_{SSD} is the mass of surface-dry aggregate (g), M_E is the equilibrium mass of aggregate at a relative humidity (g), M_{OD} is the mass of oven-dry aggregate (g).

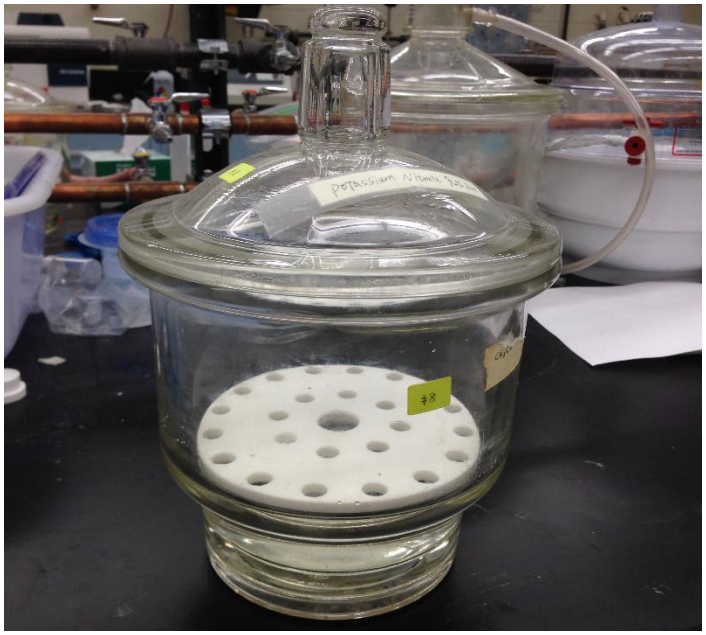

Figure 3.11 Desiccator with supersaturated solution

CHAPTER 4

LENGTH CHANGE OF ORDINARY PORTLAND CEMENT (OPC) MORTAR WITH PRE-SOAKED LIGHTWEIGHT AGGREGATES

4.1. Introduction

The objective of this chapter is to investigate the effects of the dosage of pre-soaked LWA, w/c ratio and soaking time of LWA on the deformation of ordinary Portland cement (OPC) mortar with pre-soaked lightweight aggregates.

In this chapter, the measured deformations of ordinary Portland cement (OPC) mortar specimens with pre-soaked lightweight aggregate under both sealed and unsealed conditions are presented and discussed. Eight mixtures at 0.34 or 0.44 w/c ratio and with 0%, 7%, 14% or 21% LWA-OT, which is a manufactured expanded blast furnace slag, replacement were prepared and cured under sealed or unsealed conditions. An extra mixture with the LWA-OT pre-soaked for a longer period of time (7 days) was prepared and cured under sealed or unsealed conditions.

4.2. Materials, mixture proportioning and mixing procedure

ASTM C150 Type I ordinary Portland cement (OPC) was used with a Blaine fineness of 423 m^2/kg and estimated Bogue composition of 59% C_3S, 12% C_2S, 10% C_3A, 7% C_4AF and a Na_2O equivalent of 0.28%, all by mass fraction.

A high-range water-reducing admixture (HRWRA) was added in varying dosages depending on the volume fractions of LWA replacing normal-weight sand and the w/c ratios. For a w/c ratio of 0.34, HRWRA was added at a dosage in the range of 8 to 10 fl oz/cwt. For a w/c ratio of 0.44, HRWRA was added at a dosage in the range of 2 to 3 fl oz/cwt. Different dosages were used to keep fair and similar consistencies of the mixtures.

The normal weight sand used was natural river sand with a specific gravity of 2.60. Parts of the normal weight sand were replaced LWA-OT, with a specific gravity of 1.88. The 24-hour absorption of the normal weight sand and LWA-OT were measured to be 1.7% and 15.0% by mass, respectively, according to ASTM C128. The absorption isotherms and desorption isotherms for LWA-OT is shown in Figure 4.1 and Figure 4.2, respectively.

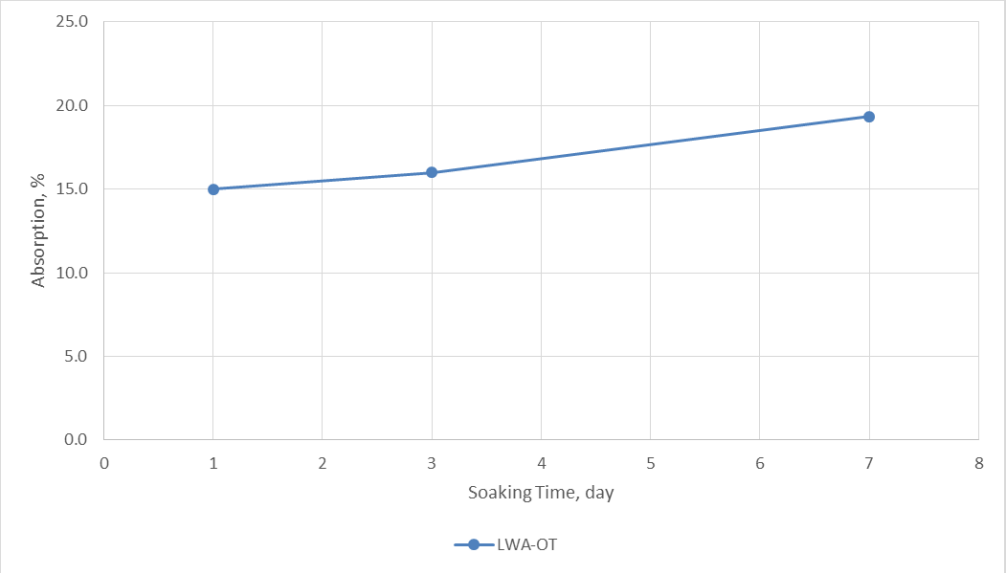

Figure 4.1 Absorption isotherm of LWA-OT

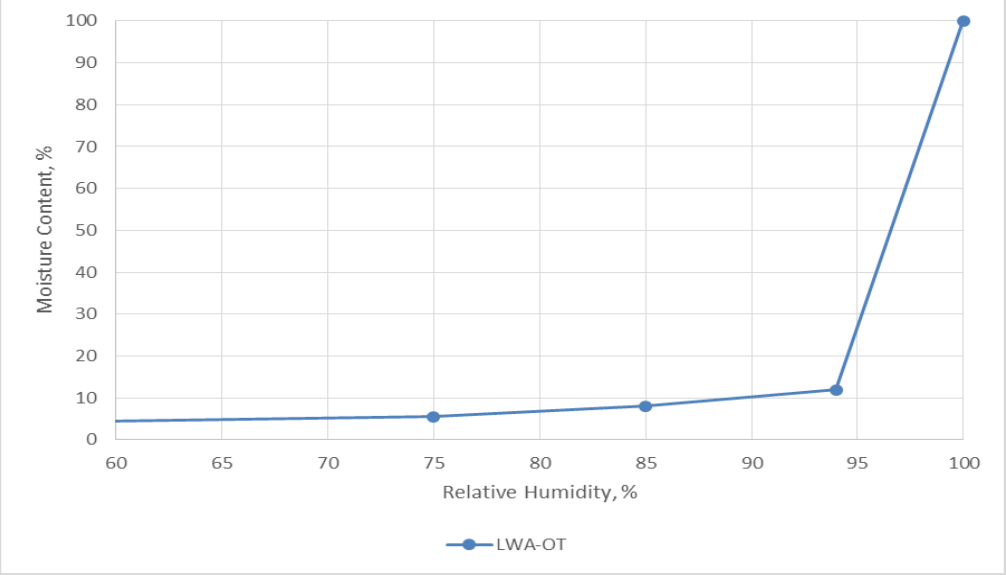

Figure 4.2 Desorption isotherm of LWA-OT

Four different mixtures were prepared with an effective w/c of 0.34 and 0.44, respectively. Effective w/c ratio indicates the w/c ratio that is calculated based on only the mixing water without considering the additional water provided by pre-soaked LWA. The four mixtures at each w/c ratio includes a plain mixture with 0% LWA-OT and three mixtures with 7%, 14% and 21% of normal weight sand replaced by saturated LWA-OT. It should be mentioned that replacements were on a total volume basis. The volume of aggregate (normal weight sand and LWA) was maintained constant at 55% since only the sand was replaced with LWA-OT. The mixture proportions are shown in Table 4.1.

Table 4.1 Mixture proportions of ordinary Portland cement mortar with LWA-OT

Materials	0.34 w/c				0.44 w/c			
	0% LWA	7% LWA	14% LWA	21% LWA	0% LWA	7% LWA	14% LWA	21% LWA
OPC (lbs/yd^3)	1154	1154	1154	1154	1002	1002	1002	1002
Water (lbs/yd^3)	433	428	422	417	481	476	471	466
OD sand (lbs/yd^3)	2371	2069	1767	1466	2371	2069	1767	1466
SSD LWA (lbs/yd^3)	0	222	444	666	0	222	444	666

The mixing procedure used was in accordance with ASTM C305. The LWA was oven dried, air cooled, and then mixed thoroughly with the amount of water corresponding to a 24-hour absorption period. The wetted LWA was kept sealed for at least 24 hours before being used.

4.3. Results and discussion

4.3.1. Effects of the dosage of pre-soaked lightweight aggregate

The measured autogenous deformations for mortar specimens from corrugated tubes and sealed prisms are provided in Figure 4.3 and Figure 4.4, respectively. The deformations of

corrugated tubes were measured from the moment of final setting, which was determined by penetration resistance test. The deformation measurements for the sealed prisms started at 24 hours and the deformation data up to 24 hours from corrugated tubes tests were added to them.

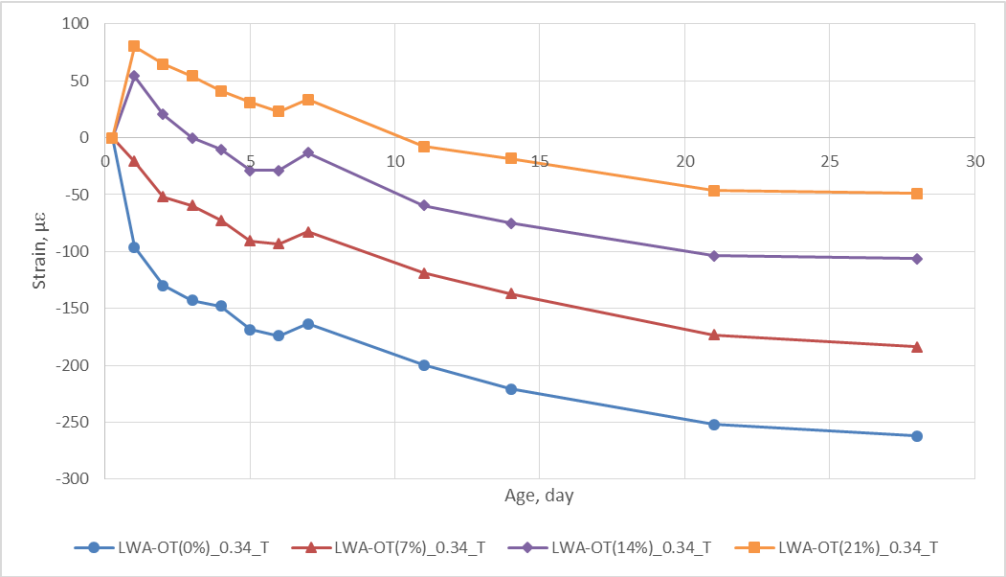

(a)

Figure 4.3 Deformation for mortar specimens from corrugated tubes at: (a) 0.34 w/c; (b) 0.44 w/c

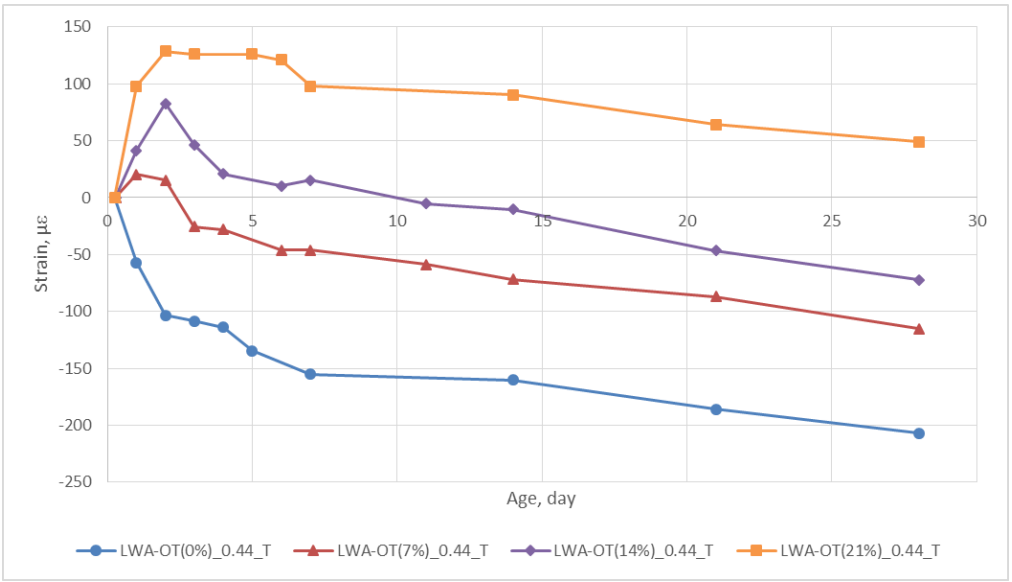

(b)

Figure 4.3 (cont.)

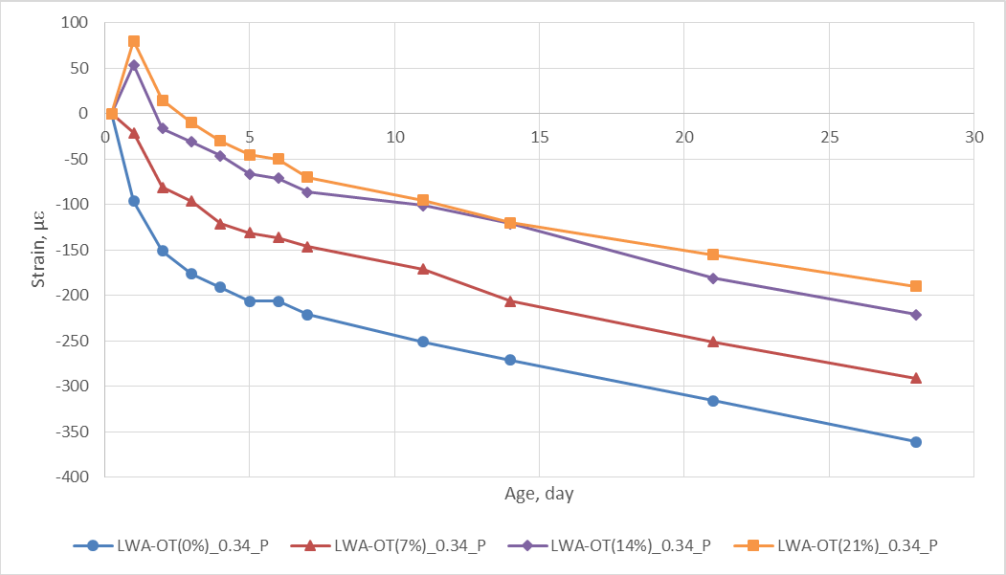

(a)

Figure 4.4 Deformation for mortar specimens from sealed prisms at: (a) 0.34 w/c; (b) 0.44 w/c

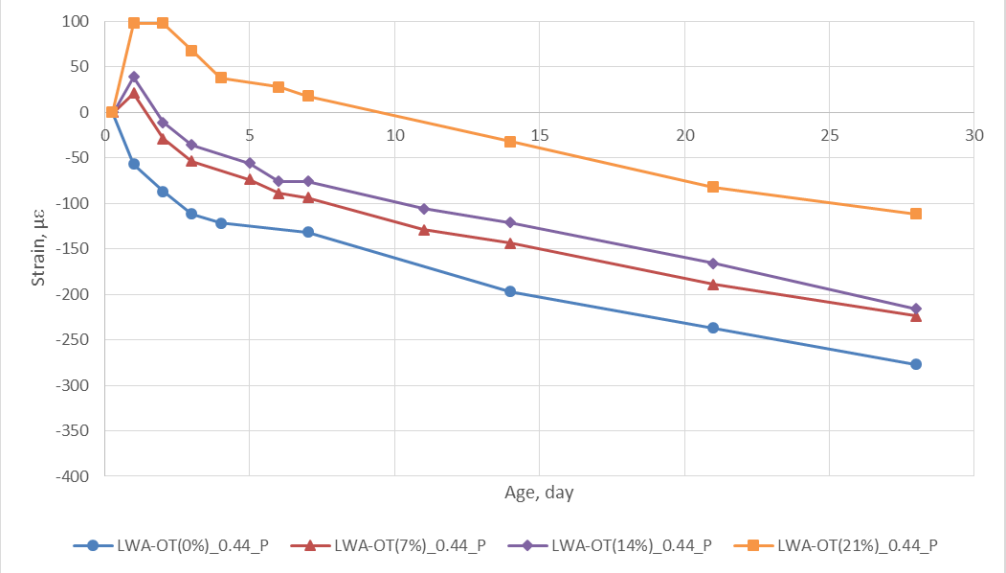

(b)

Figure 4.4 (cont.)

It was shown that for both sealed prisms and corrugated tubes and at both w/c ratios, the total shrinkage decreased as the dosage of the LWA-OT increased. This was expected because higher dosage of pre-soaked LWA could provide an even higher amount of extra water and, thus, could maintain a higher internal relative humidity of the specimens and for a longer time (Henkensiefken et al., 2009; Radlinska et al. 2008). Henkensiefken (2008) also explained this

phenomenon by measuring the critical pore size of Laplace equation (section 2.3.3.1) with mercury intrusion porosimetry (MIP). It was found that addition of pre-soaked LWA increased the critical pore size, which, in turn, minimized the self-desiccation and shrinkage. Additionally, the early-age expansion increased with the increase of LWA-OT dosage. This trend may be related to reduction in stiffness and increased hydration due to the addition of LWA.

By comparing the results of sealed prisms and corrugated tubes, some deviations were observed between them. The shrinkage of corrugated tubes were always smaller than that of the sealed prisms. However, the similar results were expected because both tests were designed to monitor autogenous shrinkage. One possible reason is that the drying shrinkage due to the small amount of water loss of sealed prisms cannot be neglected. To verify this explanation, an extra test was conducted. A mixture with a w/c ratio of 0.44 and 0% LWA was prepared, whereas besides the specimens of corrugated tubes and sealed prisms, extra double-sealed prisms were cast by sealing the sealed prisms with two more layers of Ziploc bags. The specimens are shown in Figure 4.5. The measured results are presented in Figure 4.6. It can be observed that at a very early age, the length change of double-sealed prisms were very close to that of corrugated tubes, which were assumed to have no water loss according to Jensen (1996) and Lura (2003). However, as time elapsed, the length change of double-sealed prisms deviated from that of corrugated tubes and eventually became larger than that of the tubes but still smaller than that of the sealed prisms. Comparing the aforementioned trend of length change with the weight loss for three types of specimens shown in Table 4.2, a good match could be found. Thus, it is believed that the drying shrinkage due to those small amount of water loss from sealed prisms caused the deviations. Also, it indicates that the deformation of sealed prisms is not only autogenous shrinkage but also with some amount of drying shrinkage.

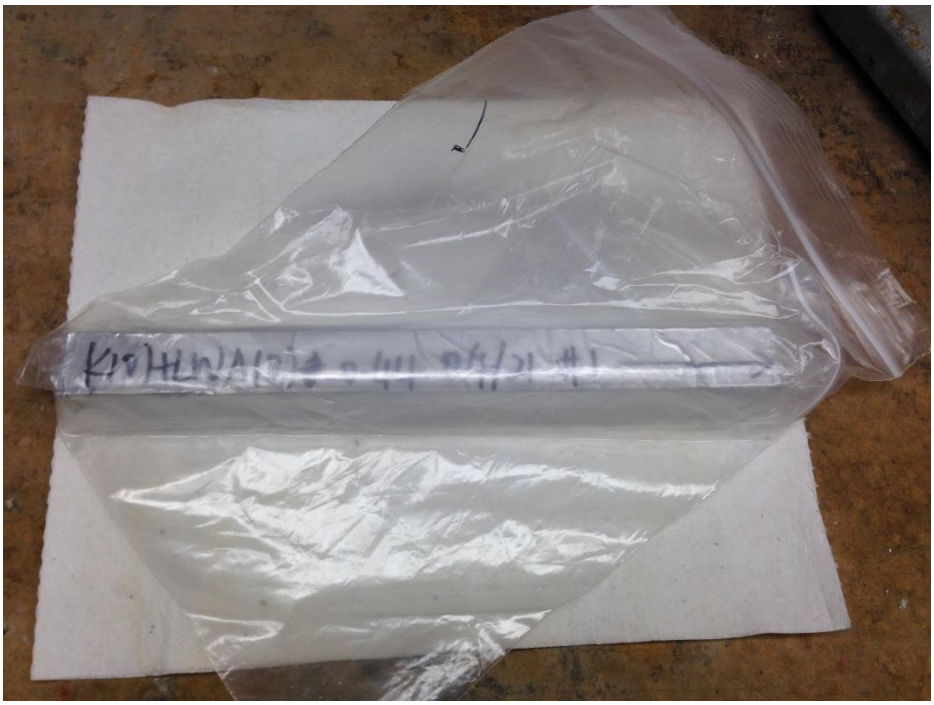

Figure 4.5 Double-sealed prisms

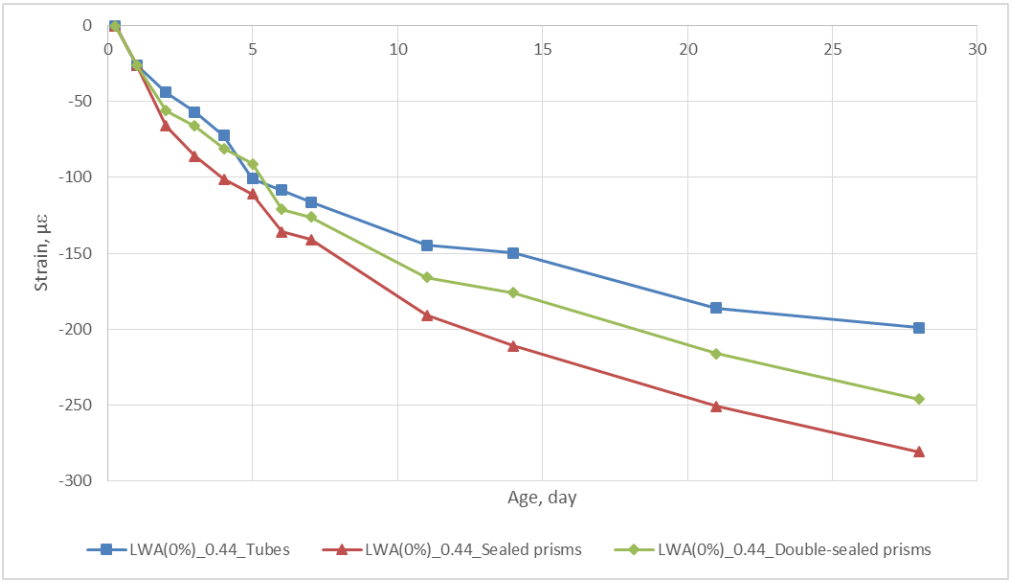

Figure 4.6 Comparison of the deformations of corrugated tubes, sealed prisms and double-sealed prisms

Table 4.2 Weight loss of corrugated tubes, sealed prisms and double-sealed prisms at different ages

Age	Sealed prisms, %	Double-sealed prisms, %
1	0	0
2	0.035	0.023
3	0.057	0.023
4	0.069	0.023
5	0.080	0.034
6	0.103	0.034
7	0.103	0.034
11	0.149	0.080
14	0.161	0.092
21	0.195	0.092
28	0.241	0.126

The measured deformations for unsealed mortar prisms at both w/c ratios are shown in Figure 4.7. The deformations before 24 hours were from corrugated tubes tests. It is shown that for the first 24 hours, the specimens with pre-soaked LWA-OT expanded while the plain specimens shrunk. After the first 24 hours, all the unsealed specimens kept expanding when cured under lime-saturated water until 7 days. The expansion increased as the dosage of the pre-soaked LWA-OT increased. However, after a 7-day curing period, when the unsealed prisms were exposed in air, it was shown that for both w/c ratios, the length change of all unsealed prisms were very close at 28 days. It seemed like the addition of pre-soaked LWA-OT did not influence the shrinkage behavior under unsealed condition. However, the reverse trend was observed when the expansion during the lime saturated water curing for the first 7 days was discarded and only the drying shrinkage after 7 days was considered. As shown in Figure 4.8, for both w/c ratios, the unsealed prisms with more addition of LWA showed larger drying shrinkage after 7-day curing. This trend is more obvious at lower w/c ratio.

One possible explanation for this phenomenon is as follows:

Based on Mackenzie-Bentz equation (section 2.3.3.1), capillary pressure and stiffness of specimens are two main factors that affect the shrinkage but function in opposite directions. Capillary pressure is the driving force for shrinkage while stiffness is the resistant force. The shrinkage behavior depends on the interaction of these two factors. In the aforementioned case, under exposed conditions the benefit of adding pre-soaked LWA on maintaining higher internal RH, which is proportional to capillary pressure, is less pronounced while the addition of LWA reduced the modulus of specimens and lead to larger shrinkage.

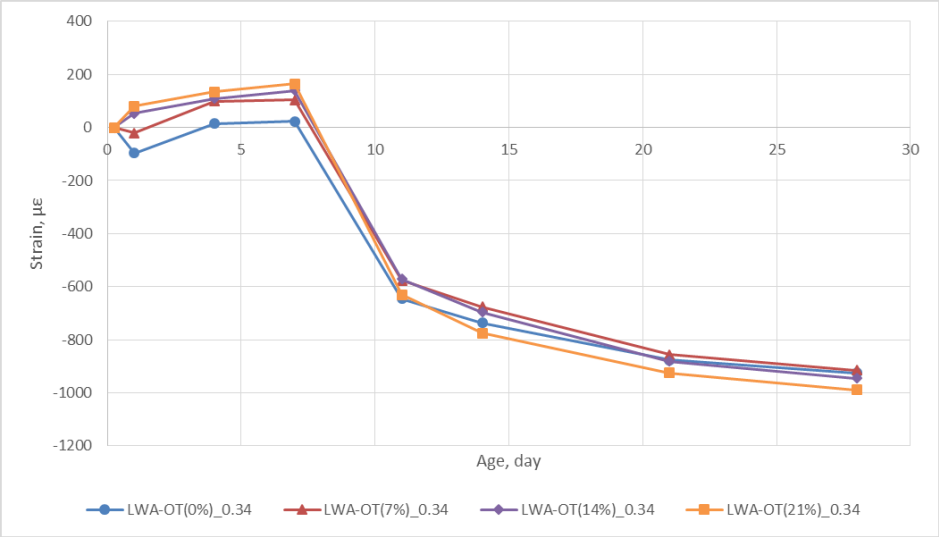

(a)

Figure 4.7 Deformation for unsealed mortar prisms at: (a) 0.34 w/c; (b) 0.44 w/c

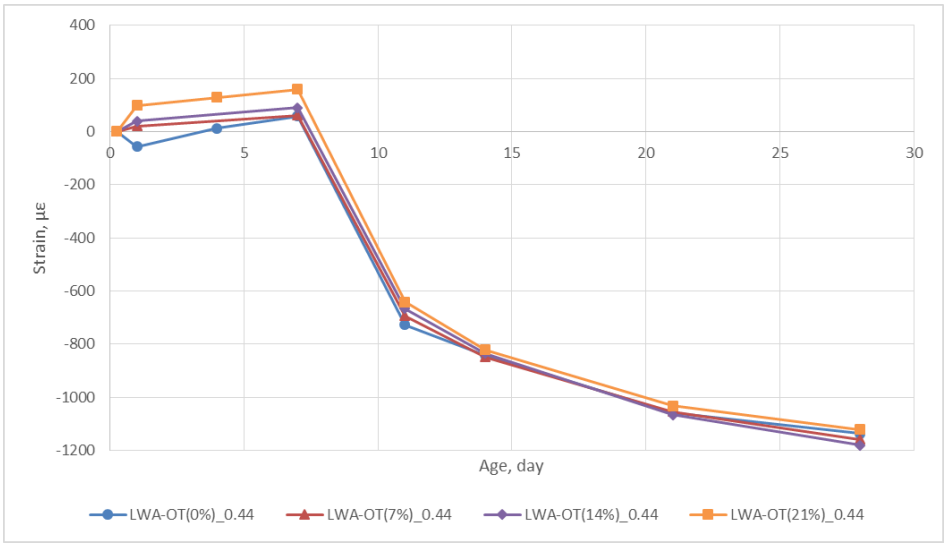

(b)

Figure 4.7 (cont.)

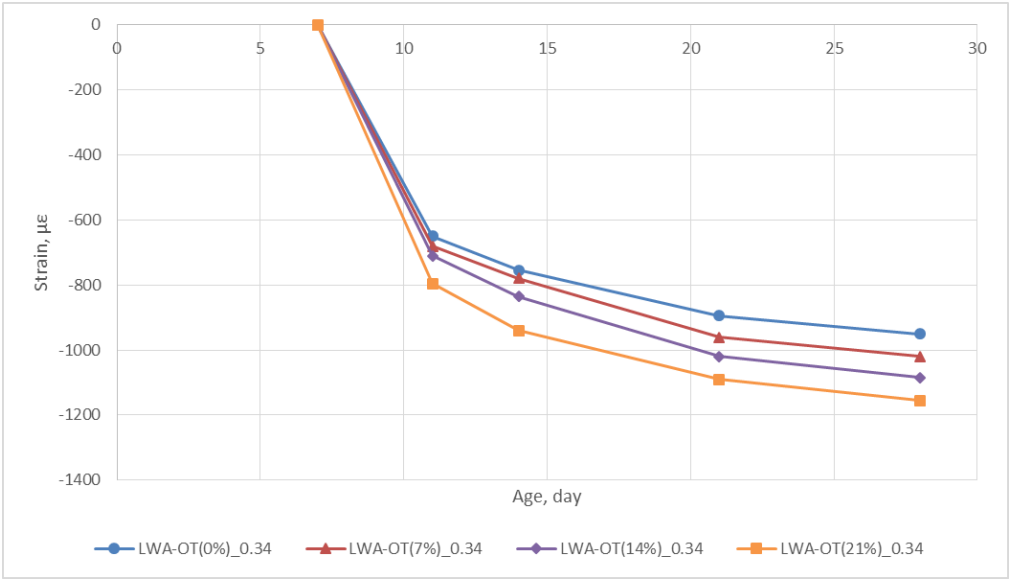

(a)

Figure 4.8 Drying shrinkage for unsealed mortar prisms after 7-day curing at: (a) 0.34 w/c; (b) 0.44 w/c

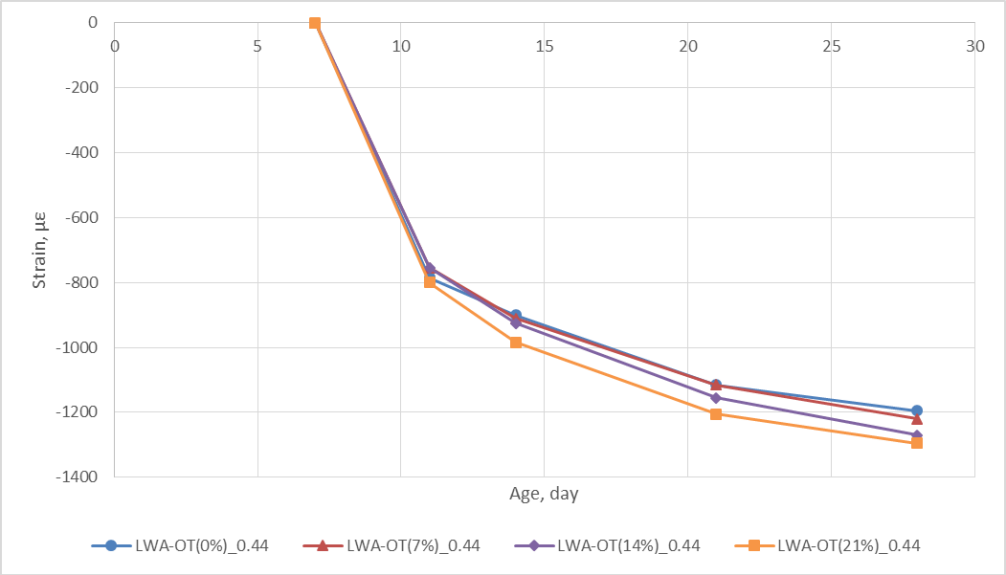

(b)

Figure 4.8 (cont.)

4.3.2. Effects of water-to-cement ratio

The comparison of deformations of two w/c ratios at each pre-soaked LWA dosage under sealed conditions is presented in Figure 4.9. It can be observed that under sealed conditions, for any of LWA dosage, the specimens with 0.44 w/c ratio showed higher early-age expansion and less shrinkage later on than those with 0.34 w/c ratio. This is because higher w/c ratios could maintain the internal RH at a higher level and for a longer period of time, which could mitigate shrinkage. Cusson and Hoogeven (2008) observed that when the total w/c ratio was kept constant, the effectiveness of pro-soaked LWA on shrinkage mitigation increased as the effective w/c ratio increased under sealed condition.

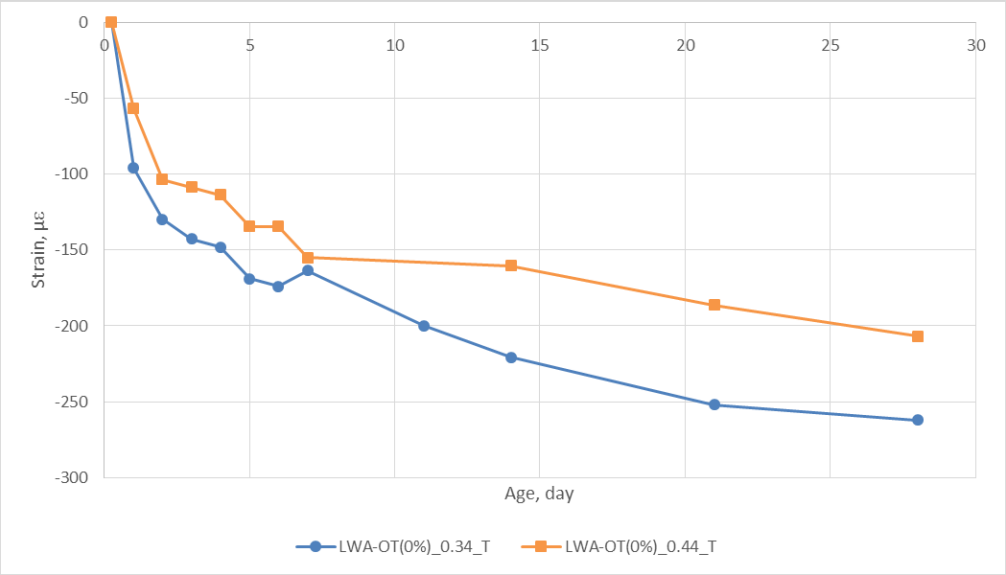

(a)

Figure 4.9 Comparison of deformations of corrugated tubes at two w/c ratios with the LWA dosage of: (a) 0%; (b) 7%; (c) 14%; (d) 21%

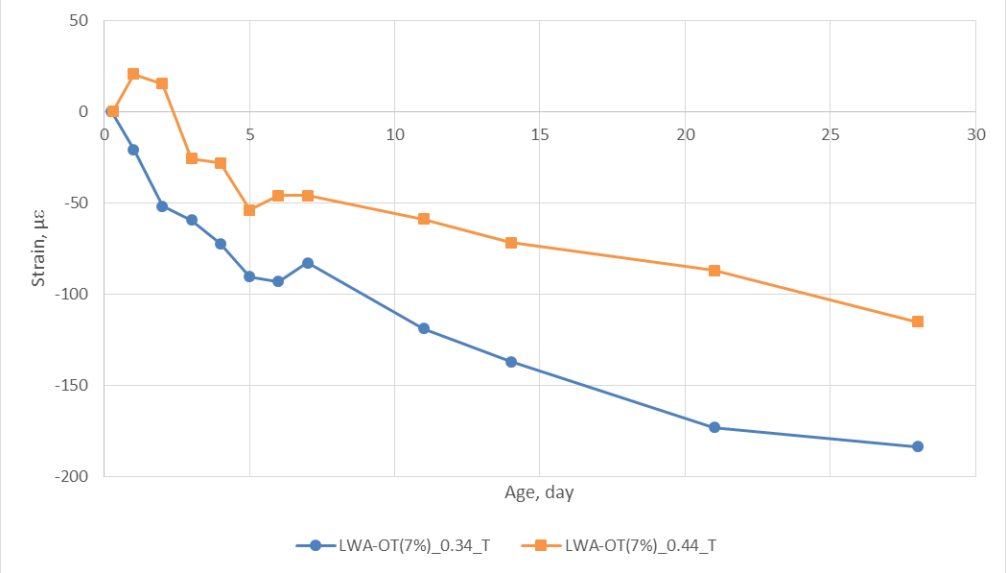

(b)

Figure 4.9 (cont.)

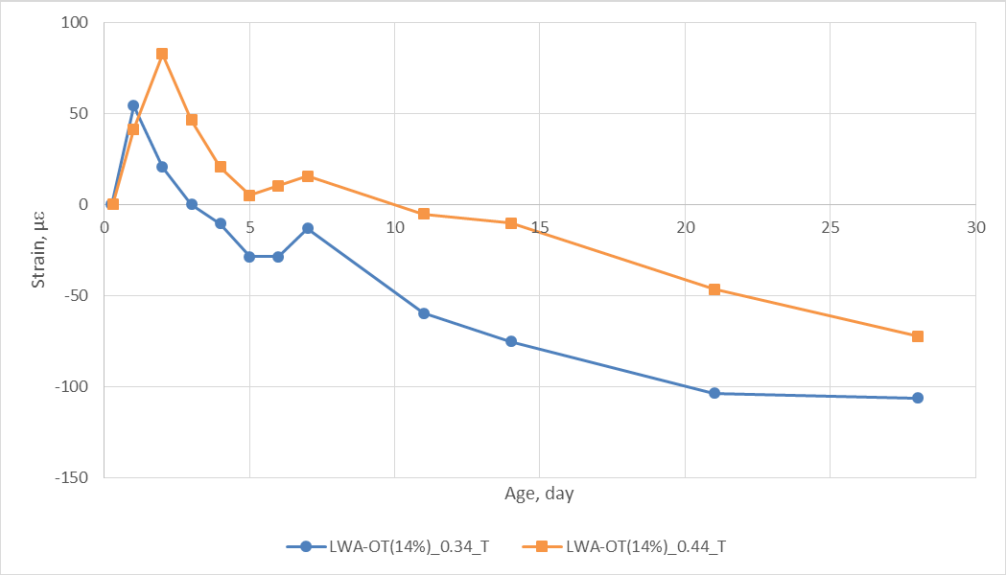

(c)

Figure 4.9 (cont.)

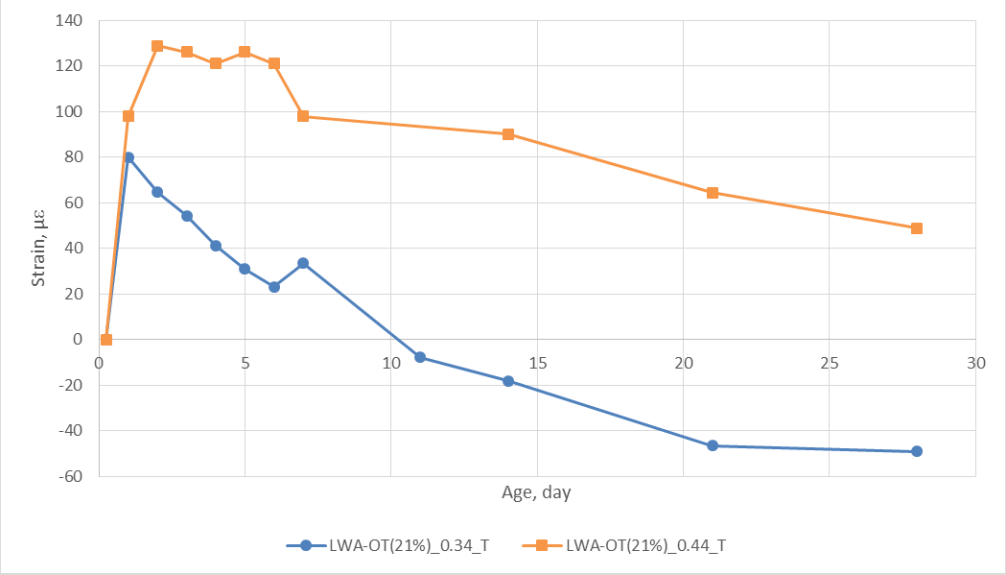

(d)

Figure 4.9 (cont.)

The comparison of deformations of two w/c ratios at each LWA dosage under unsealed conditions is presented in Figure 4.10. The figure shows that under unsealed conditions for all dosages of LWA replacement, the specimens with 0.44 w/c ratio show larger amount of shrinkage, which is the opposite of the phenomenon observed under sealed conditions. That is probably due to the fact that exposed conditions rendered the modulus of specimens the dominant factor, as

opposed to internal RH. Consequently, the larger reduction of modulus caused by a higher w/c ratio lead to larger shrinkage.

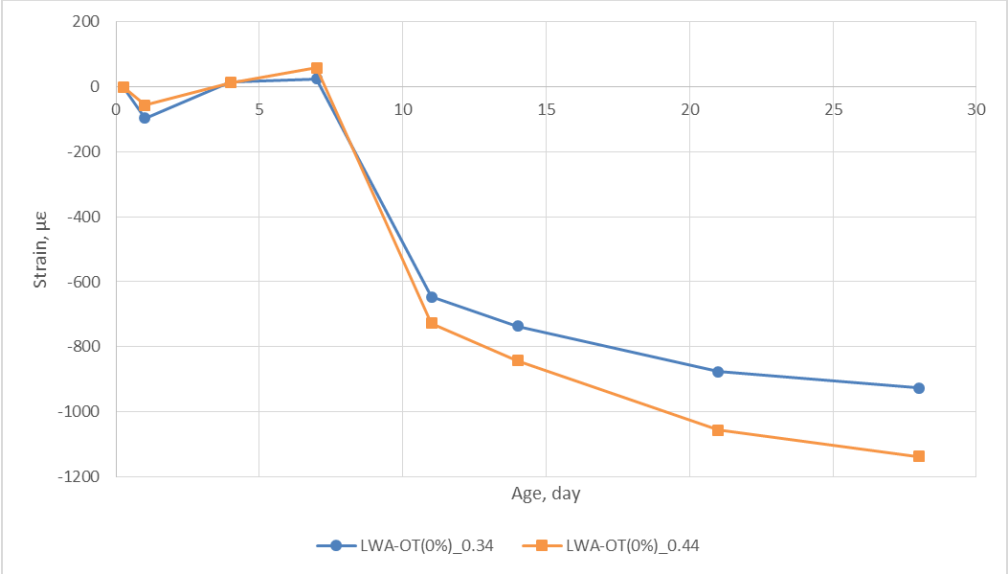

(a)

Figure 4.10 Comparison of deformations of unsealed mortar prisms at two w/c ratios with the LWA dosage of: (a) 0%; (b) 7%; (c) 14%; (d) 21%

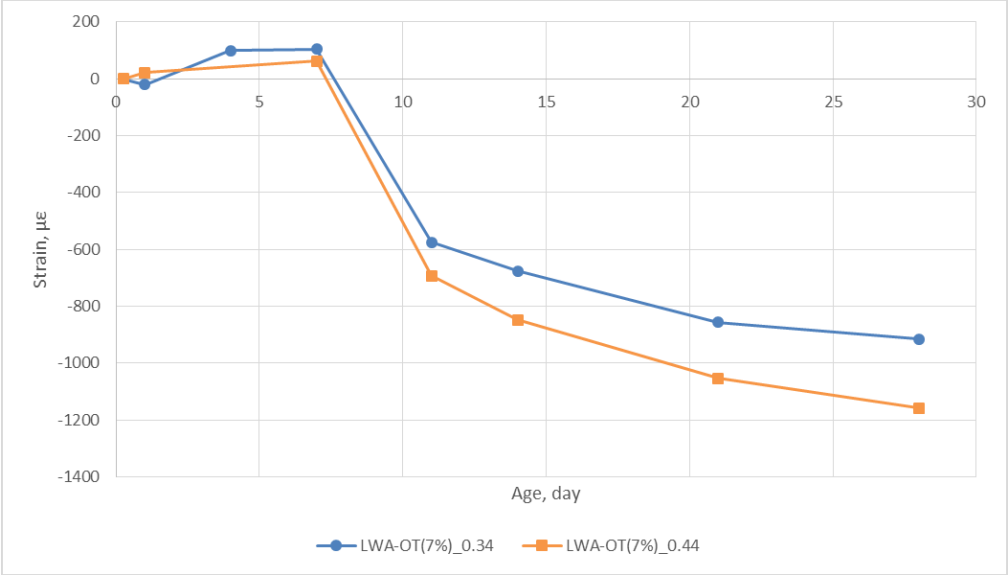

(b)

Figure 4.10 (cont.)

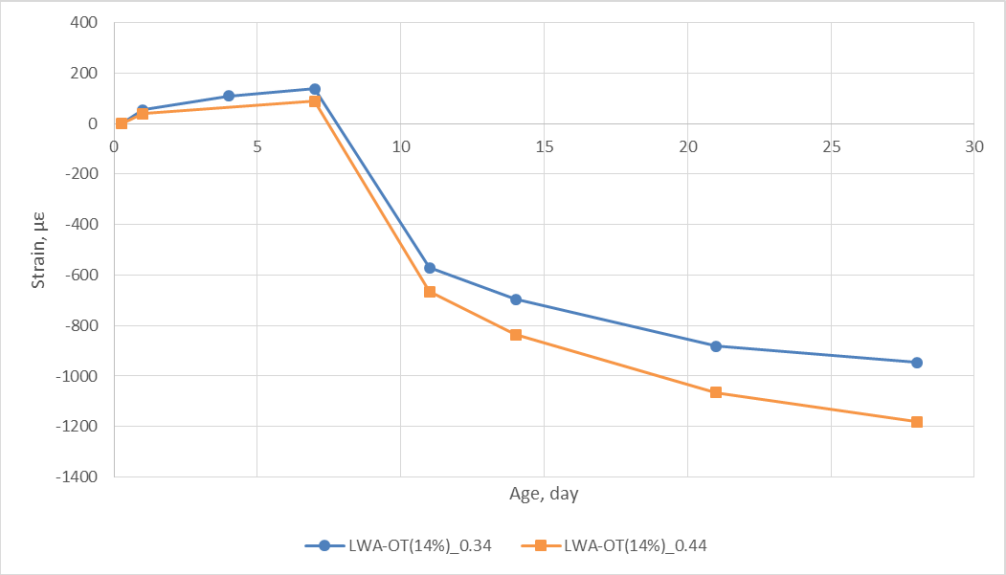

(c)

Figure 4.10 (cont.)

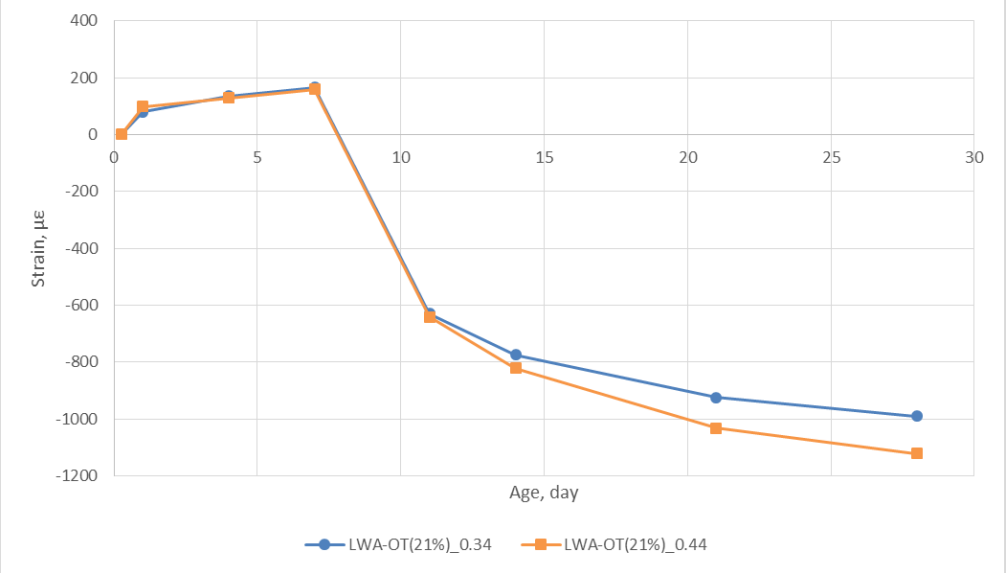

(b)

Figure 4.10 (cont.)

4.3.3. Effects of soaking time of LWA

To determine the effect of soaking time of LWA (which correlates to the amount of water stored in LWA), the LWA was prepared in the following manner. Instead of mixing the oven-dried LWA with the amount of water that corresponds to a 24-hour absorption period, the LWA was first mixed thoroughly with the amount of water enough for a 7-day absorption period. The LWA

was then allowed to absorb the added water for at least 7 days. Figure 4.11 provides the comparison of the deformation of 21% replacement of LWA soaked for 1 day and LWA soaked for 7 says at 0.34 w/c. It can be seen that longer soaking periods not only increased the early-age expansion, but also mitigated the shrinkage later on. It is because the extra water in LWA further minimized self-desiccation and kept the internal RH at a higher value (Golias et al., 2012). This, in turn, promoted the shrinkage reduction effects of pre-soaked LWA.

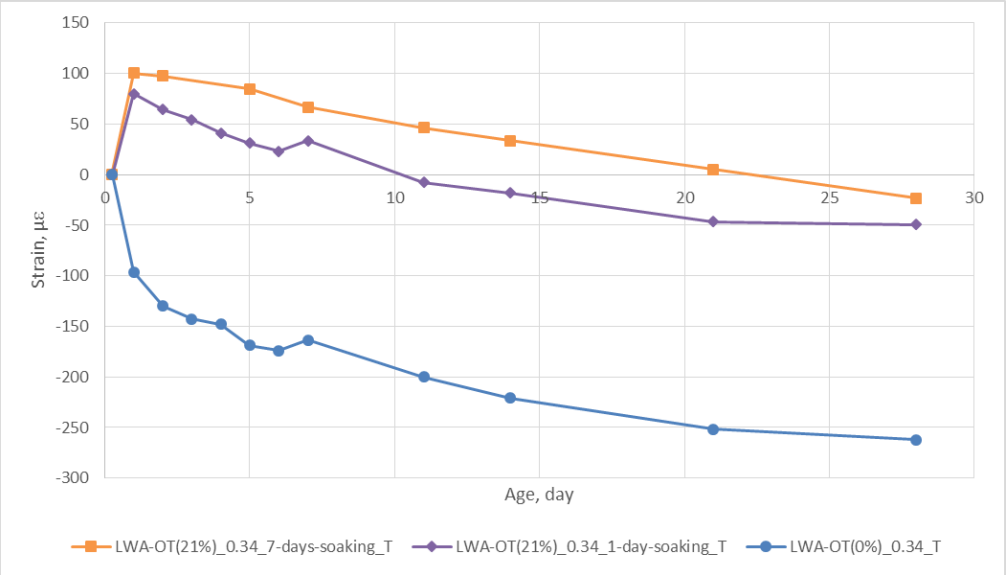

(a)

Figure 4.11 Effects of soaking time of LWA: (a) corrugated tubes; (b) sealed prisms

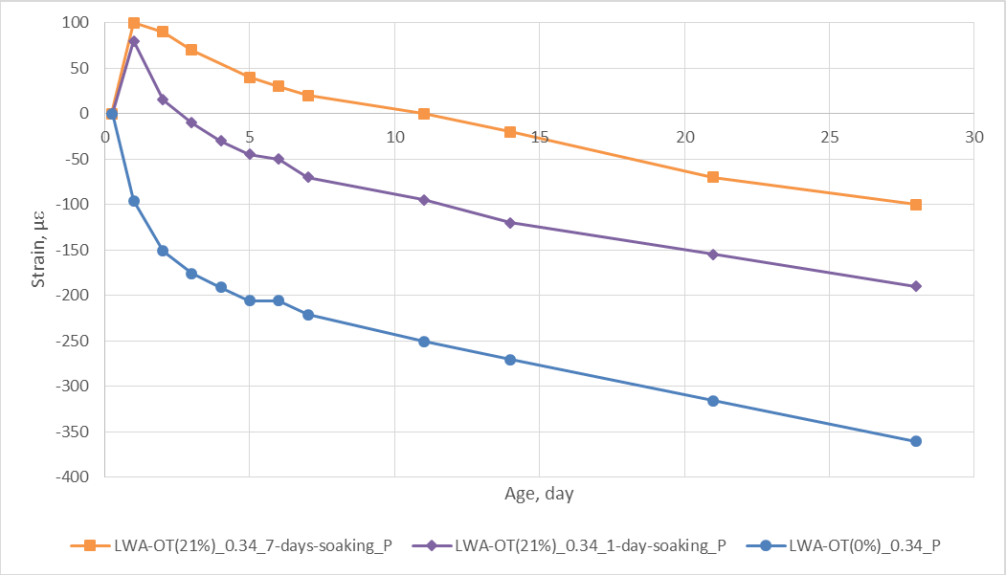

(b)

Figure 4.11 (cont.)

4.4. Conclusions

From the analysis of the experimental results of ordinary Portland cement (OPC) mortar specimens with pre-soaked lightweight aggregate under sealed and unsealed conditions, the following conclusions can be drawn:

1) Under sealed conditions, the total shrinkage decreased while the early-age expansion increased as the dosage of the LWA increased.
2) The drying shrinkage caused by small amounts of water loss from sealed prisms was believed to be the cause for the deviations between deformations of corrugated tubes and sealed prisms.
3) Under unsealed conditions, the addition of LWA did not influence the total deformation. However, the net drying shrinkage after curing increased as the dosage of the LWA increased. This trend is even more obvious at lower w/c ratios.

4) Under sealed conditions, specimens with higher w/c ratios showed higher early-age expansion and less shrinkage later on than those with lower w/c ratios. However, under unsealed conditions, the observed trend was opposite.
5) Longer soaking times for LWA could improve the effectiveness of LWA in reducing shrinkage.

CHAPTER 5

COMPARISON OF THE EFFECTIVENESS OF THREE TYPES OF LWA ON SHRINKAGE MITIGATION

5.1.Introduction

The objective of this chapter is to compare three different types of LWA and to investigate the properties of a LWA that influence its effectiveness on shrinkage mitigation under sealed and unsealed conditions.

In this chapter, the measured deformation of ordinary Portland cement (OPC) mortar specimens with three types of pre-soaked lightweight aggregates under both sealed and unsealed conditions are presented and discussed. Three types of lightweight aggregates were used in this chapter. Two of them are manufactured expanded blast furnace slag, assigned as LWA-OT and LWA-NT, respectively, and the other one is manufactured rotary kilned expanded shale, assigned as LWA-H. The LWA-OT is the same one as mentioned in chapter 4 and it is from the same manufacturer of LWA-NT but obtained at a different time. Four different mixtures were prepared at an effective w/c of 0.34 or 0.44, respectively, with 0% LWA, 21% of LWA-OT, 29.7% of LWA-NT and 19.3% of LWA-H replacement.

5.2.Materials, mixture proportioning and mixing procedure

The cement, normal weight sand and high-range water reducing admixture (HRWRA) were the same as those described in chapter 4.

Parts of the normal weight sand were replaced with three different types of LWA. The properties of three types of LWA are presented in Table 5.1. The sieve analysis results, absorption and desorption isotherms of three types of LWA are shown in Figure 5.1, Figure 5.2 and Figure

5.3, respectively. As shown in the figures, the absorption capacity of LWA-H is close to that of LWA-OT and is higher than that of LWA-NT. The gradation of LWA-NT and LWA-H is similar, and LWA-OT is coarser but all of them could be regarded as fine aggregates. The desorption capacity of LWA-NT and LWA-H is similar and is higher than that of LWA-OT.

Table 5.1 Properties of three types of LWA

Properties	LWA-OT	LWA-NT	LWA-H
Specific gravity (SSD)	1.88	2.15	1.69
Water absorption at 6 h (%)	-	6.9%	12.8%
Water absorption at 24 h (%)	15.0%	7.8%	15.5%
Water absorption at 3 d (%)	16.0%	8.8%	17.7%
Water absorption at 7 d (%)	19.3%	10.3%	19.2%

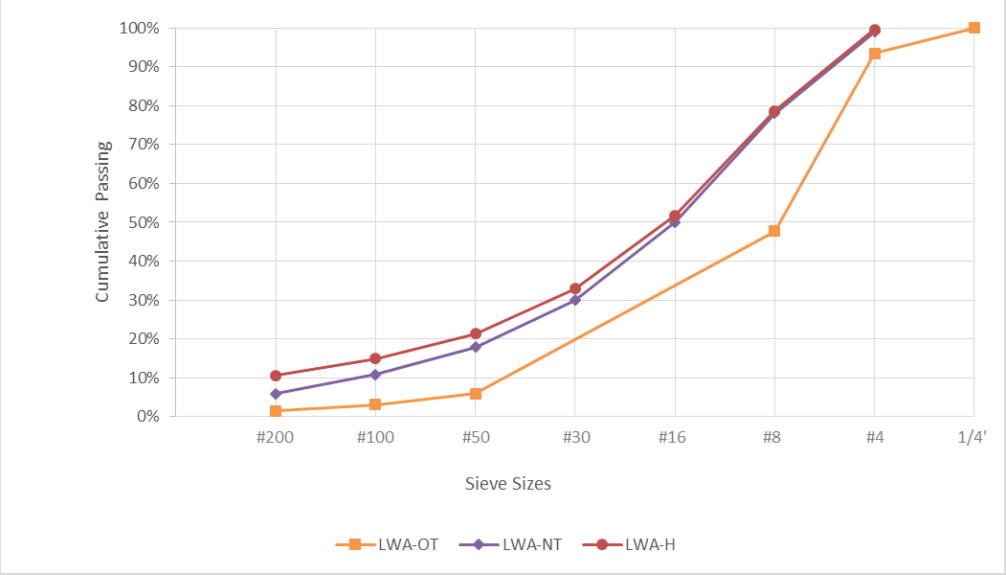

Figure 5.1 Sieve analysis of three types of LWA

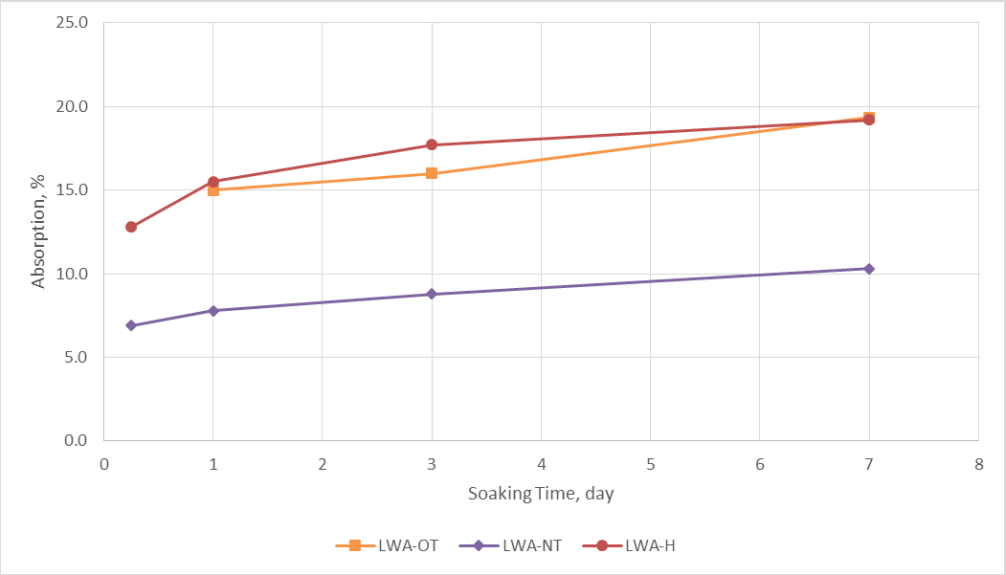

Figure 5.2 Absorption isotherms of three types of LWA

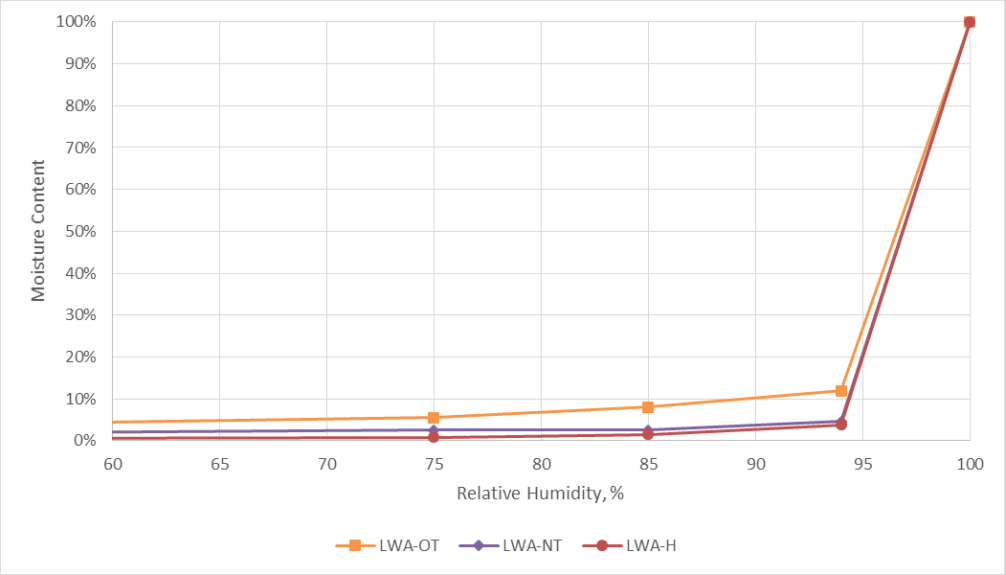

Figure 5.3 Desorption isotherms of three types of LWA

Four different mixtures were prepared with an effective w/c of 0.34 or 0.44, respectively. The four mixtures at each w/c ratio include a plain mixture with 0% LWA and three mixtures with 21%, 29.7% and 19.3% of normal weight sand replaced by pre-soaked LWA-OT, LWA-NT and LWA-H, respectively. The replacements were on basis on total volume. The volume of aggregate (normal weight sand and LWA) was maintained constant at 55%. The 21% of LWA-OT, 29.7% of LWA-NT and 19.3% of LWA-H were chosen based on the method provided by Castro et al.

(2011) as mentioned in section 2.4.2. By using the aforementioned dosage for each LWA, they could provide same amount of water for internal curing. The mixture proportions are shown in Table 5.2.

Table 5.2 Mixture proportions of ordinary Portland cement mortar with three types of lightweight aggregates

Materials	0.34 w/c				0.44 w/c			
	0% LWA	21% LWA-OT	29.7% LWA-NT	19.3% LWA-H	0% LWA	21% LWA-OT	29.7% LWA-NT	19.3% LWA-H
OPC (lbs/yd^3)	1154	1154	1154	1154	1002	1002	1002	1002
Water (lbs/yd^3)	433	417	411	419	481	466	459	467
OD Sand (lbs/yd^3)	2371	1466	1090	1539	2371	1466	1090	1539
SSD LWA (lbs/yd^3)	0	666	1077	550	0	666	1077	550

The mixing procedure and LWA preparation were the same as mentioned in chapter 4.

5.3. Results and discussions

5.3.1. Under sealed conditions

The measured deformations for mortar specimens from sealed prisms and corrugated tubes at 0.34 w/c and 0.44 w/c ratios are presented in Figure 5.4 and Figure 5.5, respectively. It can be seen that all three types of LWA improved the shrinkage behavior under sealed conditions. Additionally, the effectiveness of three types of LWA on shrinkage mitigation was very close. They all reduced a similar amount of shrinkage by providing same amount of internal curing water. A reasonable deduction is that under sealed conditions, when same amount of internal curing water was provided, the improvement of shrinkage behavior would be similar by using different pre-soaked LWA. This conclusion did not take the gradation of LWA into consideration. It does not mean the gradation is not an important factor on internal curing but probably because the spatial distribution was not a dominant factor in this case. Additionally, the differences of the reduction

of modulus by using different types and different amount of LWA were also not considered. However, as mentioned in chapter 4, under sealed conditions, the internal RH (which correlates to the capillary pressure) is the dominant factor, as opposed to the modulus of specimens.

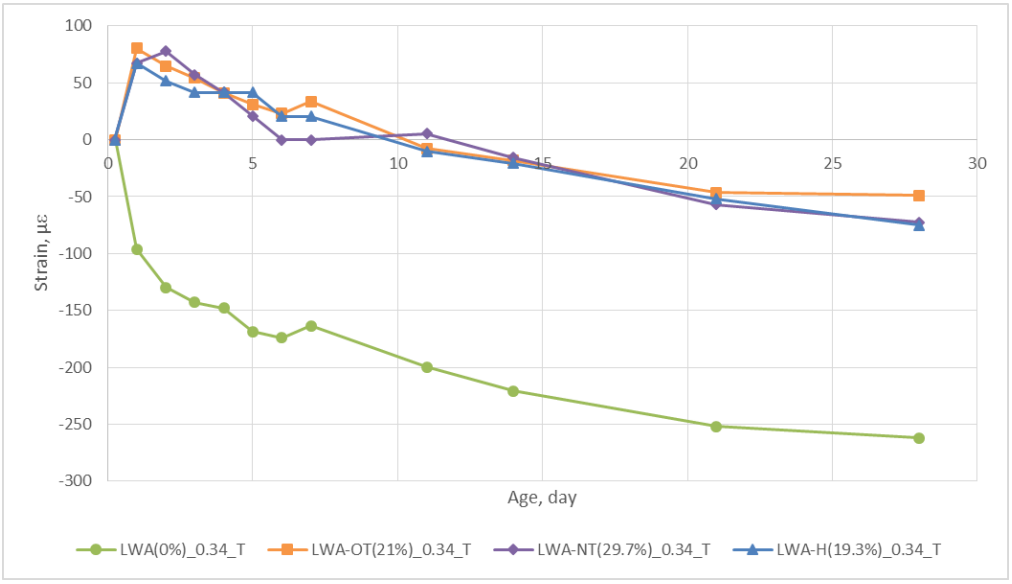

(a)

Figure 5.4 Deformation for mortar specimens from corrugated tubes at: (a) 0.34 w/c; (b) 0.44 w/c

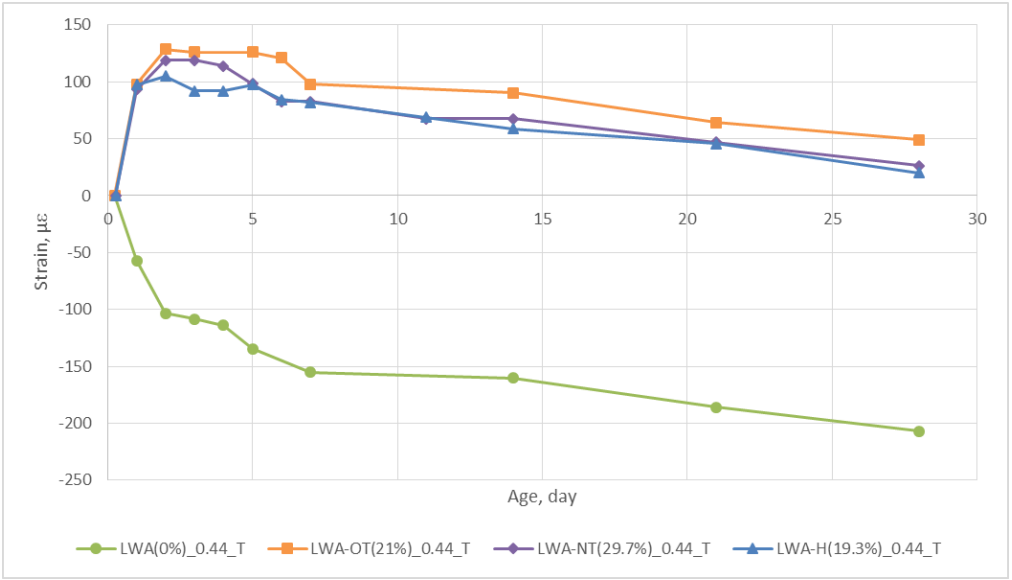

(b)

Figure 5.4 (cont.)

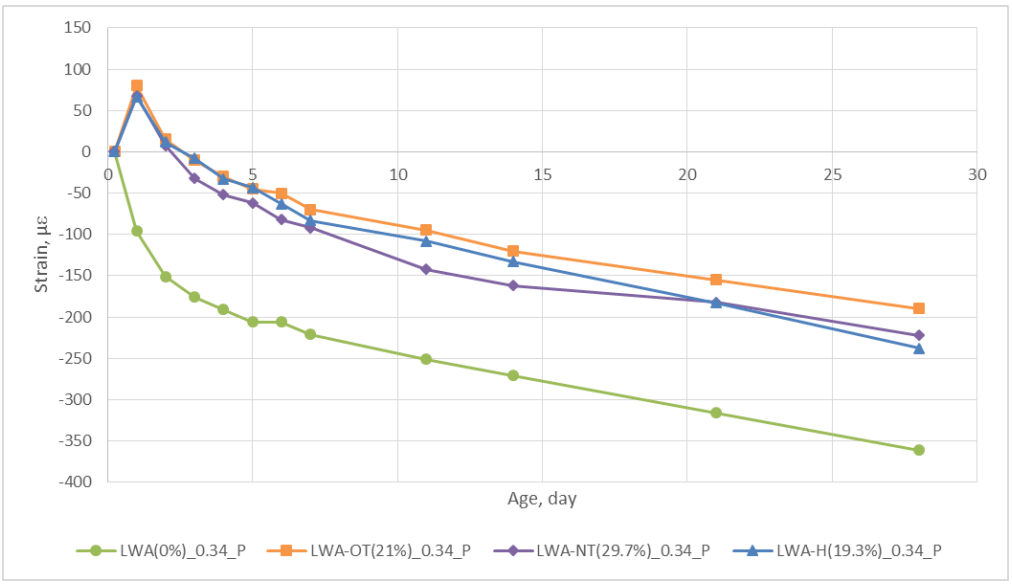

(a)

Figure 5.5 Deformation for mortar specimens from sealed prisms at: (a) 0.34 w/c; (b) 0.44 w/c

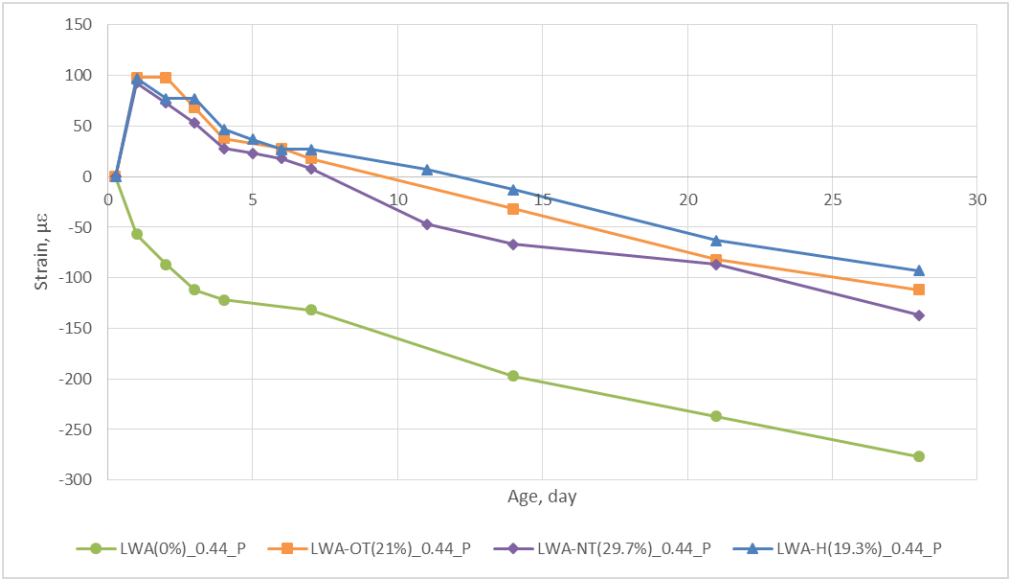

(b)

Figure 5.5 (cont.)

5.3.2. Under unsealed conditions

For unsealed conditions, two plain mixtures (0% LWA replacement) with exactly same mixture proportioning were casted and cured as control mixtures at different time with mixtures with different LWA. The first plain mixture was casted and cured together with the mixture with 21% LWA-OT and second plain mixture was casted and cured together with the mixtures with

29.7% LWA-NT or 19.3% LWA-H. Their deformation behavior was expected to be similar. However, a difference between two plain mixtures was found as shown in Figure 5.6. A reasonable deduction is that the environment in the air storage room was changed between two times of curing. Thus, in order to properly compare three types of LWA under unsealed conditions, their results have to be modified based on the difference between two plain mixtures which is caused by environmental change. The modification procedures are as following:

1) Calculating differences between two plain mixtures at 0.34 w/c and 0.44 w/c, respectively. The differences are presented in Table 5.3.

2) Modifying the result of unsealed prisms with 21% LWA-OT based on the differences in Table 5.3. The modification process is shown in Figure 5.7, and the arrows indicate the changing direction.

Table 5.3 Differences between two plain mixtures

Age (day)	Difference at 0.34 w/c (με)	Difference at 0.44 w/c (με)
11	120	165
14	75	150
21	105	195
28	90	197

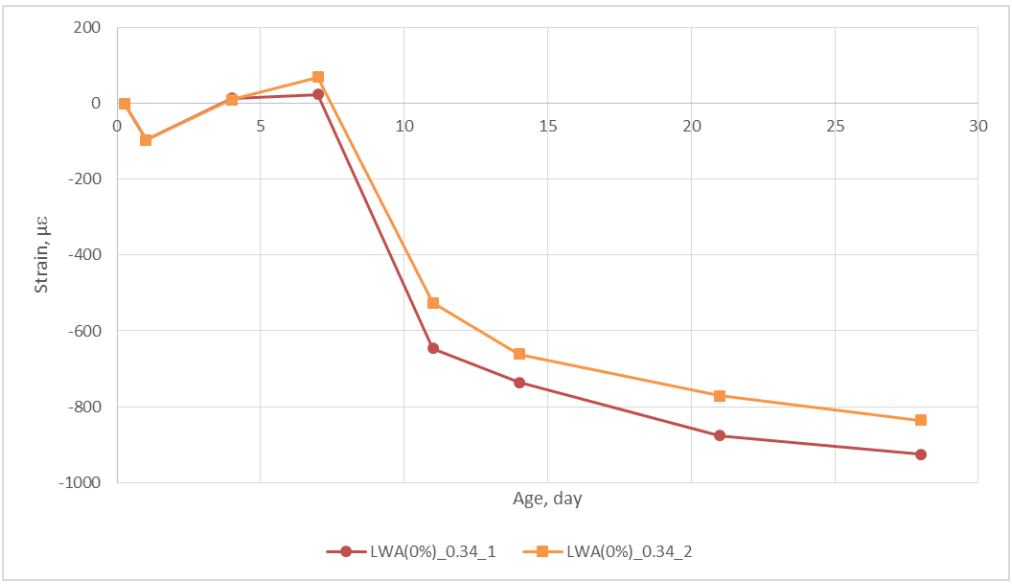

(a)

Figure 5.6 Difference of the deformation between two plain mixtures at: (a) 0.34 w/c; (b) 0.44 w/c

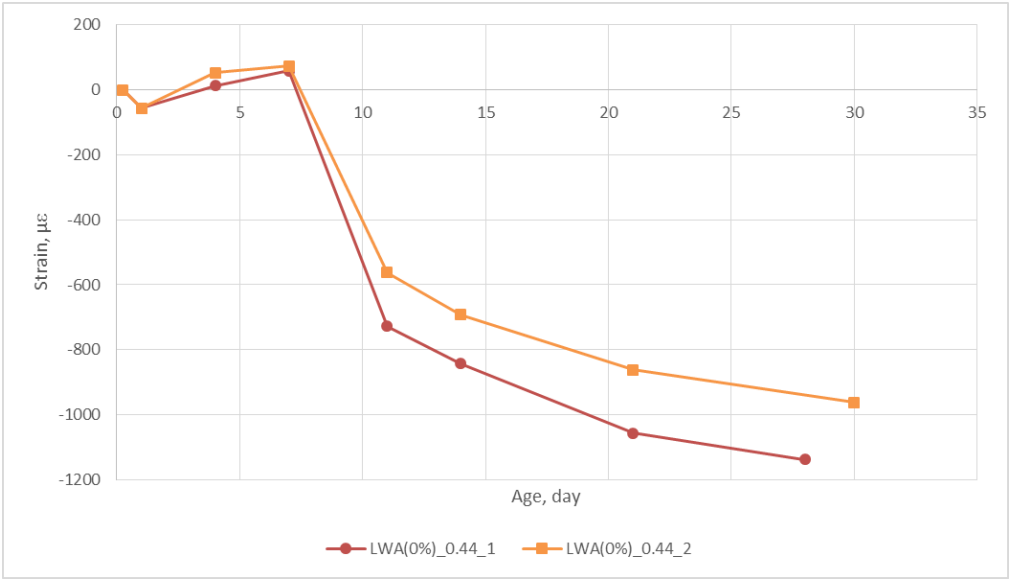

(b)

Figure 5.6 (cont.)

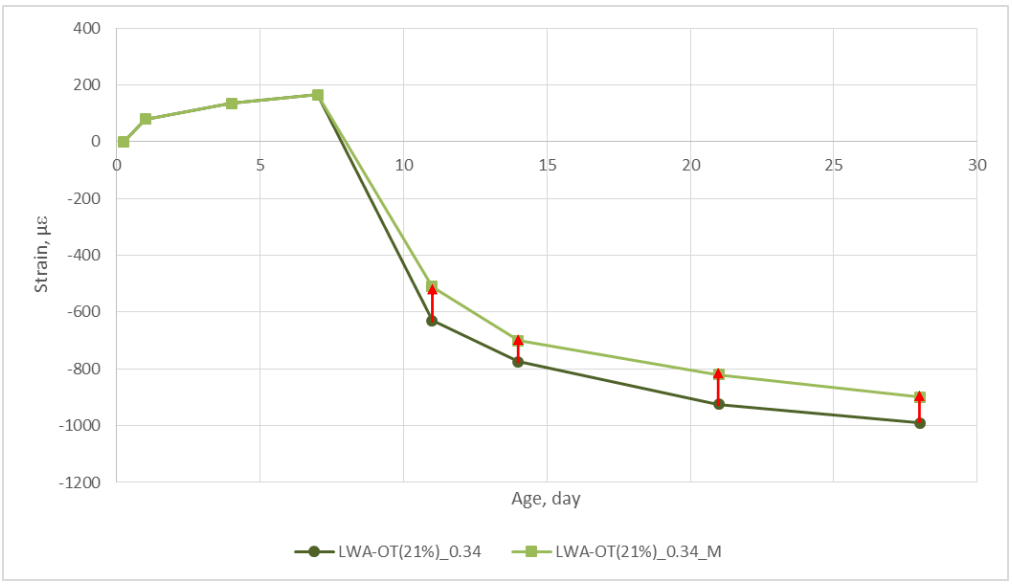

(a)

Figure 5.7 Modification process of the result of unsealed mortar prisms with 21 % LWA-OT at: (a) 0.34 w/c; (b) 0.44 w/c

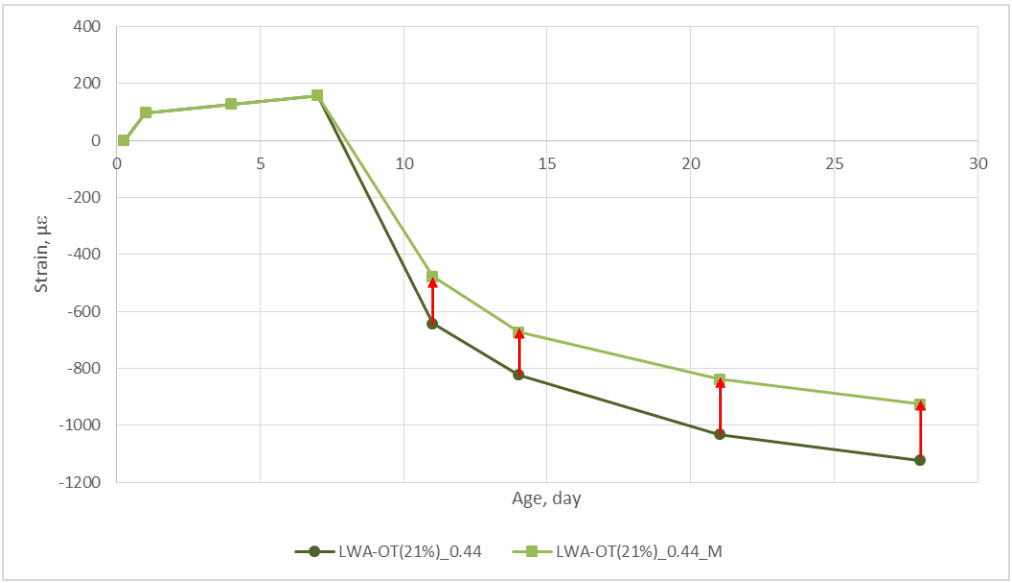

(b)

Figure 5.7 (cont.)

The modified measured deformations for unsealed mortar prisms from final set at 0.34 w/c and 0.44 w/c ratios are presented in Figure 5.8. The deformations before 24 hours are from corrugated tubes tests. The modified net drying shrinkage after 7-day curing for unsealed mortar prisms at 0.34w w/c and 0.44 w/c ratios are shown in Figure 5.9. It can be seen that the unsealed mortar prisms with 21% of pre-soaked LWA-OT, 29.7% of pre-soaked LWA-NT or 19.3% of pre-

soaked LWA-H expanded almost the same amount within the first 7 days and the expansion was higher than that of the plain mixture. Additionally, the drying shrinkage of unsealed mortar prisms with 21% of pre-soaked LWA-OT and 29.7% of pre-soaked LWA-NT was very close and larger than that of the unsealed mortar prisms with 19.3% of pre-soaked LWA-H which was close to the drying shrinkage of plain mixture. This difference is probably caused by the difference lying in stiffness. The modulus of the mixture with 19.3% of LWA-H is higher than those of the mixtures with 21% of LWA-OT and 29.7% of LWA-NT. The more specific explanation was mentioned in chapter 4. The original data is presented in Figure 5.10.

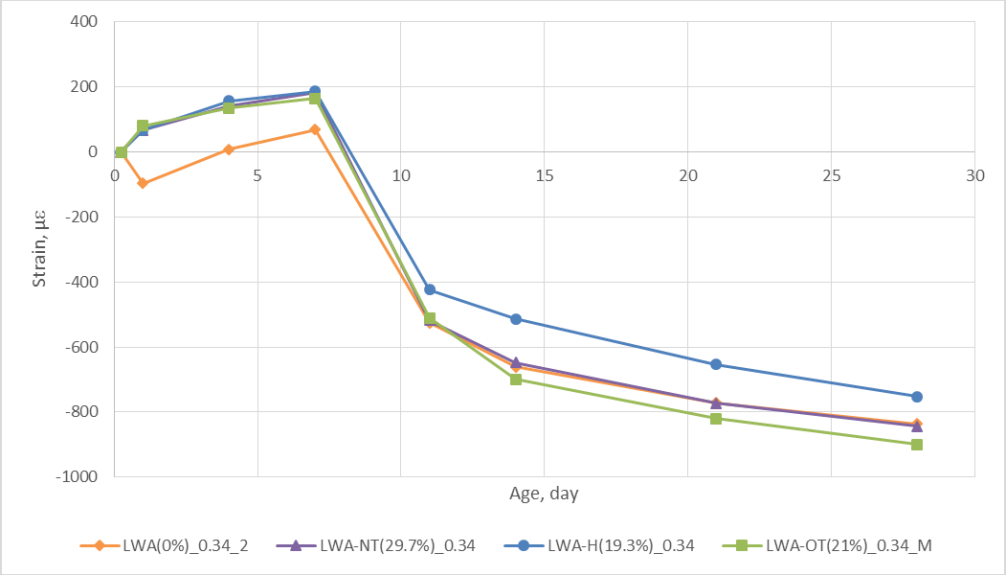

(a)

Figure 5.8 Modified deformations for unsealed mortar prisms at: (a) 0.34 w/c; (b) 0.44 w/c

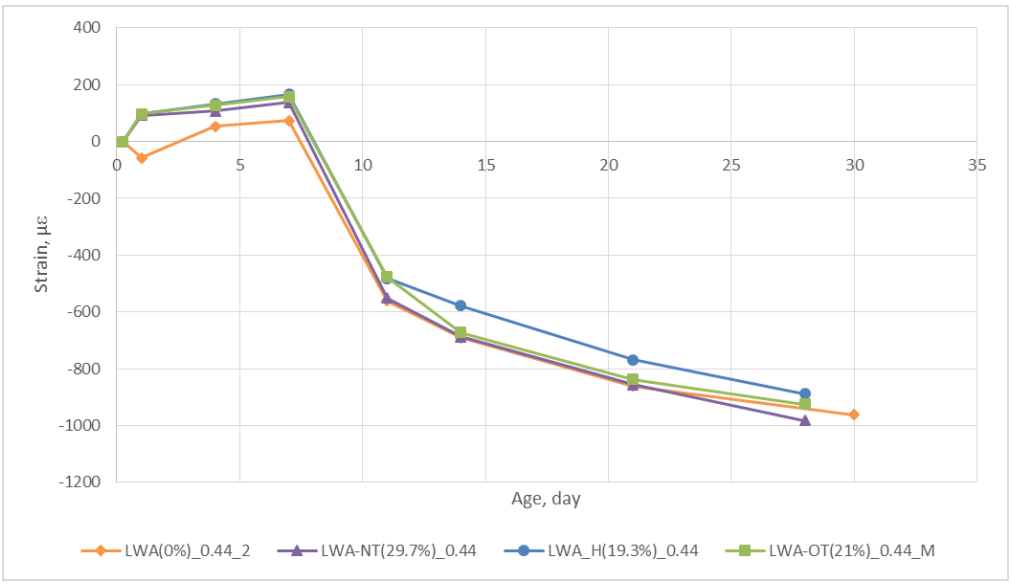

(b)

Figure 5.8 (cont.)

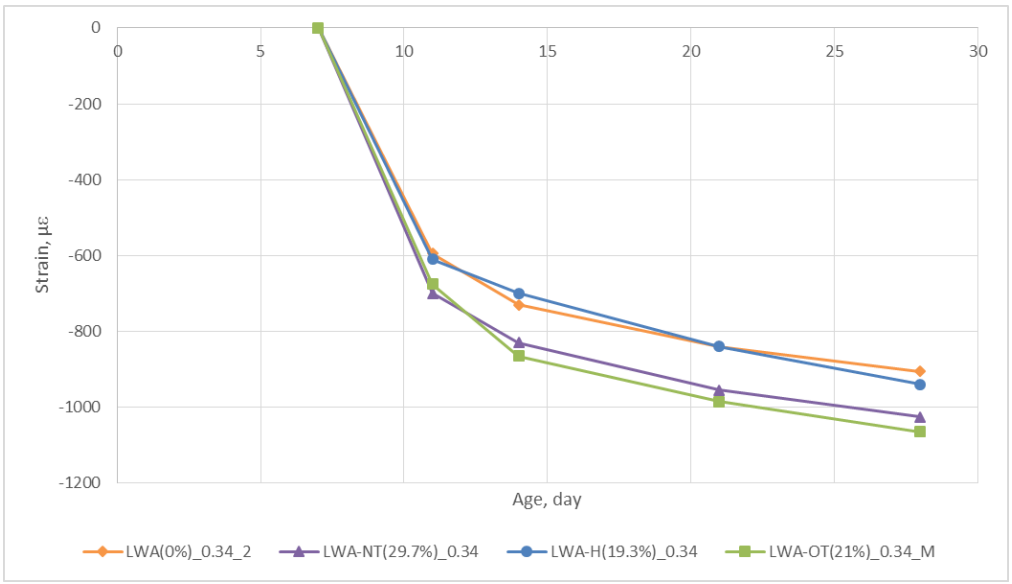

(a)

Figure 5.9 Modified drying shrinkage for unsealed mortar prisms after 7-day curing at: (a) 0.34 w/c; (b) 0.44 w/c

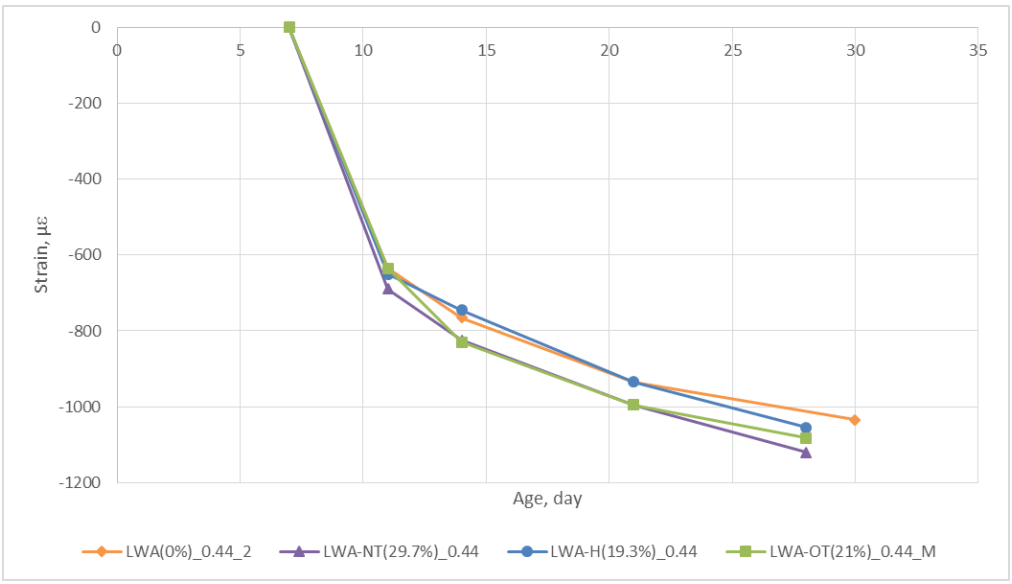

(b)

Figure 5.9 (cont)

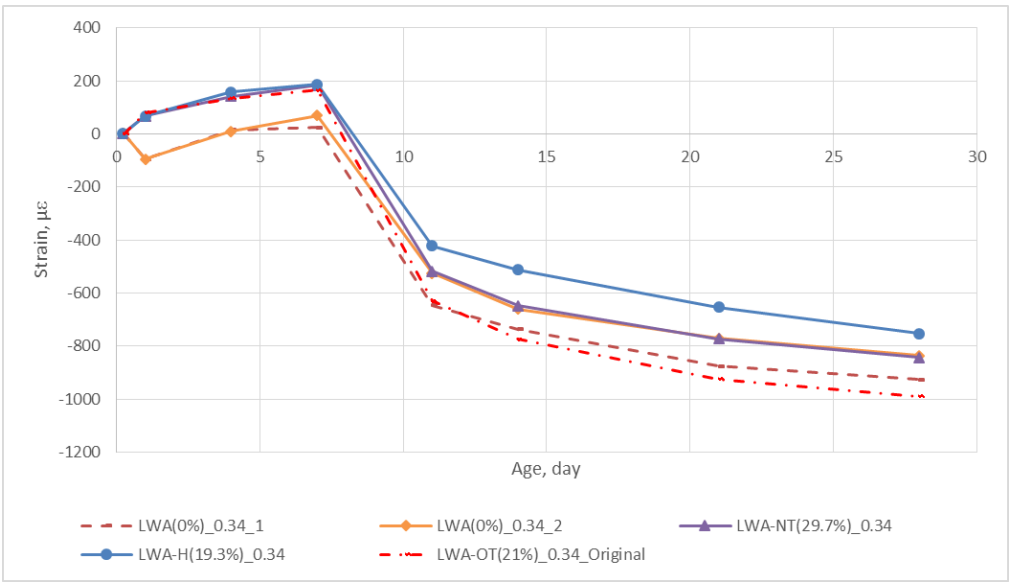

(a)

Figure 5.10 Original deformations for unsealed mortar prisms at: (a) 0.34 w/c; (b) 0.44 w/c

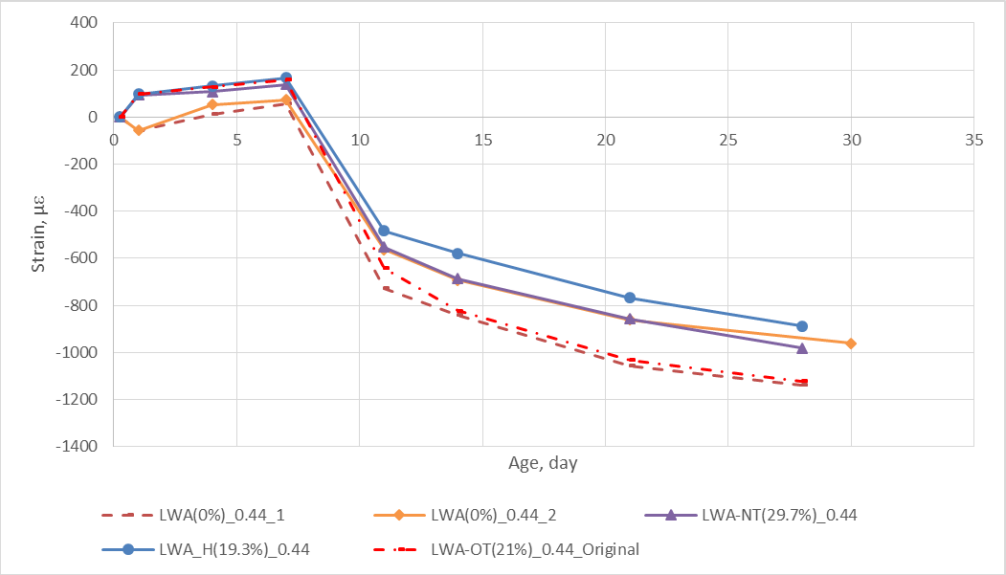

(b)

Figure 5.10 (cont.)

5.4. Conclusions

From the analysis of the experimental results of ordinary Portland cement (OPC) mortar specimens with three different types of lightweight aggregates under sealed and unsealed conditions, the following conclusions can be drawn:

1) Three types of lightweight aggregates (LWA-OT, LWA-NT and LWA-H) performed similarly under sealed conditions while LWA-H performed better under unsealed conditions on shrinkage mitigation.
2) Under sealed conditions, regardless of the spatial distribution, when same amount of internal curing water was provided, different types of pre-soaked LWA behaved similarly on shrinkage mitigation.
3) Under unsealed conditions, the effectiveness of pre-soaked LWA mostly depends on their influence on stiffness.

CHAPTER 6

LENGTH CHANGE OF ORDINARY PORTLAND CEMENT (OPC) AND CALCIUM SULFOALUMINATE (CSA) CEMENT MORTAR WITH PRE-SOAKED LIGHTWEIGHT AGGREGATES

6.1. Introduction

The objective of this chapter is to investigate the effects of the combination of pre-soaked LWA and CSA cement on shrinkage mitigation. Also, it tries to explain the causes leading to different magnitudes of early-age expansion when different dosages of pre-soaked LWA were used.

In this chapter, the measured deformations of ordinary Portland cement (OPC) and calcium sulfoaluminate (CSA) cement mortar with pre-soaked lightweight aggregate under both sealed and unsealed conditions are presented and discussed. Four mixtures at a w/c ratio of 0.34 and with 0%, 6.4%, 12.9% or 19.3% pre-soaked LWA-H replacement were prepared and cured under sealed or unsealed conditions. The results of XRD, TGA and dynamic modulus tests on the samples with the same mixture proportioning as aforementioned were also presented and discussed.

6.2. Materials, mixture proportioning and mixing procedure

The OPC, normal weight sand and high-range water-reducing admixture (HRWRA) were the same as those described in chapter 4. The calcium sulfoaluminate (CSA) cement had 19% ye'elimite ($C_4A_3\hat{S}$), 15% gypsum ($C\hat{S}H_2$), 9.4% hemihydrate ($C\hat{S}H_{0.5}$), 16.1% anhydrite ($C\hat{S}$), 34.8% belite (C_2S) and 2.1% ferrite (C_4AF). Parts of the normal weight sand were replaced with LWA-H, which is the same as described in chapter 5.

Four different mixtures were prepared with an effective w/c ratio of 0.34. The four mixtures include a plain mixture with 0% LWA and three mixtures with 6.4%, 12.9% and 19.3% of normal

weight sand replaced by pre-soaked LWA-H. The replacements were based on the total volume. For all four mixtures, 15 % of the OPC was replaced by CSA cement by weight. The volume of aggregate (normal weight sand and LWA) was maintained constant at 55%. The mixture proportions are shown in Table 6.1.

Table 6.1 Mixture proportions of ordinary Portland cement (OPC) and calcium sulfoaluminate (CSA) cement mortar with LWA-H

Materials	0.34 w/c			
	0% LWA	6.4% LWA-H	12.9% LWA-H	19.3% LWA-H
OPC (lbs/yd^3)	981	981	981	981
CSA (lbs/yd^3)	173	173	173	173
Water (lbs/yd^3)	433	428	423	419
OD Sand (lbs/yd^3)	2371	2095	1815	1539
SSD LWA (lbs/yd^3)	0	182	368	550

The mixing procedure and LWA preparation method were the same as mentioned in chapter 4. The CSA cement and OPC were mixed together properly before adding water.

6.3. Results and discussions

6.3.1. Under sealed conditions

The measured deformations for sealed prisms and corrugated tubes at 0.34 w/c ratio are presented in Figure 6.1. The deformation before 24 hours was from corrugated tubes tests. The result of the mixture with 0% CSA cement and 0% LWA is shown as a control group. It is shown that for all sealed prisms and corrugated tubes with CSA cement, the specimens kept expanding until 2 or 3 days, and the most of the expansion occurred in the first 24 hours. It is believed that the expansion was mainly due to CSA cement hydration. Additionally, the magnitude of the expansion was proportional to the dosage of pre-soaked LWA. It also can be seen that the shrinkage after the early-age expansion was not significantly affected by the dosage of pre-soaked LWA, thus, the mitigation of total shrinkage was mainly because of the early-age expansion.

Furthermore, for all of the mixtures, the length at 28 days was still longer than the initial length, which means adding CSA cement effectively mitigated the shrinkage, and adding pre-soaked LWA promoted this trend.

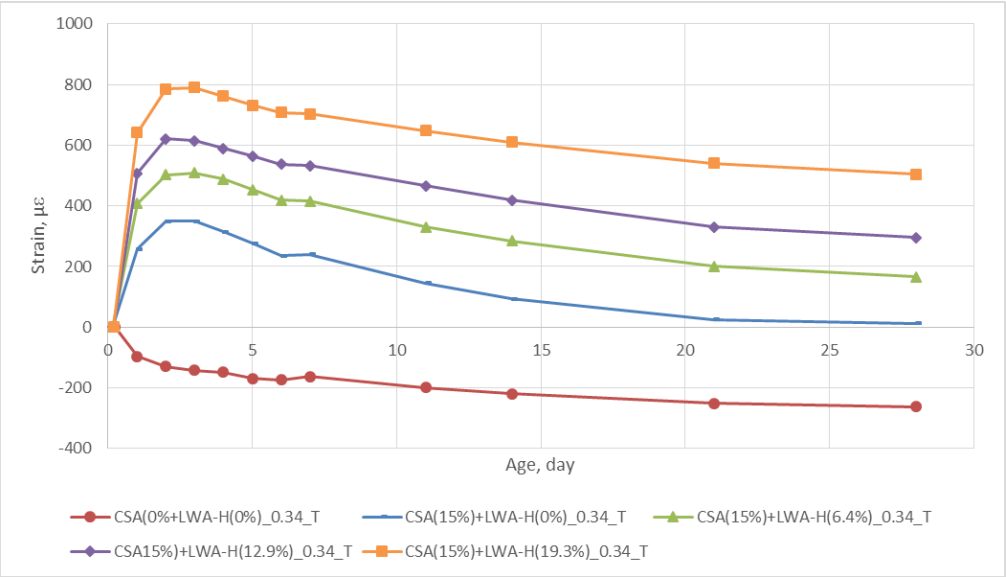

(a)

Figure 6.1 Deformations for mortar specimens with 15% CSA replacement at 0.34 w/c: (a) corrugated tubes; (b) sealed prisms

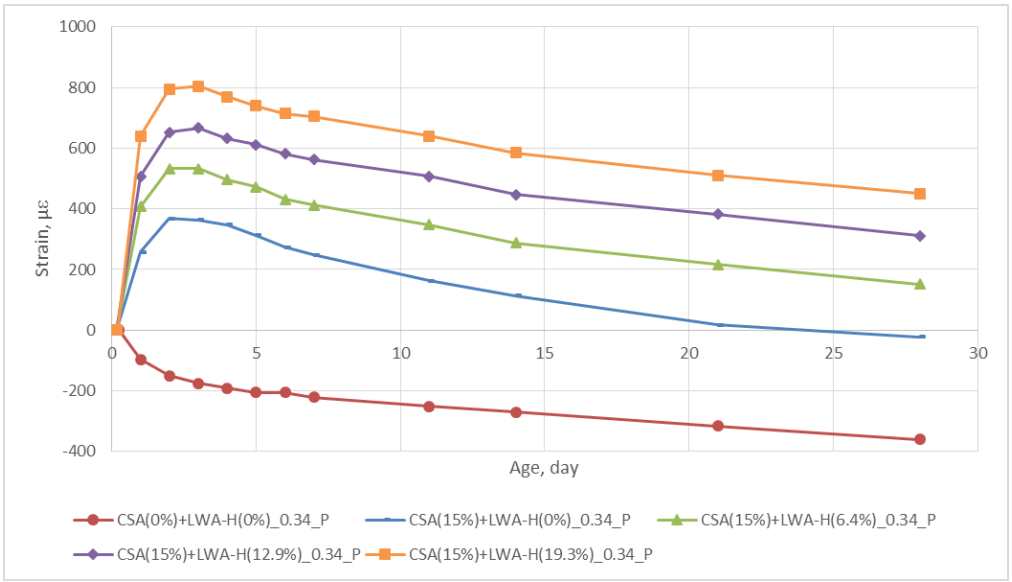

(b)

Figure 6.1 (cont.)

6.3.2. Under unsealed conditions

The measured deformations of unsealed prisms at 0.34 w/c ratio is presented in Figure 6.2. The deformation before 24 hours was from corrugated tubes tests. The result of the mixture with 0% CSA cement and 0% LWA is shown as a control group. It can be seen that the unsealed prisms with CSA cement kept expanding when cured in lime saturated water until 7 days. The magnitude of expansion was proportional to the dosage of pre-soaked LWA, however, the drying shrinkage after curing was not significantly influenced by the addition of pre-soaked LWA. Additionally, the length at 28 days for unsealed prisms was still longer than the initial length. Therefore, similar to the sealed conditions, under unsealed conditions, adding CSA cement effectively mitigated the shrinkage, and adding pre-soaked LWA promoted this trend.

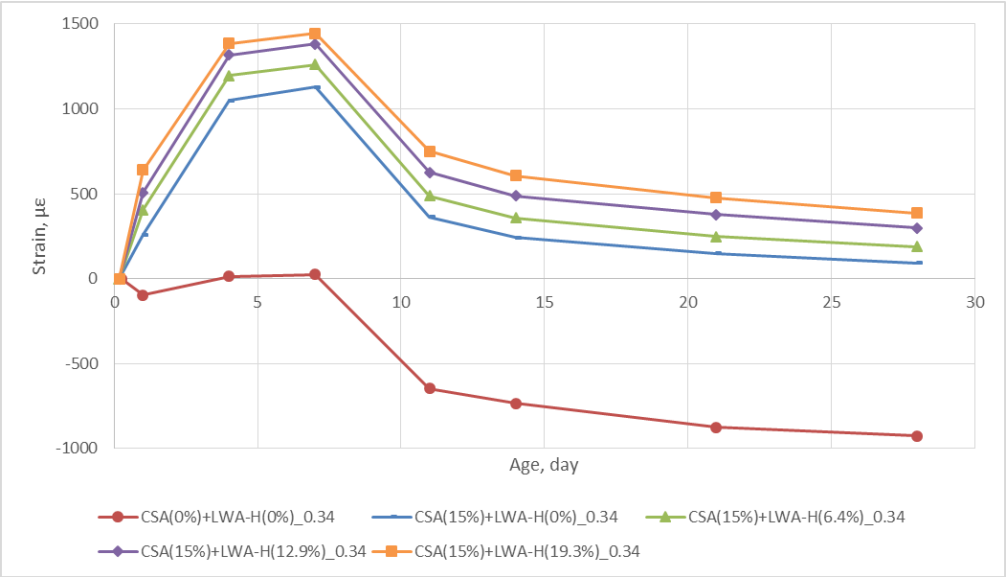

Figure 6.2 Deformations for unsealed mortar prisms with 15% CSA replacement at 0.34 w/c

6.3.3. Reasons for different magnitudes of early-age expansion

One of the factors that contributed to the observed phenomenon could be the amount of ettringite formed, which is related to the magnitude of expansion. It is possible that pre-soaked LWA facilitated the hydration of CSA cement and, therefore, more ettringite was formed with

more pre-soaked LWA. To test this hypothesis, X-ray diffraction (XRD) and Thermogravimetric analysis (TGA) tests were conducted. The four samples that were tested include a plain mixture with 0% LWA and three mixtures with 6.4%, 12.9% and 19.3% of normal weight sand replaced by pre-soaked LWA-H at a w/c ratio of 0.34. The replacements were based on the total volume. For all four mixtures, 15 % of the OPC was replaced by CSA cement by weight. All the samples were cured under sealed conditions. The thermal analysis results are shown in Figure 6.3. The first peak is mainly attributed to the decomposition of ettringite. It can be seen that at 15 hours, the first peaks of samples with 6.4%, 12.9 and 19.3% of pre-soaked LWA-H are overlapped together and they are lower than that of the sample with 0% of pre-soaked LWA-H. It means that at 15 hours the addition of pre-soaked LWA-H increased the amount of ettringite formed but the further adding did not keep promoting the formation of ettringite. the Additionally, it shows that at 24 hours, the first peaks are overlapped together, which indicates that the amounts of ettringite are very close to each other with different dosages of pre-soaked LWA-H. In other words, adding pre-soaked LWA did not affect the amount of ettringite at this age. However, for the samples at 7 days, the first peaks are slightly separated and appear on the plot in following order, from bottom to top: 0%, 6.4%, 12.9 and 19.3% of LWA-H. It means that at 7 days, the addition of pre-soaked LWA-H slightly promoted the formation of ettringite. Semi-quantitative information of ettringite content can also be extracted from the derivative thermogravimetric plot. A range of 70 to 120°C was considered as the decomposition temperature range of ettringite (Pelletier et al., 2010; Winnefeld et al., 2010; Chaunsali and Mondal, 2015). The weight loss between 70 to 120°C was shown in Table 6.2. It can be observed that the amounts of ettringite at 15 hours and 24 hours are very close, while at 7 days the amount of ettringite slightly increased with the addition of pre-soaked LWA-H. The results of weight loss are consistent with aforementioned discussion, which is that adding

pre-soaked LWA-H slightly promoted the formation of ettringite only at 7 days under sealed conditions.

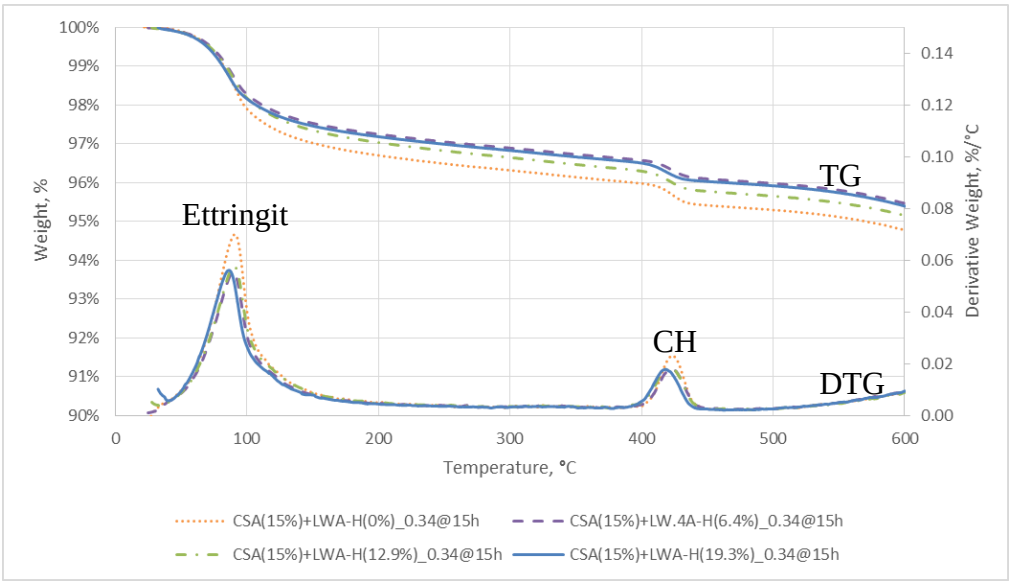

(a)

Figure 6.3 Thermogravimetric (TG) and derivative thermogravimetric (DTG) plots at: (a) 15 hours; (b) 24 hours; (c) 7 days

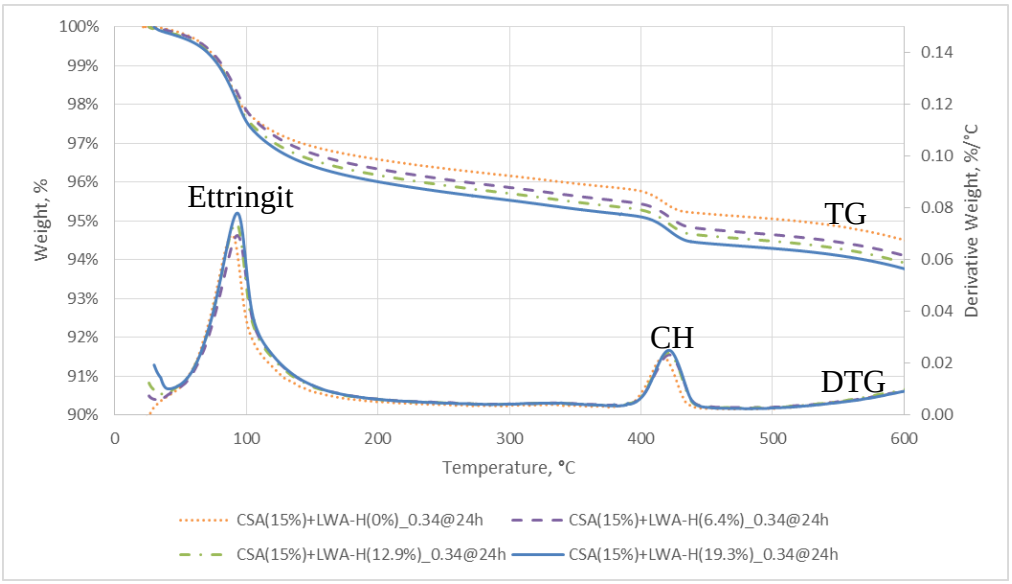

(b)

Figure 6.3 (cont.)

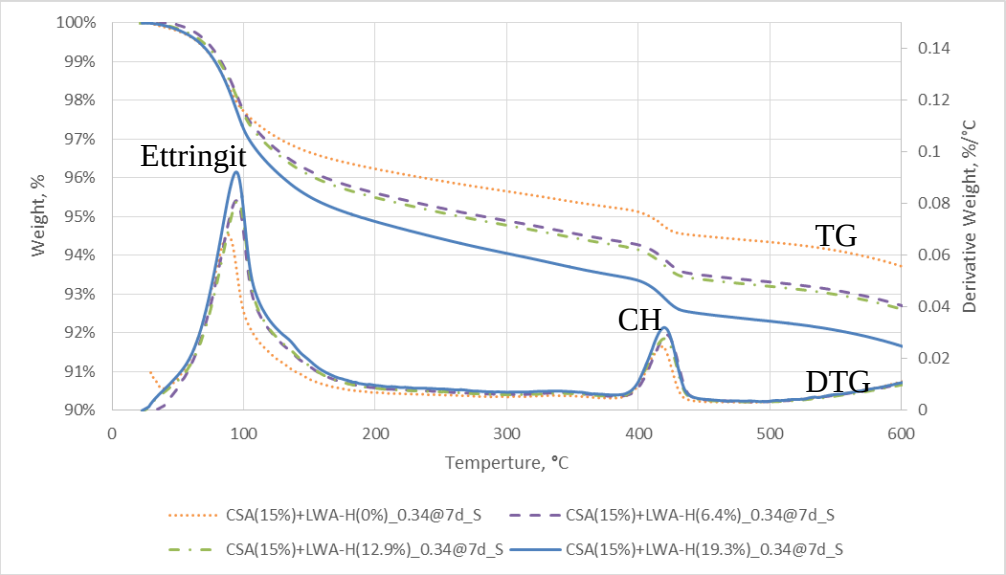

(c)

Figure 6.3 (cont.)

Table 6.2 Weight loss between 70 to 120°C from TGA tests

LWA-H dosage	15 hours		24 hours		7 days	
	Weight loss	Percentage with respect to 0% LWA	Weight loss	Percentage with respect to 0% LWA	Weight loss	Percentage with respect to 0% LWA
0%	2.13%	100.0%	2.13%	100.0%	2.20%	100.0%
6.4%	1.72%	80.7%	2.24%	104.9%	2.70%	122.3%
12.9%	1.83%	85.7%	2.34%	109.5%	2.69%	122.0%
19.3%	1.72%	80.8%	2.45%	114.8%	3.05%	138.5%

The X-ray diffraction results are shown in Figure 6.4. The very big peaks around 20.85 degree, which are related to quartz, are disregarded manually in order to enlarge other peaks. It is shown that ye'elimite, which is the main composition of CSA cement, still existed until 14 days for all samples. It indicates that the addition did not dramatically facilitate the hydration of CSA cement.

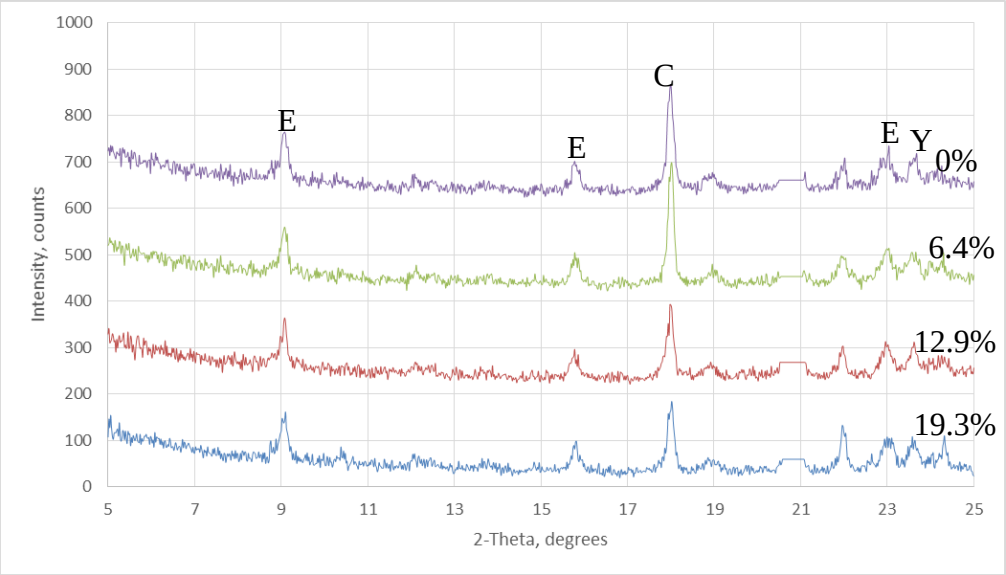

(a)

Figure 6.4 X-ray diffraction tests plots at: (a) 24 hours; (b) 7 days; (c) 14 days (Note: E is ettringite; CH is portlandite; and Y is ye'elimite)

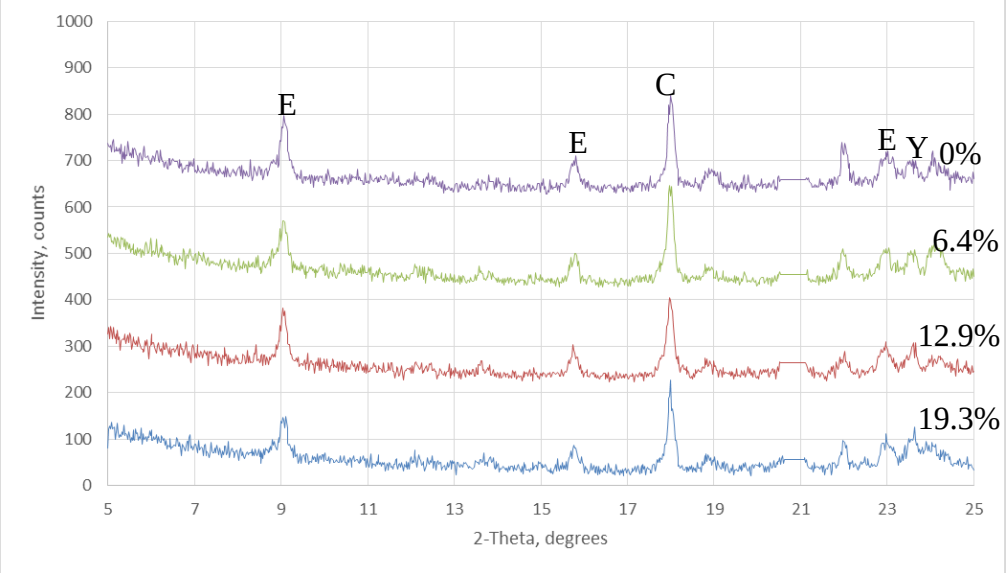

(b)

Figure 6.4 (cont.)

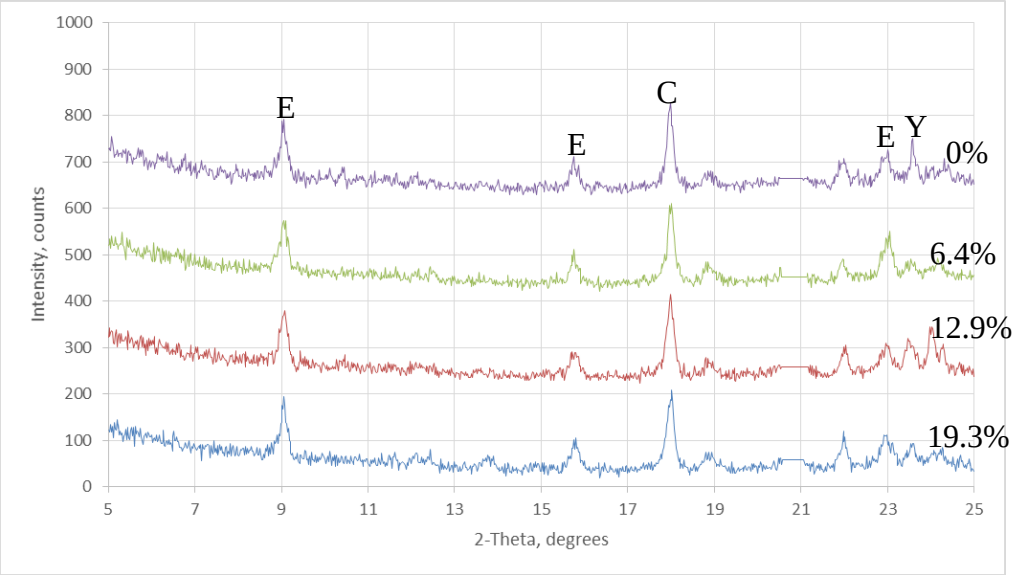

(c)

Figure 6.4 (cont.)

The other possible reason is that the addition of LWA reduced the modulus of the matrix. This is because the modulus of LWA is much lower than that of the normal weight sand and, therefore, promotes expansion. The mixture proportioning for dynamic modulus samples was the same as that of XRD and TGA tests. The dynamic modulus results are presented in Figure 6.5. Figure 6.5 (b) shows the relative dynamic modulus when the sample with 0% LWA-H was taken as the reference. It can be observed that the addition of pre-soaked LWA did lower the dynamic modulus of the mortar matrix and the amount of reduction was proportional to its dosage. To be more specific, 3-7%, 11-15% and 16-22% reductions of dynamic modulus were caused by adding 6.4%, 12.9% and 19.3% of pre-soaked LWA-H, respectively. This trend is consistent with the trend of the magnitude of early-age expansion with different amounts of pre-soaked LWA.

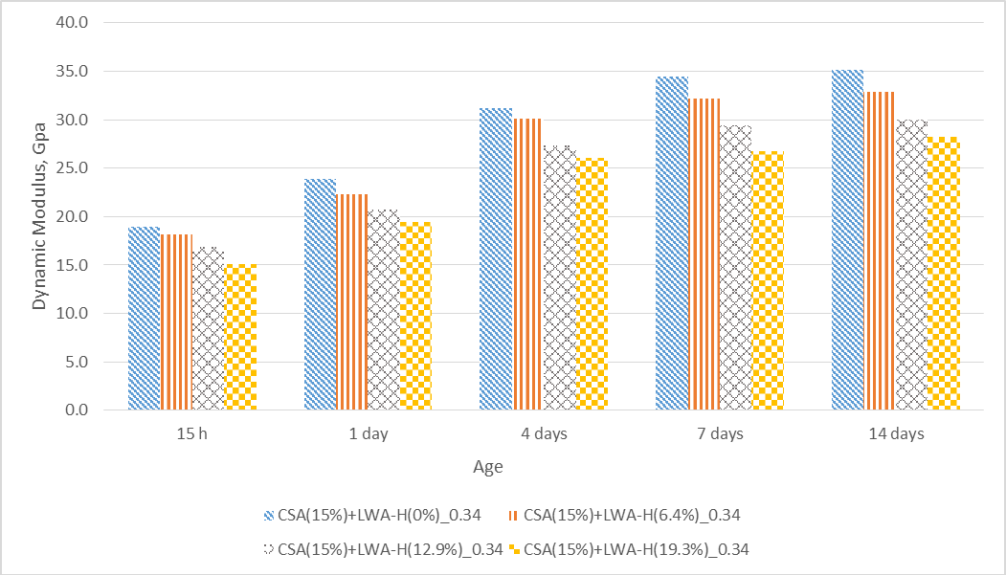

(a)

Figure 6.5 Dynamic modulus of mortars with 15% of CSA cement and different dosages of pre-soaked LWA: (a) absolute values (b) relative values

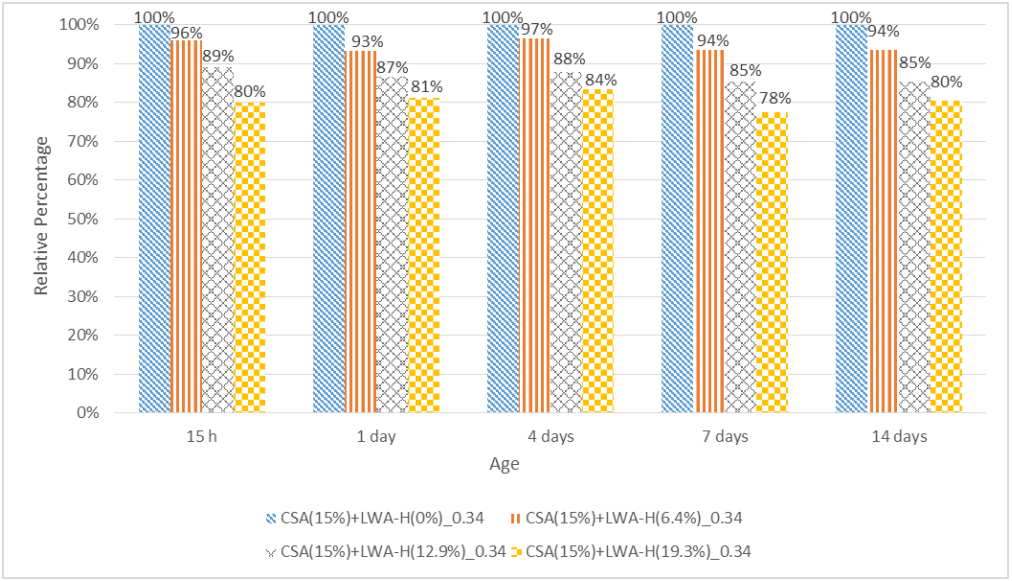

(b)

Figure 6.5 (cont.)

By taking the results of XRD, TGA and dynamic modulus tests into consideration, it was concluded that the main cause of differing magnitudes of early-age expansion by using different dosages of pre-soaked LWA is the different amounts of reduction in the dynamic modulus.

6.4. Conclusions

From the analysis of the experimental results of ordinary Portland cement (OPC) and calcium sulfoaluminate (CSA) cement mortar with pre-soaked lightweight aggregate under sealed and unsealed conditions, the following conclusions can be drawn:

1) The addition of pre-soaked LWA promoted the early-age expansion of specimens with CSA cement for both sealed conditions and lime saturated water curing conditions.
2) For both sealed and unsealed curing, the shrinkage after early-age expansion was not significantly influenced by adding pre-soaked LWA. Therefore, the mitigation of shrinkage was mainly due to the early-age expansion.
3) For both sealed and unsealed curing, adding CSA cement could effectively mitigate shrinkage and adding pre-soaked LWA could promote this trend.
4) The addition of pre-soaked LWA did not significantly facilitate the hydration of CSA cement and the formation of ettringite.
5) The addition of pre-soaked LWA reduced the dynamic modulus of matrix, and the amount of reduction was proportional to its dosage.
6) The main reason leading to differing magnitudes of early-age expansion by using different dosages of pre-soaked LWA is the different amounts of reduction in the dynamic modulus.

CHAPTER 7

LENGTH CHANGE OF ORDINARY PORTLAND CEMENT (OPC) CONCRETE WITH PRE-SOAKED LIGHTWEIGHT AGGREGATES

7.1. Introduction

The objective of this chapter is to investigate the effects of pre-soaked LWA on the deformation of ordinary Portland cement (OPC) concrete specimens.

In this chapter, the measured deformations of ordinary Portland cement (OPC) concrete specimens with pre-soaked lightweight aggregate under both sealed and unsealed conditions are presented and discussed. Two mixtures at 0.39 w/c ratio and with 0% and 19.3% of pre-soaked LWA-H were prepared and cured under sealed and unsealed conditions.

7.2. Materials, mixture proportioning and mixing procedure

The cement, normal weight sand and high-range water reducing admixture (HRWRA) were the same as those described in chapter 4. The coarse aggregate was limestone with a nominal maximum size of 19 mm. The SSD specific gravity and absorption for the coarse aggregate is 2.69 and 2%, respectively. The coarse aggregate was sieved into four ranges of sizes, 4.75-9.5 mm, 9.5-12.5 mm, 12.5-19 mm and 19-25 mm, and then mixed accordingly to meet the No. CA 7 gradation according to Bureau of Materials and Physical Research Policy Memorandum, "Aggregate Gradation Control System". Parts of the normal weight sand was replaced by LWA-H, which is the same on as described in chapter 5.

Two mixtures were prepared with an effective w/c of 0.39, a cement factor of 6.1 and a mortar factor of 0.86. These two mixtures include a control mixture with 0% of LWA-H and

another mixture with 19.3% of the normal weight sand was replaced by pre-soaked LWA-H. The replacement is on basis on total volume. The mixture proportions are shown in Table 7.1.

Table 7.1 Mixture proportions of ordinary Portland cement (OPC) concrete with pre-soaked LWA-H

Materials		0.39 w/c	
		0% LWA	19.3% LWA-H
OPC (lbs/yd^3)		610	610
Water (lbs/yd^3)		294	280
OD Coarse Agg. (lbs/yd^3)	19-25 mm	358	358
	12.5-19 mm	537	537
	9.5-12.5 mm	358	358
	4.75-9.5 mm	537	537
OD Sand (lbs/yd^3)		1188	356
SSD LWA (lbs/yd^3)		0	550

The mixing procedure was in accordance with ASTM C192. The LWA was prepared in the same way as described in section chapter 4.

7.3. Results and discussions

7.3.1. Under sealed conditions

The measured deformations for sealed concrete prisms at 0.39 w/c ratio is presented in Figure 7.1. It was shown that by adding 19.3% of pre-soaked LWA-H the shrinkage of sealed concrete prisms at 28 days was reduced about 75% – from 170 με to 45 με. Additionally, for the concrete prisms with 19.3% of pre-soaked LWA-H, in the first several days almost no shrinkage occurred. Therefore, it shows that the addition of pre-soaked LWA could effectively mitigate the shrinkage of concrete under sealed conditions.

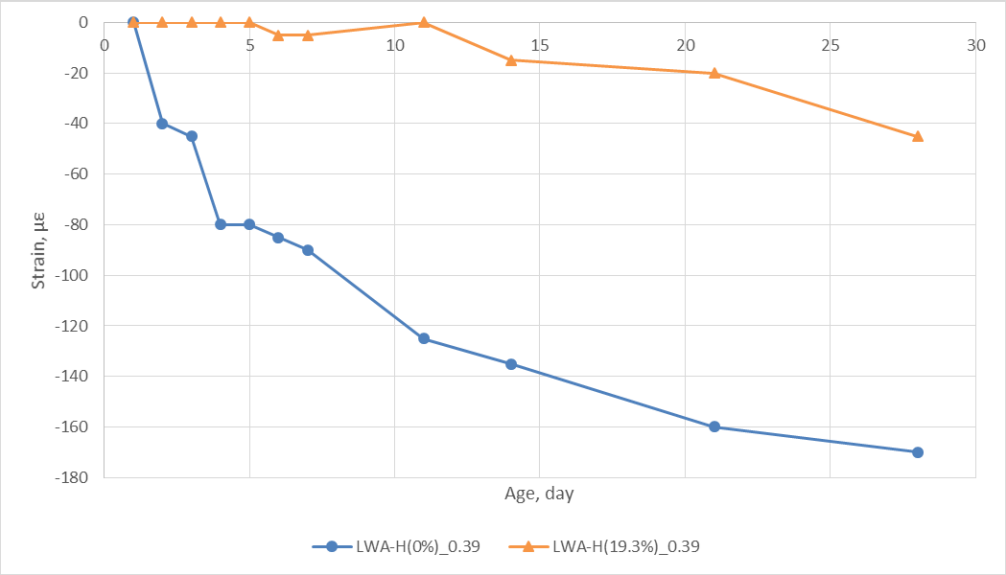

Figure 7.1 Deformation for sealed concrete prisms

7.3.2. Under unsealed conditions

The measured deformations for unsealed concrete prisms at 0.39 w/c ratio is presented in Figure 7.2. The drying shrinkage after 7-day curing is shown in Figure 7.3. It can be seen that the control unsealed concrete prisms expanded larger amount than the prisms with 19.3% of pre-soaked LWA-H in the first 7 days. Moreover, their drying shrinkage after the curing were very close. Therefore, the total shrinkage of the control mixture was smaller. Thus, the addition of pre-soaked LWA cannot reduce the shrinkage under unsealed conditions.

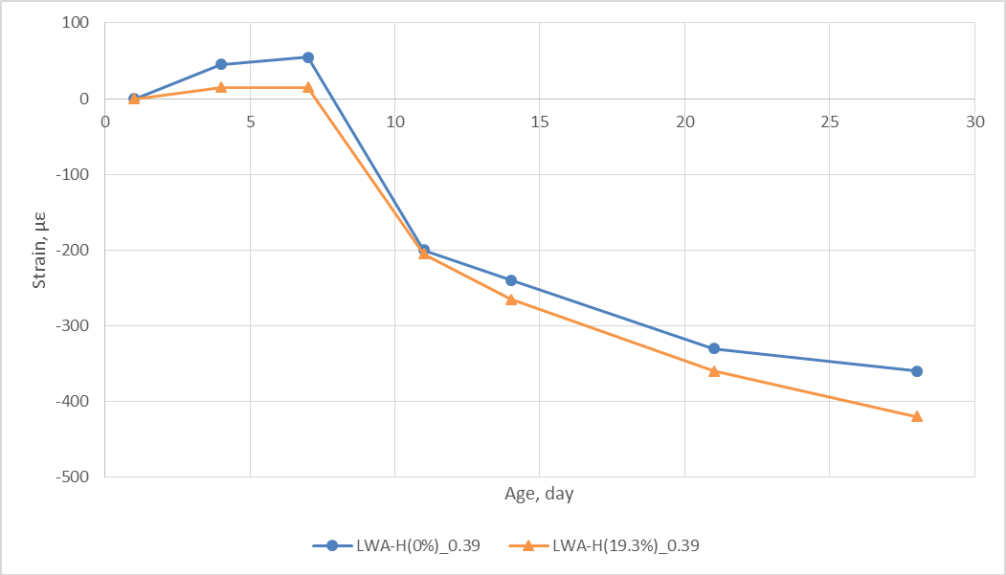

Figure 7.2 Deformation for unsealed concrete prisms

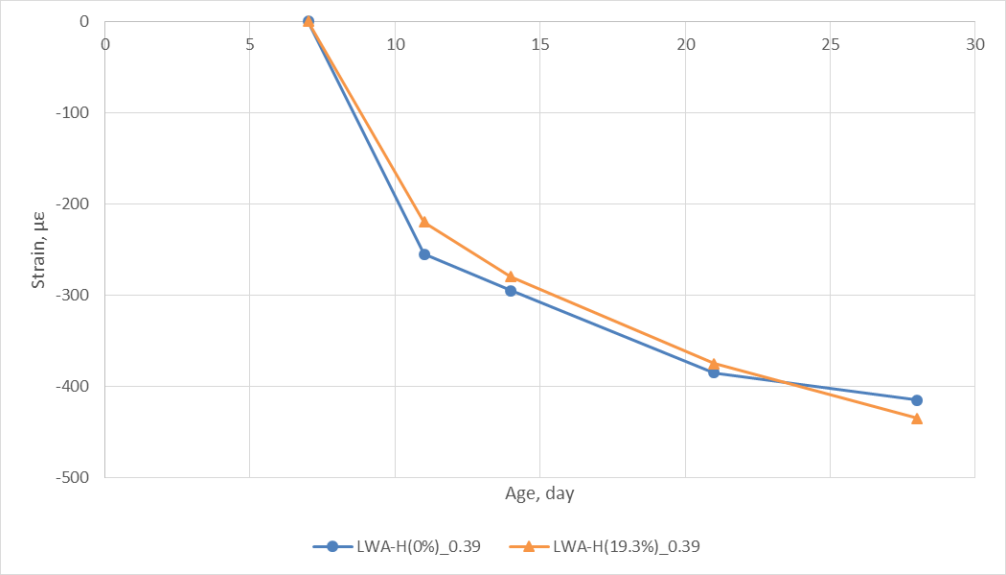

Figure 7.3 Drying shrinkage for unsealed concrete prisms after 7-day curing

7.4. Conclusions

From the analysis of the experimental results of ordinary Portland cement (OPC) concrete with pre-soaked lightweight aggregate under sealed and unsealed conditions, the following conclusions can be drawn:

1) Under sealed conditions, adding pre-soaked LWA could dramatically reduce the shrinkage of concrete, especially at early age.
2) Under unsealed conditions, adding pre-soaked LWA inhibited the expansion under lime saturated water curing and did not affect the drying shrinkage later on.
3) Addition of pre-soaked LWA could effectively mitigate the shrinkage of concrete under sealed conditions but not under unsealed conditions.

CHAPTER 8

LENGTH CHANGE OF ORDINARY PORTLAND CEMENT (OPC) AND CALCIUM SULFOALUMINATE (CSA) CEMENT CONCRETE WITH PRE-SOAKED LIGHTWEIGHT AGGREGATES

8.1. Introduction

The objective of this chapter is to investigate the effects of pre-soaked LWA on deformation of ordinary Portland cement (OPC) and calcium sulfoaluminate (CSA) cement concrete specimens.

In this chapter, the restrained and unrestrained deformation of ordinary Portland cement (OPC) and calcium sulfoaluminate (CSA) cement concrete specimens with pre-soaked lightweight aggregate under both sealed and unsealed conditions are presented and discussed. Two mixtures at 0.39 w/c ratio and with 0% and 19.3% of pre-soaked LWA-H were prepared and cured under sealed and unsealed conditions.

8.2. Materials, mixture proportioning and mixing procedure

The OPC, normal weight sand and high-range water-reducing admixture (HRWRA) were the same as those described in chapter 4. The calcium sulfoaluminate (CSA) cement was the same as mentioned in section chapter 6. The coarse aggregate was the same as described in chapter 7. Parts of the normal weight sand was replaced by LWA-H, which is the same on as described in chapter 5.

Two mixtures were prepared with the same proportioning as described in chapter 7, only in this case, 15 % of the OPC was replaced by CSA cement by weight. The mixture proportions are presented in Table 8.1.

Table 8.1 Mixture proportioning of ordinary Portland cement (OPC) and calcium sulfoaluminate (CSA) cement concrete with pre-soaked LWA-H

Materials		0.39 w/c	
		0% LWA	19.3% LWA-H
OPC (lbs/yd^3)		518.5	518.5
CSA (lbs/yd^3)		91.5	91.5
Water (lbs/yd^3)		294	280
OD Coarse Agg. (lbs/yd^3)	19-25 mm	358	358
	12.5-19 mm	537	537
	9.5-12.5 mm	358	358
	4.75-9.5 mm	537	537
OD Sand (lbs/yd^3)		1188	356
SSD LWA (lbs/yd^3)		0	550

The mixing procedure was in accordance with ASTM C192. The LWA was prepared in the same way as described in chapter 4.

8.3. Results and discussions

8.3.1. Under sealed conditions

The measured deformations for sealed concrete prisms with and without restrain are presented in Figure 8.1. It should be noted that the deformations in Figure 8.1 take the length at 24 hours as the reference. It could be observed that the sealed concrete prisms with 19.3% of pre-soaked LWA-H expanded at early age with and without restrain, while the sealed concrete prisms without pre-soaked LWA-H only expanded at early age without restrain. Additionally, the addition of 19.3% of pre-soaked LWA-H effectively reduced the amount of shrinkage with and without restrain. For the sealed concrete prisms with19.3% of pre-soaked LWA-H without restrain, even no total shrinkage occurred at 28 days. It is also shown that the magnitudes of deformations for the unrestrained sealed concrete prisms with or without pre-soaked LWA-H were lower than those of restrained sealed concrete prisms. It is reasonable because the compressive force caused by restrain could increase the shrinkage.

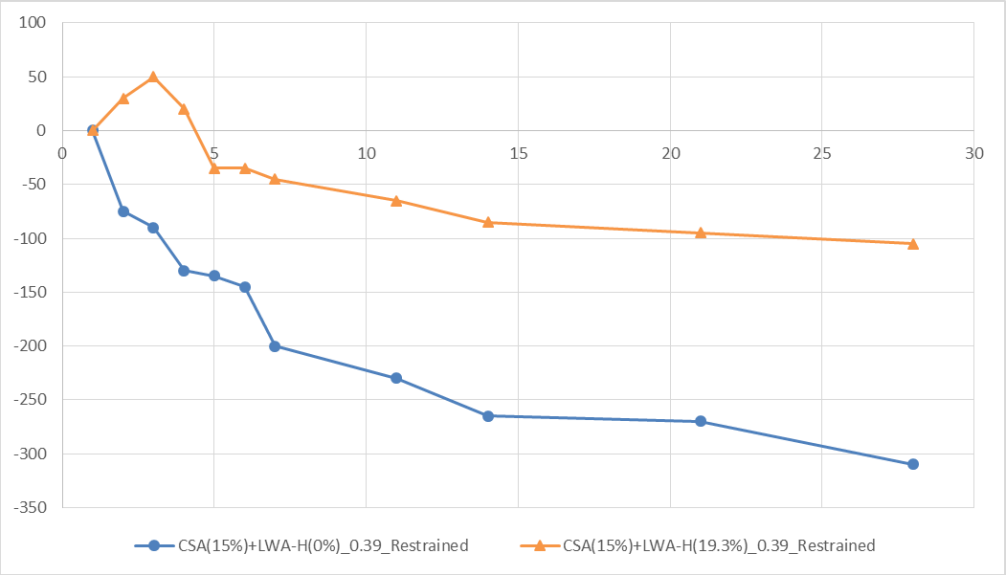

(a)

Figure 8.1 Deformations of sealed concrete prisms: (a) with restrain; (b) without restrain

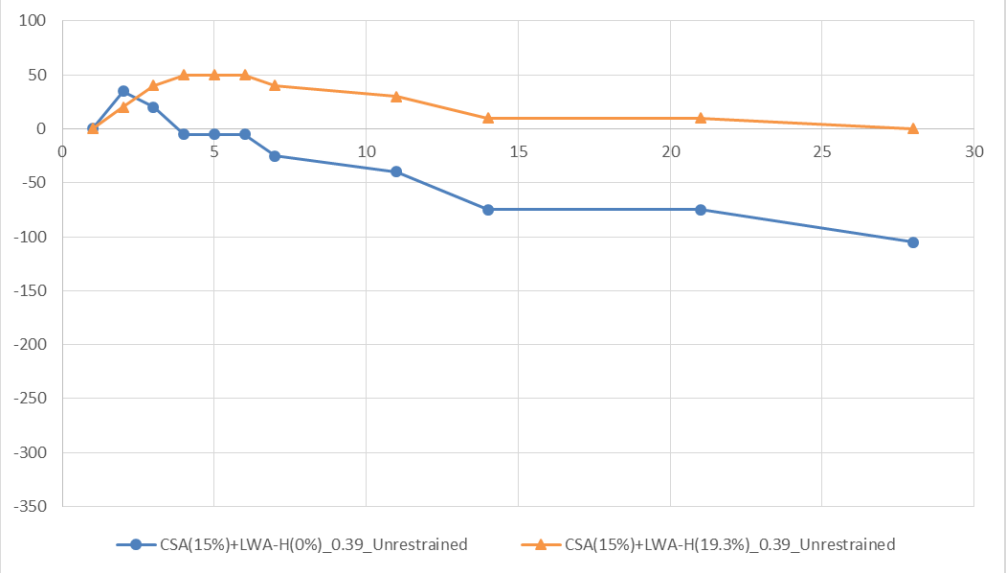

(b)

Figure 8.1 (cont.)

8.3.2. Under unsealed conditions

The measured deformations for unsealed concrete prisms with and without restrain are presented in Figure 8.2. It should be noted that the deformations in Figure 8.2 take the length at 24 hours as the reference. It can be seen that when cured in lime saturated water in the first 7 days, the concrete prisms expanded until the fourth day and after that they started shrinking. This is

different from the behavior of mortar prisms which kept expanding when cured in lime saturated water until the seventh day. Additionally, the expansion of the concrete prisms without pre-soaked LWA was larger than that of the concrete prisms with pre-soaked LWA. Moreover, the total shrinkage of the concrete prisms without pre-soaked LWA was smaller than that of the concrete prisms with pre-soaked LWA. It seemed like that based on aforementioned discussions, adding pre-soaked LWA into concrete adversely affected its shrinkage behavior. However, a different trend was observed when the data before 24 hours was added to the deformations of unsealed concrete prisms with restrain. As shown in Figure 8.3, the early-age expansion for concrete prisms with pre-soaked LWA became larger than that of the concrete prisms without pre-soaked LWA. It also can be seen that the total shrinkage of two kinds of prisms became very close. It was observed that the specimens undergo significant changes from hour 6 to hour 24. As a result, the recorded deformation vary significantly depending on the starting time of recording. It is possible that a lot of deformation is unaccounted for when starting deformation recording at a later point in time. Therefore, only when the entire deformation is recorded can a reliable observation be obtained. However, the unrestrained unsealed concrete prisms were not stiff enough to allow readings to be taken at an earlier time. Thus, the expansion before 24 hours could only be recorded for restrained unsealed concrete prisms.

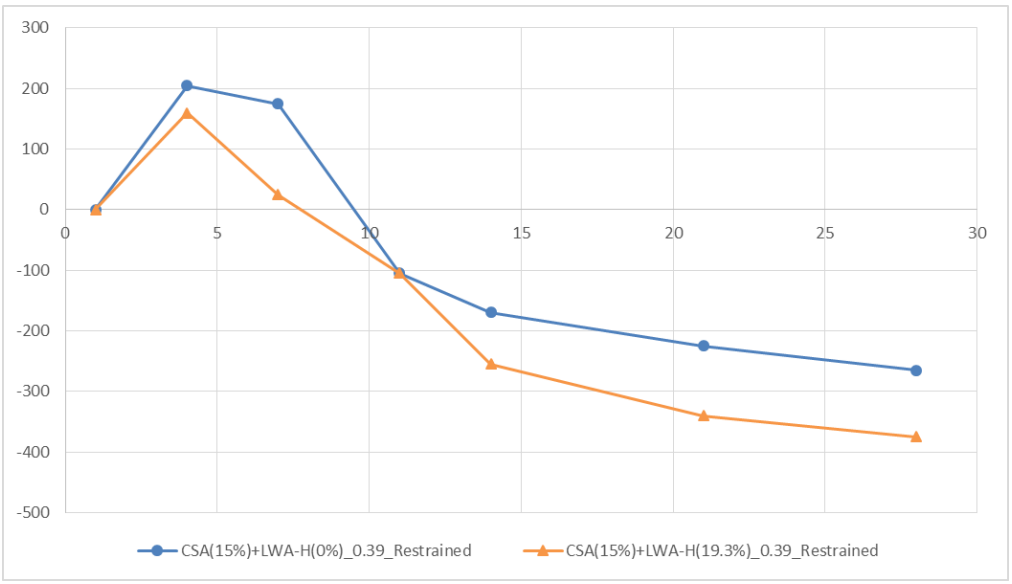

(a)

Figure 8.2 Deformations for unsealed concrete prisms: (a) with restrain; (b) without restrain

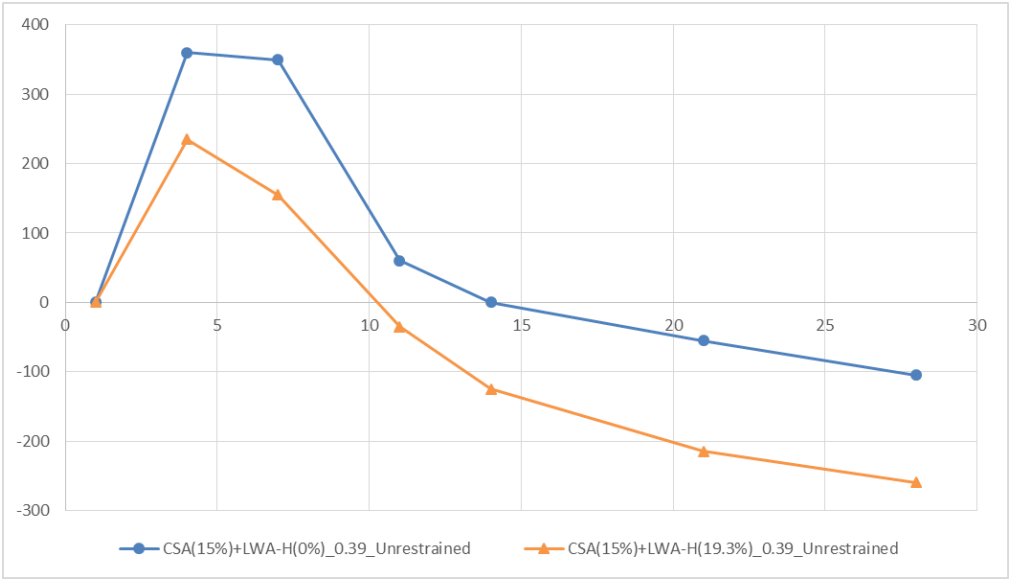

(b)

Figure 8.2 (cont.)

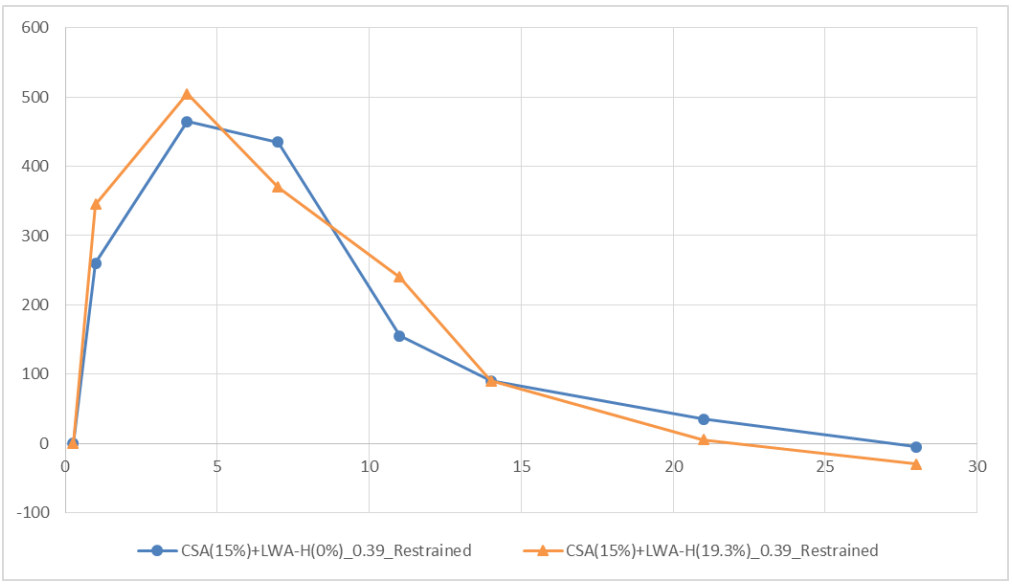

Figure 8.3 Deformations for restrained unsealed concrete prisms starting at 6 hours

The drying shrinkage of the unsealed concrete prisms after being cured in lime saturated water for 7 days is shown in Figure 8.4. It can be observed that the addition of pre-soaked LWA-H reduced the amount of drying shrinkage whether with or without restrain.

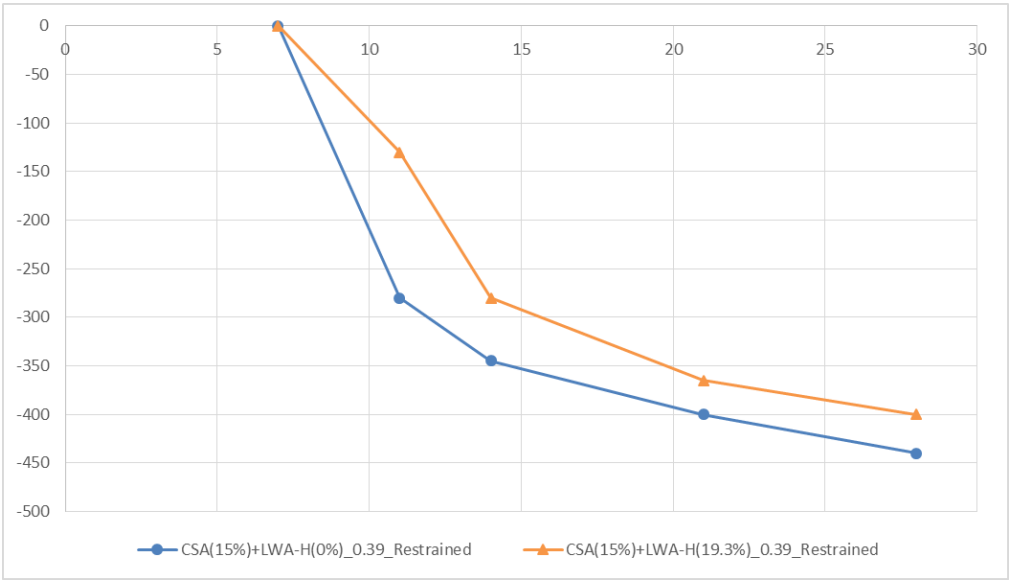

(a)

Figure 8.4 Drying shrinkage for unsealed concrete prisms after 7-day curing: (a) with restrain; (b) without restrain

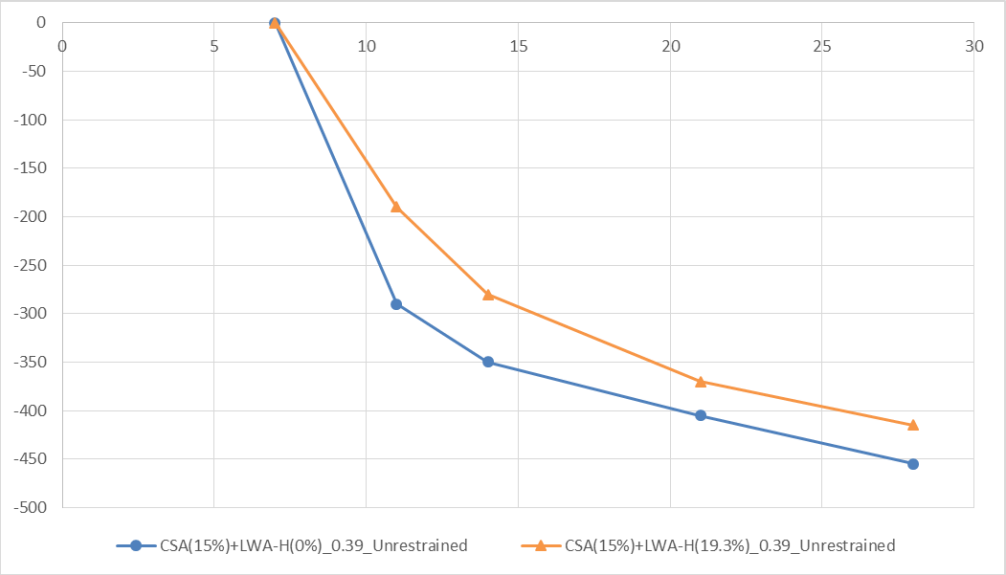

(b)

Figure 8.4 (cont.)

8.4. Conclusions

From the analysis of the experimental results of ordinary Portland cement (OPC) and calcium sulfoaluminate (CSA) cement concrete with pre-soaked lightweight aggregate under sealed and unsealed conditions, the following conclusions can be drawn:

1) Under sealed conditions, the addition of pre-soaked LWA-H effectively reduced the amount of shrinkage of the concrete with CSA cement whether with or without restrain.
2) Under unsealed conditions, after adding the expansion before 24 hours into the deformation, the restrained concrete prisms with pre-soaked LWA showed a similar amount of total shrinkage to that of the restrained concrete prisms without pre-soaked LWA.
3) Under unsealed conditions, the addition of pre-soaked LWA reduced the amount of drying shrinkage of concrete prisms after being cured for 7 days.

CHAPTER 9

CONCLUSIONS AND FURTHER RESEARCH

A wide range of tests that focused on the effects of pre-soaked lightweight aggregate and calcium sulfoaluminate cement on shrinkage mitigation of mortar and concrete were carried out. The main conclusions and recommendations are presented as follows.

9.1. Conclusions

9.1.1. Mortar

The addition of pre-soaked LWA decreased the total shrinkage and increased the early-age expansion under sealed curing. However, under unsealed curing, the addition of pre-soaked LWA did not influence the total shrinkage, but instead increased the drying shrinkage after being cured in lime saturated water for 7 days. Additionally, higher w/c ratio is beneficial to shrinkage mitigation for sealed curing, but had adverse effects when unsealed curing is employed. Longer soaking times for pre-soaked LWA could improve the effectiveness of LWA in reducing shrinkage.

Under sealed conditions, when the same amount of internal curing water was provided, different LWA had similar influence on the shrinkage behavior. Under unsealed conditions, LAW's effectiveness mostly depended on their influence on the stiffness of the cement matrix. Greater reductions of the modulus led to more shrinkage.

The combined use of pre-soaked LWA and CSA cement effectively mitigated the shrinkage. The effectiveness increased as the dosage of pre-soaked LWA increased. This increase was mainly due to the reduction of stiffness rather than the promotion of hydration by adding LWA.

9.1.2. Concrete

The addition of pre-soaked LWA dramatically reduced the shrinkage under sealed curing, while it did not affect the drying shrinkage significantly under unsealed curing. Therefore, the addition of pre-soaked LWA could effectively mitigate the shrinkage of concrete under sealed conditions but not under unsealed conditions.

The combined use of pre-soaked LWA and CSA cement effectively reduced the shrinkage under sealed curing with or without restrain. Under unsealed conditions, the addition of pre-soaked LWA into concrete with CSA cement did not reduce its total deformation. Instead, this combination affected the drying shrinkage after 7 days of lime saturated water curing.

9.2. Recommendations for future research

The tests in this thesis were mainly on small-scale specimens. However, in order to better predicate the performance of pre-soaked LWA and CSA cement on shrinkage mitigation in field, the further research on large-scale specimens has to be conducted. This is because that several differences, such as surface-to-volume ratio and the way the specimens are restrained, exist between small-scale and large-scale specimens and may affect the effectiveness of pre-soaked LWA and CSA cement.

As shown in this thesis, the early-age deformation is very critical on deformation study. Thus, proper methods of early-age deformation measurement have to be adopted.

The properties of a LWA that determine its effectiveness on shrinkage mitigation need to be examined more carefully. An evaluation method needs to be developed so the effectiveness of the LWA on shrinkage could be measured based on the properties of the LWA.

Furthermore, in this thesis, the influences of thermal deformation, plastic deformation and early-age creep were not taken into consideration. For future research, these factors need to be considered in order to predict shrinkage behavior more accurately.

REFERENCES

ACI Committee 231, "Report on Early-Age Cracking: Causes, Measurement, and Mitigation (ACI 231R-10)," American Concrete Institute, Farmington Hills, MI, 2010, 46 pp.

Bazant, Z. P., & Wittmann, F. H. (1982). *Creep and shrinkage in concrete structures* Wiley Chichester.

Beltzung, F., Wittmann, F., & Holzer, L. (2001). Influence of composition of pore solution on drying shrinkage. *Creep, Shrinkage and Durability Mechanics of Concrete and Other Quasi-Brittle Materials, Edited by Ulm, F.-J., Bazant, ZP and Wittmann, FH, Elsevier Science Ltd,*

Bentz, D. P. (2002). Influence of curing conditions on water loss and hydration in cement pastes with and without fly ash substitution. *Nistir, 6886*, 15.

Bentz, D. P. (2007). Internal curing of high-performance blended cement mortars. *ACI Materials Journal, 104*(4)

Bentz, D. P., Garboczi, E. J., & Quenard, D. A. (1998). Modelling drying shrinkage in reconstructed porous materials: Application to porous vycor glass. *Modelling and Simulation in Materials Science and Engineering, 6*(3), 211.

Bentz, D. P., Halleck, P. M., Grader, A. S., & Roberts, J. W. (2006). Four-dimensional X-ray microtomography study of water movement during internal curing. *Proceedings of the International RILEM Conference-Volume Changes of Hardening Concrete: Testing and Mitigation,* pp. 11-20.

Bentz, D. P., Lura, P., & Roberts, J. W. (2005). Mixture proportioning for internal curing. *Concrete International, 27*(2), 35-40.

Bentz, D. P., & Weiss, W. J. (2011). *Internal curing: A 2010 state-of-the-art review* US Department of Commerce, National Institute of Standards and Technology.

Bentz, D., Hansen, K. K., Madsen, H., Vallee, F., & Griesel, E. (2001). Drying/hydration in cement pastes during curing. *Materials and Structures, 34*(9), 557-565.

Bentz, D., Koenders, E., Mönnig, S., Reinhardt, H., van Breugel, K., & Ye, G. (2006). Materials science-based models in support of internal water curing. *RILEM Report, 41*, 29-43.

Bentz, D., & Snyder, K. (1999). Protected paste volume in concrete: Extension to internal curing using saturated lightweight fine aggregate. *Cement and Concrete Research, 29*(11), 1863-1867.

Bentz, D., & Weiss, W. (2008). REACT: Reducing early-age cracking today. *Concrete Plant International, 3*, 56-61.

Bizzozero, J., Gosselin, C., & Scrivener, K. L. (2014). Expansion mechanisms in calcium aluminate and sulfoaluminate systems with calcium sulfate. *Cement and Concrete Research, 56*, 190-202.

Castro, J., De la Varga, I., Golias, M., & Weiss, W. (2010). Extending internal curing concepts to mixtures containing high volumes of fly ash. *International Bridge Conference,*

Castro, J., Keiser, L., Golias, M., & Weiss, J. (2011). Absorption and desorption properties of fine lightweight aggregate for application to internally cured concrete mixtures. *Cement and Concrete Composites, 33*(10), 1001-1008.

Chaunsali, P., Lim, S., Mondal, P., Foutch, D., Richardson, D., Tung, Y., & Hindi, R. (2013). Bridge Decks: Mitigation of Cracking and Increased Durability. Illinois Center for Transportation (ICT).

Chaunsali, P., & Mondal, P. (2015). Influence of mineral admixtures on early-age behavior of calcium sulfoaluminate cement. ACI Materials Journal, 112(1)

Collepardi, M., Turriziani, R., & Marcialis, A. (1972). The paste hydration of 4CaO· 3Al 2 O 3· SO 3 in presence of calcium sulphate, tricalcium silicate and dicalcium silicate. *Cement and Concrete Research, 2*(2), 213-223.

Cusson, D., & Hoogeveen, T. (2008). Internal curing of high-performance concrete with pre-soaked fine lightweight aggregate for prevention of autogenous shrinkage cracking. *Cement and Concrete Research, 38*(6), 757-765.

Feldman, R., & Sereda, P. (1970). A new model for hydrated portland cement and its practical implications. *Engineering Journal, 53*(8/9), 53-59.

Gartner, E., Young, J., Damidot, D., & Jawed, I. (2002). Hydration of portland cement. *Structure and Performance of Cements, 13*, 978-970.

Golias, M., Bentz, D., & Weiss, J. (2012). Influence of exposure conditions on the efficacy of internal curing. *Adv Civ Eng Mater (Submitted),*

Golias, M., Castro, J., & Weiss, J. (2012). The influence of the initial moisture content of lightweight aggregate on internal curing. *Construction and Building Materials, 35*, 52-62.

Hansen, W. (2011). Report on early-age cracking. *Concrete International, 33*(3), 48-51.

Henkensiefken, R., Nantung, T., & Weiss, J. (2011). Saturated lightweight aggregate for internal curing in low w/c mixtures: Monitoring water movement using X-ray absorption. *Strain, 47*(s1), e432-e441.

Henkensiefken, R., Nantung, T., & Weiss, W. (2009). Internal curing-from the laboratory to implementation. *International Bridge Conference,*

Henkensiefken, R., Bentz, D., Nantung, T., & Weiss, J. (2009). Volume change and cracking in internally cured mixtures made with saturated lightweight aggregate under sealed and unsealed conditions. *Cement and Concrete Composites, 31*(7), 427-437.

Henkensiefken, R., Briatka, P., Bentz, D., Nantung, T., & Weiss, J. (2010). Plastic shrinkage cracking in internally cured mixtures made with pre-wetted lightweight aggregate. *Concrete International, 32*(2), 49-54.

Henkensiefken, R., Sant, G., Nantung, T., Weiss, J., Schlangen, E., & De Schutter, G. (2008). Comments on the shrinkage of paste in mortar containing saturated lightweight aggregate. *CONMOD, Delft, the Netherlands,*

Hiller, K. (1964). Strength reduction and length changes in porous glass caused by water vapor adsorption. *Journal of Applied Physics, 35*(5), 1622-1628.

Jensen, O. M., & Hansen, P. F. (2001). Autogenous deformation and RH-change in perspective. *Cement and Concrete Research, 31*(12), 1859-1865.

Jensen, O. M., & Hansen, P. F. (2001). Water-entrained cement-based materials: I. principles and theoretical background. *Cement and Concrete Research, 31*(4), 647-654.

Jensen, O. (1996). Dilatometer–further development. *Building Materials Laboratory, the Technical University of Denmark, Lyngby, Denmark, 8*

Kovler, K., & Zhutovsky, S. (2006). Overview and future trends of shrinkage research. *Materials and Structures, 39*(9), 827-847.

Lura, P. (2003). *Autogenous deformation and internal curing of concrete* TU Delft, Delft University of Technology.

Lura, P., Bentz, D. P., Lange, D. A., Kovler, K., Bentur, A., & van Breugel, K. (2006). Measurement of water transport from saturated pumice aggregates to hardening cement paste. *Materials and Structures, 39*(9), 861-868.

Lura, P., Jensen, O. M., & van Breugel, K. (2003). Autogenous shrinkage in high-performance cement paste: An evaluation of basic mechanisms. *Cement and Concrete Research, 33*(2), 223-232.

Mackenzie, J. (1950). The elastic constants of a solid containing spherical holes. *Proceedings of the Physical Society.Section B, 63*(1), 2.

Mehta, P. (1967). Expansion characteristics of calcium sulfoaluminate hydrates. *Journal of the American Ceramic Society, 50*(4), 204-208.

Mehta, P. (1972). Chemistry and microstructure of expansive cements. *Conference on Expansive Cement Concrete, University of California, Berkeley, California,*

Mehta, P. (1973). Mechanism of expansion associated with ettringite formation. *Cement and Concrete Research, 3*(1), 1-6.

Mehta, P. K., & Hu, F. (1978). Further evidence for expansion of ettringite by water adsorption. *Journal of the American Ceramic Society, 61*(3-4), 179-181.

Mehta, P. K., & Klein, A. (1966). Investigations on the hydration products in the system 4 cao-3al203-so3-caso4-cao-h20. *Highway Research Board Special Report,* (90)

Mindess, S., Young, J. F., & Darwin, D. (2003). *Concrete*

Pelletier, L., Winnefeld, F., & Lothenbach, B. (2010). The ternary system portland cement–calcium sulphoaluminate clinker–anhydrite: Hydration mechanism and mortar properties. *Cement and Concrete Composites, 32*(7), 497-507.

Polivka, M. (1973). Factors influencing expansion of expansive cement concretes. *ACI Special Publication, 38*

Powers, T. C. (1965). Mechanisms of shrinkage and reversible creep of hardened cement paste. *The Structure of Concrete and its Behaviour Under Load, ,* 319-344.

Powers, T. C., & Brownyard, T. L. (1946). Studies of the physical properties of hardened portland cement paste. *ACI Journal Proceedings, , 43.* (9)

Powers, T. C., Copeland, L. E., & Mann, H. (1900). *Capillary Continuity Or Discontinuity in Cement Pastes,*

Radlinska, A., Rajabipour, F., Bucher, B., Henkensiefken, R., Sant, G., & Weiss, J. (2008). Shrinkage mitigation strategies in cementitious systems: A closer look at differences in sealed and unsealed behavior. *Transportation Research Record: Journal of the Transportation Research Board, 2070*(1), 59-67.

Sant, G., Lura, P., & Weiss, J. (2006). Measurement of volume change in cementitious materials at early ages: Review of testing protocols and interpretation of results. *Transportation Research Record: Journal of the Transportation Research Board, 1979*(1), 21-29.

Schubert, H. (1982). *Kapillarität in porösen feststoffsystemen* Springer.

Shin, K., Bucher, B., & Weiss, J. (2010). Role of lightweight synthetic particles on the restrained shrinkage cracking behavior of mortar. *Journal of Materials in Civil Engineering, 23*(5), 597-605.

Steiger, M. (2005). Crystal growth in porous materials—I: The crystallization pressure of large crystals. *Journal of Crystal Growth, 282*(3), 455-469.

Steiger, M. (2005). Crystal growth in porous materials—II: Influence of crystal size on the crystallization pressure. *Journal of Crystal Growth, 282*(3), 470-481.

Trtik, P., Münch, B., Weiss, W., Kaestner, A., Jerjen, I., Josic, L., et al. (2011). Release of internal curing water from lightweight aggregates in cement paste investigated by neutron and X-ray tomography. *Nuclear Instruments and Methods in Physics Research Section A: Accelerators, Spectrometers, Detectors and Associated Equipment, 651*(1), 244-249.

Visser, J. H. M. (1998). *Extensile hydraulic fracturing of (saturated) porous materials* TU Delft, Delft University of Technology.

Wasserman, R., & Bentur, A. (1996). Interfacial interactions in lightweight aggregate concretes and their influence on the concrete strength. *Cement and Concrete Composites, 18*(1), 67-76.

Weber, S., & Reinhardt, H. (1999). Manipulating the water content and microstructure of high performance concrete using autogenous curing. *Modern Concrete Materials: Binders, Additions and Admixtures, ,* 567-577.

Winnefeld, F., & Lothenbach, B. (2010). Hydration of calcium sulfoaluminate cements—experimental findings and thermodynamic modelling. *Cement and Concrete Research, 40*(8), 1239-1247.

Zhang, J., & Scherer, G. W. (2011). Comparison of methods for arresting hydration of cement. *Cement and Concrete Research, 41*(10), 1024-1036.

Zhang, L., & Glasser, F. (2002). Hydration of calcium sulfoaluminate cement at less than 24 h. *Advances in Cement Research, 14*(4), 141-156.

Zhutovsky, S., & Kovler, K. (2012). Effect of internal curing on durability-related properties of high performance concrete. *Cement and Concrete Research, 42*(1), 20-26.

Zhutovsky, S., Kovler, K., & Bentur, A. (2004). Influence of cement paste matrix properties on the autogenous curing of high-performance concrete. *Cement and Concrete Composites, 26*(5), 499-507.